

H α emitters from the Southern Photometric Local Universe Survey (S-PLUS) Optical identification of emission line sources in the southern photometric local Universe survey (S-PLUS)

L. A. Gutiérrez-Soto,^{1*} Second Author,² Third Author^{2,3} and Fourth Author³

¹Departamento de Astronomia, IAG, Universidade de São Paulo, Rua do Matão, 1226, 05509-900, São Paulo, Brazil

²Department, Institution, Street Address, City Postal Code, Country

³Another Department, Different Institution, Street Address, City Postal Code, Country

Accepted XXX. Received YYY; in original form ZZZ

ABSTRACT

In the way to map 9000 deg² of the Southern hemisphere, the S-PLUS project is also surveying the sky in a proxy of a myriad of astrophysical processes: the H α transition. Here we explore such a capability from its DR3 to make H α emitters in evidence from the ($r - J0660$) versus ($r - i$) color-color diagram and distinguish the red from the blue ones by exploring the ($r - i$) and ($g - z$) diagram. Our catalog is composed of 9,200 objects that exhibit excess in the narrow $J0660$ band which is consistent with H α in emission. Unsupervised, clustering machine learning approach revealed two distinct populations: one with an intense blue continuum and another with a red one. The hierarchical clustering algorithm was compared with the HDBSCAN. By adopting a “soft” clustering approach, we assigned the probability of each emitter belonging to a given population, blue or red clusters. We use synthetic and observed (SDSS) spectra to emphasize the potential of color-color diagrams to distinguish several classes of emission line emitters that include planetary nebulae, H II regions, young stellar objects, symbiotic stellar systems, cataclysmic variables, blue compact galaxies, star-forming galaxies, and quasars, and trace the way to reveal new ones with S-PLUS data.

The emission line objects are very important objects in astronomy because reflects different class of objects that evolved physical mechanics that given counts of stellar formation process, presences the gas, shocks, star-burst in galaxies, the final stage of stars among others process. For this reason we have created a list of H α emitters selected from the S-PLUS data, which is mapping the southern hemisphere at relatively high latitudes. We implemented the ($r - J0660$) versus ($r - i$) color-color diagram for that task. We found 9,200 objects that exhibit um excess in emission in the $J0660$ which we have traduced as the presence of the H α emission line. In addition we have found that by combining the colors: ($r - i$) and ($g - z$) with unsupervised (clustering) machine learning it is possible separate the blue sources from red ones, then we ave divided our list of emitters in two sub-groups: one with intense blue continuum and another with intense red one. We compare hierachical clustering algorithm with the HDBSCAN. By adopting a “soft” clustering approach, we can assign each emission object a probability of belonging to a given cluster (blue or red group), allowing for more flexibility in the classification of objects according to these colours those objects with a low probability of belonging to any cluster.

Key words: surveys – stars: emission-line, Be – novae, cataclysmic variables – galaxies: dwarf – quasars: emission lines

1 INTRODUCTION

The existence of an ionizing radiation field can lead to Balmer hydrogen emission lines. From the presence of the H Balmer lines in the optical spectra of some sources it is well known the possible presence of ionized gas. Many important astronomical objects involve the physics of photo-ionized gases and the interpretation of the emission-line spectra. Emission line objects as the H II regions allow us to study the star formation history of the far reaches of our Galaxy and of distant galaxies. Planetary nebulae let us to see the remaining envelope of dying stars. Star-burst galaxies and QSOs are

one the most luminous objects and hence the most distant that can be observed. Their spectra can reveal details about of the first generation of star and the formation of heavy elements in the young universe. On the other hand, emission lines can also infer the presence or lack the accretion discs (Schwope et al. 2000; Ratti et al. 2012), the properties of single or double picked line can allow us to infer geometrical characteristics (Horne & Marsh 1986), the nature of donor stars in binary system (Steeghs & Casares 2002; van Spaandonk et al. 2010; Casares 2015) and the compact objects as black holes (Casares 2016).

Emission lines are also associated with stars in very early-type and/or very late evolutionary stage which are short phase. As already mentioned are also associated with binaries that experiencing mass transfer. These group of emission line stars includes young

* E-mail: gsoto.angel@gmail.com

stellar (YSOs) and Herbig-Haro (HH) objects, post-asymptotic and some asymptotic giant branch (AGB), some red giant stars (RGB), Wolf-Rayet (WR) stars, supernova remnants, classical Be stars, active late-type dwarfs, interacting binary system like symbiotic stars (SySt) and cataclysmic variables (CV). Most of these class of object are in-homogeneous and some contains many few identified members, for instance at the moment around 323 symbiotic system have been identified from which 257 belong to the Galaxy and ~ 66 are extra-galactic objects (Akras et al. 019a). The same occurs with PNe from which around 3500 of them are been cataloged (Parker et al. 2016), this current number of PNe represents only about 15-30% of the estimated total of Galactic PNe (Frew, 2008; Jacoby et al., 2010) showing that a small fraction of the PNe have been cataloged. Many galaxies, in addition to harbor Planetary nebulae and H II regions, show characteristic nebular in their spectra. In most of these objects, the gas is photoionized by hot stars in the nucleus, which is thus much like giant H II region, or perhaps many H II regions. The galactic nucleus with very strongest emission lines of this type are often called blue compact galaxies, extragalactic H II regions, star forming or starburst galaxies (Osterbrock & Ferland 2006). There are also spiral galaxies that present emission lines.

In the past $H\alpha$ surveys with modest spatial resolutions have been used to identified extended nebular emission to study supernova remnants, galaxy groups and star forming regions (Davies, Elliott & Meaburn 1976). More recently, higher resolution surveys such as the INT Photometric $H\alpha$ survey (IPHAS; Drew et al. 2005; Barentsen et al. 2014) have focused in the study of compact emission line sources on the Galactic plane, typically with objects in different stage of stellar evolution. The Anglo-Australian Observatory UKS Schmidt Telescope Supercosmos $H\alpha$ Survey (Parker et al. 2005) is another $H\alpha$ survey of the Southern Galactic Plane and Magellanic Cloud which has covered to $b \sim 10\text{--}13^\circ$ (verificar esto). Currently ongoing is the VST Photometric $H\alpha$ Survey of the Southern Galactic Plane and Bulge (VPHAS+; Drew et al. 2014) that will cover the Galactic bulge and plane in five filters.

Like VPHAS+, others ongoing surveys that are used to study the population of emission line objects are the The Javalambre Photometric Local Universe Survey (J-PLUS¹, Cenarro et al. 2018) and the Southern-Photometric Local Universe Survey (S-PLUS², Mendes de Oliveira et al. 2019) are providing observations of the Galactic halo covering both northern and southern celestial hemispheres in a systematic way with twin telescopes using the same set of multi-band filters. In addition to the $H\alpha$ filter, which is already vastly applied to systematically searching for $H\alpha$ emitters the telescopes offer 11 more filters. And more ambitious yet the JPAS survey that will the same area of J-PLUS in 56 narrow-band filters.

Traditionally, color-color diagrams based in $H\alpha$ filter are been used to identify $H\alpha$ emitters. The analysis the color-color diagram ($r - H\alpha$) versus ($r - i$) has resulted on the discovered of new emission line objects, for instance Witham et al. (2006, 2007) used the ($r - H\alpha$) versus ($r - i$) colour-colour diagram to find for new CV. On the other hand, Vink et al. (2008) reported the discovery of YSOs by using this same colour criteria. In this sense using this methodology a variety of classes of objects are been identified, which include symbiotic stars (Corradi et al. 2008; Corradi & Giammanco 2010; Corradi et al. 2011), early type emission line stars (Drew et al. 2008) and planetary nebulae (Vironen et al. 2009; Sabin et al. 2010). Recently, by using this same color diagram were also identified compact PN candidates

in VPHAS+ catalog (Akras et al. 2019). And the same diagram in conjunction with new ones shows to be very efficient to find for PN candidates (Gutiérrez-Soto et al. 2020). In general terms, Witham et al. (2006) presented a methodology and first results in looking for emission line sources in narrow-band surveys.

In this era of big data on astronomy, machine learning techniques are becoming in important statistical tools for the analysis and find meaning from massive data sets. Particularly, unsupervised machine approaches have showed a promised in various applications, especially in automatic classification task. Including object classification and selection, using galaxies with active galactic nuclei as example (Geach 2012), morphological analysis of galaxies (Martin et al. 2020), classification of variable stars, relying only on the similarity among light curves. (Valenzuela & Pichara 2018). Using unsupervised machine learning can be very advantageous because they do not require a labeled data training sets. Unlike of supervised methods like Random Forest algorithm. Instead, unsupervised techniques are generally based in the data itself to identify patrons, e. g. cluster of similar objects, in some pre-defined feature space where the data are defined.

In this work, we used S-PLUS observations of the southern hemisphere to search for objects with an excess of $H\alpha$ using automatic methods based on the ($r - H\alpha$) versus ($r - i$) color-color diagram. We have also used color criteria based in ($g - r$) and ($z - g$) in conjunction to unsupervised machine learning techniques to split the final list in those with blue and red continuum. The paper is organized as follows...

2 OBSERVATIONS: THE S-PLUS PROJECT

We are implemented data from S-PLUS DR3 (ref) to carried out our study. S-PLUS is 12-band optical photometric survey, which are formed by seven narrow-band ($J0378$, $J0395$, $J0410$, $J0430$, $J0515$, $J0660$ and $J0861$) and five broad-band like SDSS filters (u, g, r, i and z , Fukugita et al. 1996). The narrow-band set include the filter $J0660$ which detect the $H\alpha$ emission line. For more detailed about the configuration of S-PLUS filter set see Figure 1 shows the Javalambre filter system (Marín-Franch et al. 2012) overlapping are the optical spectra of several class of emission line objects on which it is possible to see that the $H\alpha$ line falls into the $J0660$ filter, except for the QSOs.

The actual data release contains about 60 millions of objects covering a total area of $\sim 8000 \text{ deg}^2$, at high Galactic latitudes ($> 30 \text{ deg}$) using a dedicated 0.83m robotic telescope, the T80-South (T80S), located at Cerro Tololo, Chile. S-PLUS will cover an additional $1,300 \text{ deg}^2$ of the Galactic plane and bulge to enable Galactic studies. In this work, we focus on the aspects that are of particular interest to the second data release of the S-PLUS main survey. Additional information about S-PLUS can be found in Mendes de Oliveira et al. (2019).

3 METHODOLOGY

We first constructed a sub-sample from all S-PLUS DR3 from which we applied an iterative and automatic technique to select objects with an excess of $H\alpha$ emission line. Once the objects were selected we also make a separation of them into two groups those with red and blue continuum by using optical colors in conjunction with unsupervised machine learning statistical tools. These procedures are described below:

¹ <https://www.j-plus.es>

² <http://www.splus.iag.usp.br>

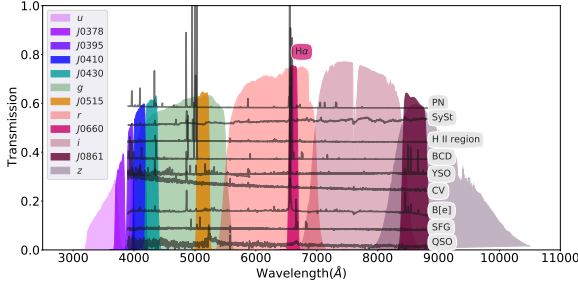


Figure 1. Transmission curves of the S-PLUS filters set. The narrow-band filter $J0660$ detects the $H\alpha$ emission line. Over-plotted are different classes of emission line objects, from upper to down PN, SySt...

3.1 Initial selection sample

The first step in our selection procedure consist in the following criteria to guarantee the quality of the observations of the objects:

- (i) The sources must have detection in the filters: r , i and $J0660$. To assure that we select object must have error minor or equal to 0.2 in each of three filters.
- (ii) Must have an r magnitude until $r = 21$.

3.2 Finding the main stellar locus and selecting the H α emitters

Once the initial cut were made, we proceed to select the objects with an excess of $H\alpha$ which is represent with a relatively high value of the filter $J0660$ in comparison with r-band filter. For that we first divided our sub-sample in for magnitude bins using the r -band magnitudes. The bins have the follow distribution:

- (i) objects with magnitude in the r -band $r < 16$
- (ii) objects with magnitude in the r -band $16 \leq r < 18$
- (iii) objects with magnitude in the r -band $18 \leq r < 20$
- (iv) objects with magnitude in the r -band $20 \leq r < 21$

To select the emission lines we used the same method created and implemented by [Witham et al. \(2008\)](#) its possible to do that because the S-PLUS has similar filters that the IPHAS project, which are r , $J0660$ and i . This technique was used by [Scaringi et al. \(2013\)](#) to identify blue objects with excess of $H\alpha$ and after that [Wevers et al. \(2017\)](#) also applied this methodology to create catalogue of candidate $H\alpha$ emission showing an high effectiveness. In this order of ideas we attempted this methodology in S-PLUS.

We first generated the $(r - J0660)$ versus $(r - i)$ color-color diagram for each magnitude bins. We then carried a out an initial straight line fit to all objects in each magnitude bin. This initial fit is an attempt to find the loci of main-sequence and giant stars. We implemented a iterative σ -clipping technique to find the best-fitting of the main stellar locus. In this order of ideas, we made four interactive σ -clipped. Once we have found the appropriate fitting for each magnitude bin, we identified those objects significantly above of this final fit as likely sources with a excesses of $H\alpha$. Objects with a significant contribution of $H\alpha$ meet the condition:

$$(r - J0660)_{\text{obs}} - (r - J0660)_{\text{fit}} \geq C \times \sqrt{\sigma_s^2 - \sigma_{\text{phot}}^2} \quad (1)$$

where σ_s is the root mean squared value of the residuals around the fit and σ_{phot} is the error on the observed $(r - J0660)$ colour index. C is a constant which has the value 4 following [Wevers et al.](#)

(2017). The fits are carried out with the aid of the python library `astropy.modeling`³.

Figure 2 illustrates the procedure used to selected the $H\alpha$ emitters in S-PLUS DR3 for each magnitude bin. The continuous black lines represent the initial fit and the dashed lines indicate the 4σ clipping fit lines. The dotted lines are the cut selection criteria for the $H\alpha$ emitters – the 4σ above of the final fit-. Note that theses cut lines are only an approximations because to trace them, it is only considered the residual around the fit. The actual selection criteria used here also include the photometric uncertainties in $r - J0660$ for each individual data source as shows on the Equation 1.

After the algorithm was applied to all data, we visually inspectioned the resulting list by seeing the S-spectra and corresponding colored image. The figure 3 shows an example of how looks like a S-spectra⁴ of sources in magnitude unities selected with methods explained above. This object clearly exhibits strong $H\alpha$ emitter.

Fig 4 exhibits the distribution of the emission on the $r - J0660$ versus $r - i$ color-color plane. At this point we can say that the algorithm implemented works well in selected objects with a excess in emission on the $J0660$ filter. It is possible to affirm that, because the identified objects are located above of the loci of the main and giant stars. The S-PLUS synthetic photometry of the stellar locus is represent by the contours in the diagram and was obtained by using the filter transmission profiles, shown in Fig. 1, and the library of stellar spectral energy distributions of [Pickles \(1998\)](#). This synthetic magnitudes were defined in the AB magnitude system ([Oke & Gunn 1983](#)). The wide distribution of fonts across the colors ($r - J060$) and ($r - i$) indicates that several types of objects were selected. For instance, higher values on the $r - J060$ color of some sources could be indicating that they are H II regions or/and blue compact galaxies and PNe. On the hand, the $r - i$ color indicates the rendered sources such as SySt and young stellar objects or source with strong blue continuum as cataclysm variables.

Fig. 5 displays the distribution of all emitters in Galactic longitude and latitude. The density map regions represent the spatial positions of the objects on the sky. The surface density of $J0660$ -excess objects is highest near the Galactic plane.

Once, we felt confident of our sample of $H\alpha$ emission lines sources, we proceeded to classify the objects into two big groups; one group containing those objects with a strong blue continuum and another with an intense emission of the continuum on the blue part of the spectrum.

3.3 Unsupervised machine learning/clustering techniques

In this work we are using unsupervised machine learning approaches to divided our sample in two groups: one represent the blue sources and the another one are the red sources. The blue are those that have strong emission of the continuum on the part blue of the spectra and the another with strong emission continuum of the red one. For that task, was implemented two clustering techniques; hierarchical clustering and Hierarchical density-based cluster selection based on the $(g - r)$ and $(z - g)$ colors.



Figure 2. An illustration of the selection criteria used to identify strong emission-line objects via colour-colour plots. The data shown here are all from the S-PLUS DR3. The data are split up into four magnitude bins, as shown in the four panels. Objects with H α excess should be located near the top of the colour-colour diagrams. The thin red lines illustrate the original linear fit to all the data (grey points). The dashed lines represent the final fits to the stellar locus of points which were obtained by applying an iterative σ -clipping technique to the initial fit. The actual cuts used to select H α emitters are shown by the dotted lines. Objects selected as H α emitters must be located above. Note that the cut lines (selection criteria) shown here are only approximate, as the actual selection criterion also considers the errors on each source. This means that an object could be in the bottom right-hand panel is not selected despite clearly lying above the cut line (EXPLICAR ESTA ÚLTIMA FRASE MEJOR).

3.3.1 $(g - r)$ versus $(z - g)$ color-color diagram

In order to find the best color-color diagram to separating the final sample of emission line objects into two color types, we first attempted constructed color-color diagrams by using the S-PLUS

simulated photometry of several classes of emission line objects⁵. The $(g - r)$ versus $(z - g)$ color-color diagram is displayed on the Fig. 6. The SySt span a wide range on the $(z - g)$ color, from approximately -0.5 to 6.0. This wide range on the color may refer to the different type spectral of the cold stellar component of the binary system. All the YSOs and many SySt are located on the top-left on the diagram indicating a reddening effect of the circumstellar disk

³ <https://docs.astropy.org/en/stable/modeling/index.html>

⁴ S-spectra signify the S-PLUS emission in flux or magnitude unities of an object in all twelve bands.

⁵ It is important to note that there are other classes of objects with emission lines that have not been included, because our main objective is to separate between two types of these objects by their photometric colors.

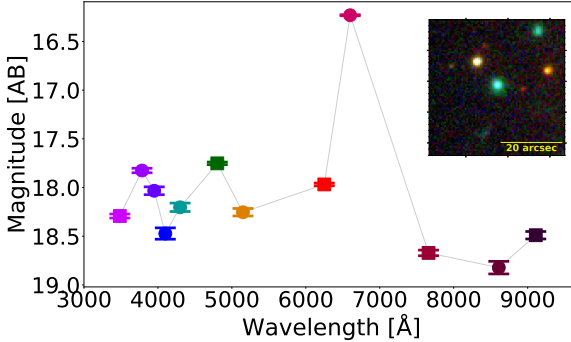


Figure 3. S-spectra of a random object with emission lines select with algorithm explained above. Squares represent the SDSS-like broad-band filters. From left to right they are u, g, r, i and z . Circle symbols are the narrow-band filters, which from left to right represent J0378, J0395, J0410, J0515, J0660 and J0861.

for many SySt (for example for those symbiotic with a Mira star) and YSOs. On the other hand, the PNe, HII regions, CVs, QSOs and emission line galaxies are located on the lower-right region in the diagram. This indicates blue continuum present in each classes of theses objects, mainly by the presence of the high excitation star, for instance, white dwarf in planetary nebulae and cataclysm variable stars and massive young stars in H II regions and the starburst galaxies. Although some SySt are located in the region where appear the blue sources, this color-color diagram seems to separate very well two color types, blue from red sources.

We constructed the $(g - r)$ versus $(z - g)$ color-color diagram using the photometry of our final list of H α emitters, which is presented in Fig. 7. As was we expected two-color population is showed in the diagram perceptible in the level of the color of the density region on which yellow areas represent a higher concentration of points. This is re-forced by the bi-modal shape of the $(g - r)$ and $(z - g)$ color distributions (see inset plots of the Fig. 7). The two peaks of the $(g - r)$ and $(z - g)$ distributions clearly correspond to blue and red sources, respectively. This histograms also show that the fraction of blue objects is considerable higher than the red ones.

3.3.2 Hierarchical agglomerative clustering

Hierarchical clustering belong to the family of clustering algorithms on which are constructed clusters by merging and splitting them successively. It is an unsupervised algorithm that yields a dendrogram⁶ represents the nested grouping of patterns and the levels of similarity at which the groupings change (Jain et al. 1999). There is two type of hierarchical clustering: one is the *hierarchical agglomerative clustering* (that we have used in this work) which is “bottom-up” approach. Hierarchical agglomerative clustering (HAC) consists of building a binary merge tree, starting from each data element stored at the leaves (interpreted as individual clusters) and proceed by merging two by two the “closest” sub-sets (stored at nodes) until it reaches the root -unique cluster- of the tree that contains all the elements of the data set. Agglomerative term is used to define it since the individual data point are successively agglomerated into higher-level. In each iteration, two cluster are selected that are considered as close as possible. These cluster are merged and replaced with a

⁶ Dendrogram is a diagram representing tree, which shows hierarchical relationship between objects.

newly created merged cluster. Thus, each merging step reduces the number of cluster by “1”. Therefore, the method needs to be designated for measuring proximity between cluster containing multiple data points, so that they may be merged (Mann & Kaur 2013; Aggarwal 2015). We could describe how to work the algorithm in three simple steps:

- (i) Initially, each data point represents the clusters i.e. leaves.
- (ii) It looping merges the nodes (clusters) that have the maximum similarity between them.
- (iii) At the end of the process all the nodes belong to an unique cluster. This is known as the root of the tree structure.

The other type is the *hierarchical divisive clustering*. This is a “top-down” approach. The data start in one cluster (the root of the tree), and splits step by step are performed recursively as one moves down the hierarchy. It is the inverse procedure of HAC.

In simple words, hierarchical clustering approaches can be interpreted as an algorithm that groups similar objects into groups called clusters or nodes. The endpoint is a set of clusters, where each cluster is distinct from each other cluster, and the objects within each cluster are broadly similar to each other.

Choosing the number of cluster. Firstly, the Hierarchical cluster output dendrogram (tree) can be implemented to obtain the desired clustering. Secondly, the dendrogram schema allows a convenient way to establish the entity relationship between at all levels of granularity. In conclusion, a dendrogram is a visualization in form of a tree showing the order and distances of merges during the hierarchical clustering.

- On the x axis you see labels. If you do not specify anything else they are the indices of your samples in X .
- On the y axis you see the distances (of the “ward” method in our case).

3.3.3 Dendrogram Truncation

As you might have noticed, the above is pretty big for many samples already and you probably have way more in real scenarios, so let me spend a few seconds on highlighting some other features of the dendrogram() function:

Starting from each label at the bottom, you can see a vertical line up to a horizontal line. The height of that horizontal line tells you about the distance at which this label was merged into another label or cluster. You can find that other cluster by following the other vertical line down again. If you don’t encounter another horizontal line, it was just merged with the other label you reach, otherwise it was merged into another cluster that was formed earlier.

Hierarchical clustering can be performed with either a distance matrix or raw data. When raw data is provided, the software will automatically compute a distance matrix in the background. The distance matrix below shows the distance between six objects.

Hierarchical clustering starts by treating each observation as a separate cluster. Then, it repeatedly executes the following two steps: (1) identify the two clusters that are closest together, and (2) merge the two most similar clusters. This iterative process continues until all the clusters are merged together. This is illustrated in the diagrams below.

Hierarchical clustering 2

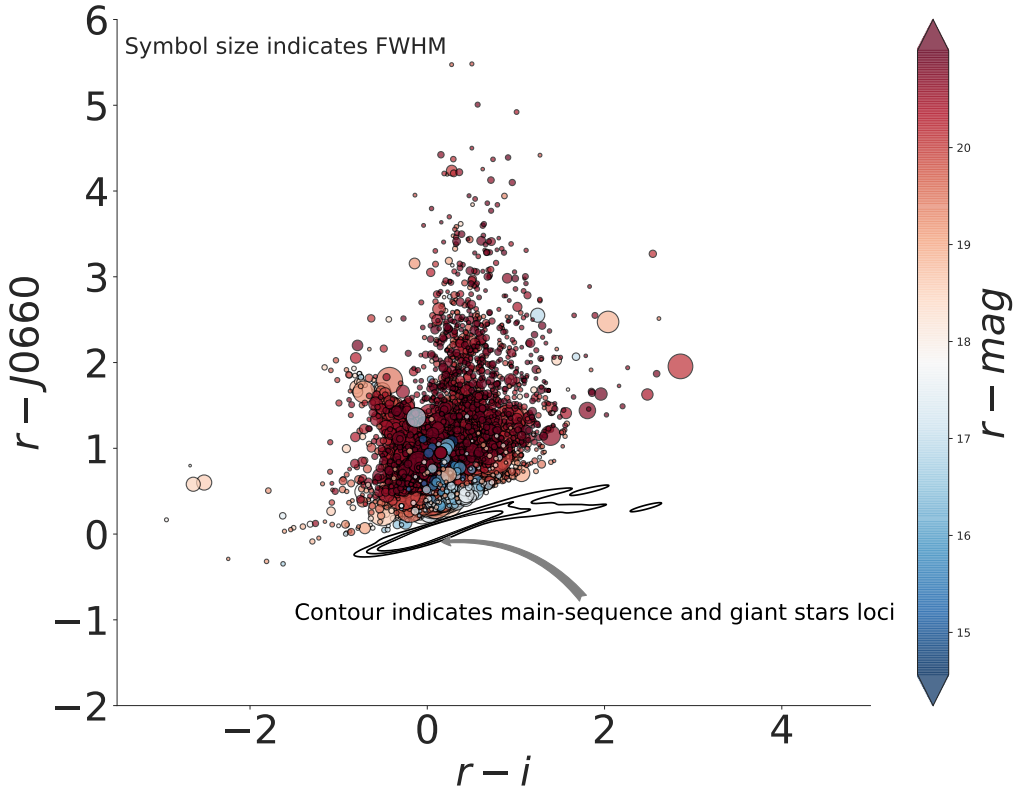


Figure 4. Colour-colour diagram with all the emission line objects selected from S-PLUS DR3. Size of the symbols represent the measured FWHM assuming a Gaussian core (for more detail see Almeida-Fernandes et al. 2021). Coloured bar indicates the magnitude values in the r-band. The contours represent the S-PLUS synthetic photometry of main-sequence and giant stars loci from the library of stellar spectral energy distributions of Pickles (1998).

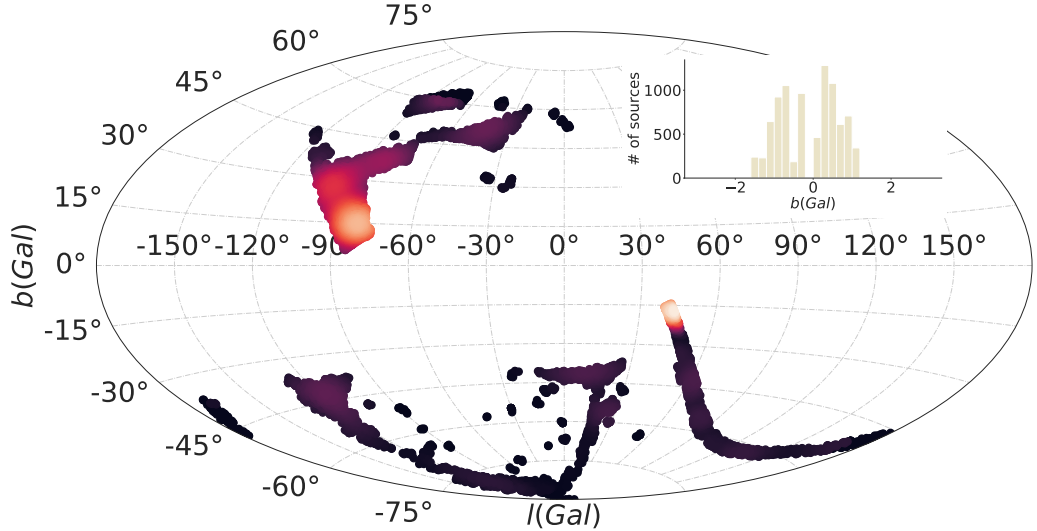


Figure 5. Distribution of H α emitters in Galactic longitude and latitude coordinate. Inset figure represents distribution of the objects in Galactic latitude.

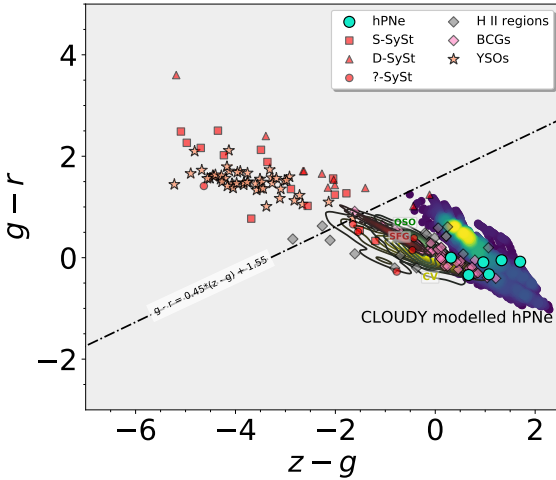


Figure 6. The $(g-r)$ versus $(z-g)$ synthetic color-color diagram of several classes of emission lines objects. Included in the diagrams, there are families of CLOUDY modelled halo PNe spanning a range of properties (density map region). Cyan circles represent S-PLUS photometry from observed spectra Grey diamonds represent H II regions in NGC 55. Red boxes display symbiotic stars, this group also includes Galactic and external SySt from NGC 205 IC 10 and NGC 185,. Yellow circles correspond to cataclysmic variables (CVs) from SDSS. Pink circles indicate blue compact galaxies (BCGs) from SDSS. Orange triangles refer to SDSS star-forming galaxies (SDSS SFGs). SDSS QSOs at different redshift ranges are shown as light blue diamonds, and YSOs from Lupus and Sigma Orionis are represented by salmon stars. The diagonal line represent a subjective criterion to separate the objects into two color types.

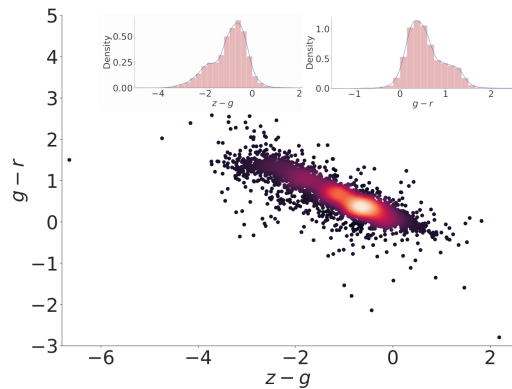


Figure 7. The $(g-r)$ versus $(z-g)$ color-color diagram with all the emission line objects selected in S-PLUS. The inset figures represent the $(g-r)$ and $(z-g)$ distributions.

3.3.4 Hierarchical density-based cluster selection

Hierarchical density-based cluster selection (HDBSCAN, Campello et al. 2013) is another unsupervised machine learning algorithm that hinges on clustering. It is based on a slightly modified version of Density-based Spatial Clustering of Applications with Noise (DBSCAN; Ester et al. 1996) which declare points as noise. It is a algorithm that assumes clusters are characterized by “islands” of high density in the sea of the parameter space, such that clusters are regarded as data partitions that have a higher density than their surroundings (Ntwaetsile & Geach 2021). HDBSCAN takes forward

the DBSCAN concept by introducing a hierarchy to the clustering, with “persistent” clusters finally extracted from the hierarchical tree. The main advantage of HDBSCAN in comparison with the predecessor consists in the possibility in finding clusters of variables densities and different shape. Following Malzer & Baum (2021) and Ntwaetsile & Geach (2021) works as follows:

(i) In HDBSCAN is consider the “core” distance for a point x , $\text{core}_k(x)$ which defines the distance of an object to the k th nearest neighbor that is an efficient way of measurement of density. Low values of $\text{core}_k(x)$ represents high density and vice-versa.

(ii) The “mutual readability distance” between two points a and b is defined as $d_m(a,b) = \min\{\text{core}_k(a), \text{core}_k(b), d(a,b)\}$, where $d(a,b)$ is the distance between a and b according, for instance, Euclidean metric. The mutual readability distance allows points in dense regions stay close together and those that are in less dense regions pushed away.

(iii) The mutual readability graph is used to construct the minimum spanning tree, and sorting its edges by the mutual readability distance results in a hierarchical tree structure. The hierarchy of connected components is defined by sorting the edges of the tree by distance in reverse order, describing a dendrogram. This is the structure from which cluster will be identified.

(iv) HDBSCAN allows to extract clusters of variable density, effectively by cutting the dendrogram at different points.

(v) The cluster tree is condensed into a simpler structure. Considering the single main trunk which contains all of the data points, the tree splits into branches. A condensed cluster hierarchy can be described by considering the number points kept in each branch as it splits. If a given branch splits into two, with a branch containing fewer points than the minimum cluster size means, the large branch “persists” and the smaller split branch “falls out” of the cluster. If a branch splits into two with both branches exceeding the minimum cluster size, both new branches persist.

(vi) The clusters are extracted on the notion of persistence in the hierarchy. The parameter $\lambda = d_m^{-1}$ is defined, and each cluster has a λ_{birth} (the point at which the cluster split off) and λ_{death} (the point when the cluster split into other clusters). In each cluster, we have λ_p describing when each point fell out of the cluster (or was split off into new cluster), $\lambda_{\text{birth}} \leq \lambda_p \leq \lambda_{\text{death}}$. Cluster stability S is defined as the sum of $\lambda_p - \lambda_{\text{birth}}$ for all points in the cluster. To extract cluster the following procedure is implemented: First, select all leaves as cluster. Then, working through the hierarchy, consider the stability of a parent cluster S_p and its n descendants $S_d^{0,1,2,\dots,n}$. If $S_p > \sum_{i=0}^n S_d^i$ we unselect all the descendants. If $S_p < \sum_{i=0}^n S_d^i$ then the cluster stability is set such that $S_p = \sum_{i=0}^n S_d^i$. At the root node we have our set of selected cluster. Any point in the sample that does not fall into one of the selected clusters is defined as noise.

(vii) The selected cluster are used the label points. Furthermore, the definition of λ_p within a cluster, when normalized between 0 and 1 provides a means of characterization a probability that a given point belongs to the cluster or alternative a measure of the strength of membership.

The algorithm starts off much the same as DBSCAN: we transform the space according to density, exactly as DBSCAN does, and perform single linkage clustering on the transformed space. Instead of taking an epsilon value as a cut level for the dendrogram however, a different approach is taken: the dendrogram is condensed by viewing splits that result in a small number of points splitting off as points “falling out of a cluster”. This results in a smaller tree with fewer clusters that “lose points”. That tree can then be used to se-

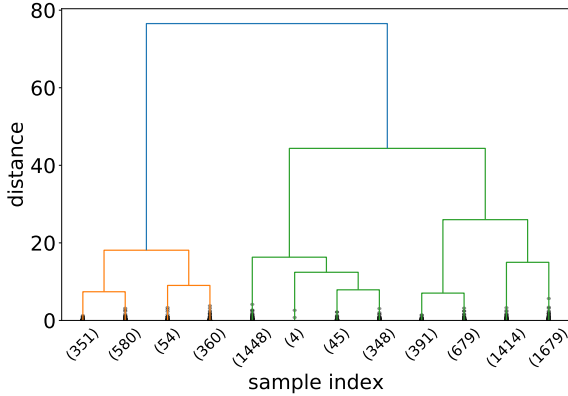


Figure 8. Customer dendrogram...

lect the most stable or persistent clusters. This process allows the tree to be cut at varying height, picking our varying density clusters based on cluster stability. The immediate advantage of this is that we can ave varying density clusters; the second benefit is that we have eliminated the epsilon parameter as we no longer need it to choose a cut of the dendrogram. Instead we have a new parameter `min_cluster_size` which is used to determine whether points are “falling out of a cluster” or splitting to form two new clusters. This trades an unintuitive parameter for one that is not so hard to choose for EDA (what is the minimum size cluster I am willing to care about?).

Hierarchical Density-Based Spatial Clustering of Applications with Noise (Campello, Moulavi, and Sander 2013), (Campello et al. 2015). Performs DBSCAN overvarying epsilon values and integrates the result to find a clustering that gives the best stability over epsilon. This allows HDBSCAN to find clusters of varying densities (unlike DBSCAN), and be more robust to parameter selection. The library also includes support for Robust Single Linkage clustering (Chaudhuri et al. 2014), (Chaudhuri and Dasgupta2010), GLOSS outlier detection (Campello et al. 2015), and tools for visualizing and exploring clusterer structures. Finally support for prediction and soft clustering is also available.

In the last years, HDBSCAN have been in astronomy for different tasks. Jayasinghe et al. (2019) presented the second data release Milky Way Project (MWP), a citizen science initiative on the Zooniverse platform, presents internet users with infrared (IR) images from Spitzer on which were aggregate ~ 3 million classifications made by volunteers during the years 2012-2017 to produce the DR2 catalogue, which contains 2600 IR bubbles and 599 candidate bow shock driving stars. The reliability of bubble identifications was made by using HDBSCAN. On the other hand, Webb et al. (2020) used HDBSCAN for transient discovery. Recently, Ntwaetsile & Geach (2021) used it to group radio sources into a sequence of morphological classes, illustrating a simple methodology to classify and label new, unseen galaxies in large samples.

3.4 Grouping the $\text{H}\alpha$ emitters into blue and red sources

3.4.1 HAC

In this work, we implemented HAC by using the python machine learning library Scikit-learn⁷ (Pedregosa et al. 2011). There are

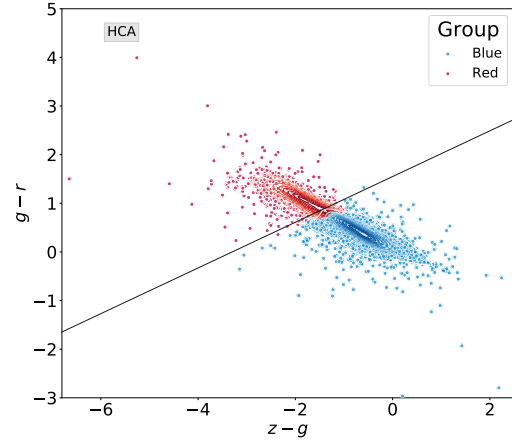


Figure 9. The $(g-r)$ versus $(z-g)$ color-color diagram with the two population found bi implementing HAC algorithm. The blue symbols represent the sources with intense blue continuum and the red symbols are the objects with intense red continuum.

some parameters to have in count when the algorithm is applied: `n_clusters` which is the number cluster to find. Given that our goal is to divide our sample in two groups we set this value in 2. `Affinity`, Metric used to compute the linkage. We found that a simple “Euclidean” distance metric was effective. `Linkage` which determines which distance to use between sets of observation. The algorithm merge the pairs of cluster that minimize this criterion. Here was implemented “ward” which minimizes the variance of the clusters being merged. As was mentioned, the input variables are the colors; $(g-r)$ and $(z-g)$.

Fig. 8 shows the dendrogram truncated diagram visualization that shows the branching of the sample from the main root. And Fig. 9 shows the position of the two groups that resulted after to applying HAC in the color-color diagram. The two clusters represent the blue sources (blue symbols) and red sources (blue symbols) as already by analyzing the diagram of the Fig. 6. Now, we have divided our list in two groups in agreement with the nature of their continuum. We found that the number of blue $\text{H}\alpha$ emitter is bigger than the red one.

3.4.2 HDBSCAN

We also used HDBSCAN to separate the blue sources from the red ones. This just for comparing the performance of two algorithms and show that the our resulted are consistent. We used the python implementation of HDBSCAN⁸ (McInnes et al. 2017). Like HAC, in addition to the colors input parameters, there are key parameters that should be considered when the algorithm is applied. “Euclidean” metric is implemented which results to be very efficient. The two most critical parameters to be implemented are the “minimum cluster size” and “minimum number of samples”. The former refers to the smallest size grouping that we wish to consider a cluster. We have adopted the value “80”. The latter provides a measure of how conservative we want our clustering to be and expressed as the fraction of data

⁷ <https://scikit-learn.org/stable/>

⁸ <https://hdbSCAN.readthedocs.io/en/latest/>

classified as noise. The value implemented was “40”. With this configuration of our model we found two cluster. If we use values of minimum number of samples smaller than “40” several small cluster are found that do not make sense.

Left panel of Fig 10 the resulted cluster found with HDBSCAN. Two group are found and these results are consistent with results found with HAC. In fact, by applying the `condensed_tree_` to the data colors two clusters are selected (for more detail about `condensed_tree_` attribute see appendix A and related Fig. A1). The two primary clusters are located in the same region in the $(g-r)$ versus $(z-g)$ color-color diagram where lie the group found by the other algorithm. The main difference between the two algorithm is that HDBSCAN is much conservative, then many data points are classified as noise. The two final cluster contain, which we are labeled blue and red sources contain xxx and xxx objects, respectively.

3.5 Soft clustering for HDBSCAN

Perhaps, the main disadvantage of HDBSCAN is that many of the sources are labelled as “noise”, on which some sources are not assigned to any cluster. As was mentioned, this comes from the conservative nature of HDBSCAN and that they are located far away of the cluster cores. An alternative to avoid the outlier classification consists in used the concept of “soft clustering”. We have carried out here soft clustering for HDBSCAN to assign every object to its most likely cluster. This means that with this approach, points are not assigned cluster labels, instead are assigned a vector of probabilities. The probability value at the i th entry of the vector is the probability that a data point is a member of the i th cluster. We can then simply assign cluster labels for every point by taking the most likely cluster it belongs to, using probability thresholds. Soft clustering for HDBSCAN is based on the Global-Local Outlier Score from Hierarchies (GLOSH) algorithm (Campello et al. 2015) and combines this with a measure of distance from a given cluster to produce an estimate of the probability that any given data point belongs to any of the fixed clusters extracted from the condensed tree.

The right panel of Fig. 10 shows at what most likely cluster belongs the data points classified as the noise by HDBSCAN. We have used blue and red colors for the points that have the highest probability of being in the blue and red groups, respectively. This fills out the clusters nicely. We see that there were many noise points that are most likely to belong to the clusters we would expect, e. g. in agreement we the results obtained with HAC. Indeed, We now have improved our classification of our list into sources with blue and red continuum because we have estimated the probability of each source to belong to every group.

4 RESULTS AND DISCUSSION

We found a total of 389 emission line sources in all S-PLUS DR3. To understand the nature of the objects and the fractional contribution of different classes of objects with emission lines to the overall sample cross-matching with some catalogs available were carried out.

4.1 Simbad

We made cross-match between our sample of objects with a excess of emission of the J0660 and SIMBAD. We searched for all objects in SIMBAD using a radius of 2 arcsec around the position of the optical source in question. We found 1000 matches that include a great

variety of emission line objects. In table 1 is showed the different categories of objects found in SIMBAD.

4.1.1 Nebulae

As was mentioned, objects with nebulosity include several types of objects such as H II region and planetary nebulae. The H II regions are objects with gas that being ionized by amounts of UV light come from massive stars (OB type) on which are formed the emission lines. In these clouds of ionized gas, new stars are formed. Unlike H II regions, planetary nebulae represent the final stages of low- and intermediate-mass stars where the gas previously ejected in the phase of AGB is ionized by the high energetic radiation come from their central stars.

In our list of H α emission line a PN appears cataloged in SIMBAD on which the S-PLUS photometry and spectrum is displayed on panel (a) of Fig 11. Emission lines like H α and [N II] are clearly perceptible in its spectrum, agreeing with PLUS photometry. This objects is a very interesting because is one of the twelves PNe that belong to the Galactic halo. These PNe are low metallizite and present large velocities that can give count of the origin and nucleosynthesis of the early universe. 30 objects cataloged as HII regions on the SIMBAD database are in our list of H α emitters. Panel (b) of the figure shows the S-PLUS photometry and SDSS spectrum of the extragalactic HII region GALEX 2417063145906373262.

4.1.2 Binary systems

25 known CVs and 5 candidate CVs (from SIMBAD) were selected with algorithm. CVs are binary systems of very short orbital period, in which a low-mass and early-type star fills its Roche region and transfers mass to a companion stars, a dwarf white (Patterson 1984). Fig. 11 the S-PLUS photometry overlapped to the SDSS spectrum of the CV FASTT 1560. As expected, this object was classified as blue source by the machine learning approaches. Other binary system in our list are the X-binary sources, eclipsing binary, variable stars of RR Lyr type.

4.1.3 Stars

Several stars were selected as shows the matches with SIMBAD. The SIMBAD types include normal stars, white dwarf stars (WD*), white dwarf candidates (Candidate_WD*), blue stars, blue supergiant stars (BlueSG*), high proper-motion stars (PM*) and low-mass star (low-mass*, M<1M $_{\odot}$). All these objects appears in the S-PLUS catalog as H α emitters. Some of them can be early/late-type emission-line stars and/or different types of stars with the H α emission lines. Although some of these stars could represent the fraction of contaminant of our sample.

4.1.4 Galaxies

Several type of emission line galaxies were selected. This category include several class of galaxies according to SIMBAD class: emission-line galaxy (EmG), blue compact galaxy (BlueCompG), HII galaxy (HII G), galaxy in cluster of galaxies (GinCl), galaxy in group of galaxies (GinGroup), low surface brightness galaxy (LSB G), interacting galaxies (IG), part of a Galaxy (PartofG), Seyfert 1 and Seyfert 2 galaxies, AGN and galaxy.

All the emission line galaxies of these category form part of the universe local. This mean that their redshift cover the range on which

Table 1. A summary of the results obtained of the positional cross-match between the S-PLUS list of emission line objects and the SIMBAD database. We used a search radius of 2 arcsec.

Main type	Associated SIMBAD types	Number of S-PLUS objects with SIMBAD match
H II region	HII	26
Planetary nebula	PN	1
Supernova	SN, Candidate_SN*	9
Nova	Nova	1
Cataclysmic variable star	CataclyV*, Candidate_CV*	30
Variable star of RR Lyr type	RRLyr, Candidate_RRLyr	19
X-ray source	HMXB, X	6
Eclipsing binary	EB*	8
BL Lac - type object	BLLac	2
Emission object	EmObj	4
Star	star, WD*, Candidate_WD*, Blue, BlueSG*, PM*, low-mass*	57
UV-emission source	UV	2
Cluster of stars	Cl*	3
Far-infrared source	FIR	2
Mid-infrared source	MIR	1
Radio-source	Radio	7
Molecular cloud	MolCld	2
Emission line galaxy	EmG, HII_G, StarburstG, BlueCompG	102
Part of a galaxy	PartofG	9
Interacting galaxies	IG	10
Radio galaxy	RadioG	2
Galaxy in pair of galaxies	GinPair	12
Galaxy in group of galaxies	GinGroup	18
Galaxy in cluster of galaxies	GinCl	23
Low surface brightness galaxy	LSB_G	10
Brightest galaxy in a cluster	BCIG	3
Globular cluster	GICl	1
QSO	QSO, QSO_Candidate	225
AGN	AGN, AGN_Candidate	18
Seyfert 1	Seyfert_1	38
Seyfert 2	Seyfert_2	7
Galaxy	Galaxy	421
Possible gravitationally lensed image	Possible_lensImage	1
Total		10

the H α emission line still falls into the $J0660$ filter. Objects with $z > 0.02$ the H α is outside of the $J0660$ filter. Table B1 of the appendices shows the red-shift of the emission line galaxies of our sample that have SIMBAD matches, probing that mostly of these galaxies are real H α emitters. In these kind of galaxies such as the blue compact and/or H II galaxies their starburst regions that consist of ensemble of massive ionizing stars and their respective giant H II regions cover the extension of the optical images and the emission lines of their spectra.

On the other hand, several AGN, Seyfert 1 and Seyfert 2 galaxies have red-shift between 0.31 and 0.37 indicating that the excess on the $J0660$ filter is not due to the H α emission but if due to the H β and [O III] 4959, 5007 Å emission lines. These emission lines at the red-shift range $0.306 < z < 0.376$ are detected in the $J0660$ band. It is well known that the AGNs have very strong emission lines such as H β , [O III] 4959, 5007 Å and H α .

One interesting discussion here, is that the type part of a Galaxy (PartofG) on SIMBAD are actually galaxies with Wolf-Rayet (WR) signature in the low red shift universe also named “WR galaxy” ([Osterbrock & Cohen 1982](#)). WR stars in galaxies is perceptible in their spectra with strong emission lines such as H α and [NII]. These spectral features can be of them very similar to extragalactic H II regions present typically of the outskirt of spiral galaxies. Panel (e) of

Fig. 11 displays the S-PLUS and SDSS spectra of the Wolf-Rayet [BKD2008] WR 14 which belong to the galaxy nnnnn.

Many of the objects have as main type “galaxy” in SIMBAD. This galaxies could be spiral galaxies on which the star formation is present. It is known that in the spiral arms of the galaxies are present H II regions as well as neutral gas (H I) and molecular gas. Actually some of these galaxies haves for secondary type H I. The reservoir of H I gas in galaxies must ultimately feed their star formation, after cooling and forming molecular clouds ([van Driel et al. 2016](#)). Fig. shows the S-PLUS photometry and the SDSS spectra of star-forming galaxy with clearly emission lines. Note that almost all these galaxies are classified as blue color type objects by the HAC and HDBSCAN. However, Mostly of the Seyfert 2 galaxies and a handful of galaxies are classified as red sources, why?

4.1.5 QSOs

Other extragalactic objects with emission lines that were selected are the QSOs. In the case of the QSOs is not the H α emission line who impact on the $J0660$ filter. This filter is affected by strong emission lines present in these objects that to specific redshift drop into the $J0660$ filter. Some of these emission lines are H β , C IV 1550 Å, C III] 1909 Å, Mg II 2798 Å (see, also [Gutiérrez-Soto et al. 2020](#);

Nakazono et al. 2021). All the objects were classified as blue sources which was the expected. Fig. show the S-PLUS photometry and SDSS spectrum of the QSO 2SLAQ J220529.34-003110.6 which has red-shift of ~ 2.45 indicating that the emission line corresponds to the line C III].

4.1.6 Other type of objects

Miscellanies the objects were selected on which are include as it can see in the table 1. They include FIR sources, MIR objects, molecular clouds,

4.2 SDSS and LAMOST

We also made cross-match between the sample of H α emission line objects and SDSS DR16 (Ahumada et al. 2020). We used use the 2σ error circle as the cross-matching radius. We got 200 spectra from which 195 objects exhibit strong emission lines. 5 objects do not show emission lines, they probably are stars or galaxies.

We also cross-correlate our list with Large Sky Area Multi-Object Fiber Spectroscopic Telescope (LAMOST; Wu et al. 2011) using a radius of 2 arcsec for the match. These spectra also show strong emission lines. These results shows that this technique actually are very effective for selecting sources with strong emission lines.

4.3 Magnitudes and color distributions

Fig. 13 shows the magnitude and color distribution of the blue and red sources –classification performed with machine learning on Section 3.3–. Upper panel of the figure shows the distribution of the blue and red sources of the r magnitude. The peaks of the r distribution is the same for the blue and red sources, which is around $r \sim 19.9$. However, the density at the peak is higher in red sources than the blue ones indicating that the proportion of objects with value r of 19.9 is higher than the blue sources. The fraction of object is very small at $r < 16$ for each group of objects. The distribution of the objects for both group increase in the range $16 \geq r \geq 19.9$. However the density as indicating the Kernel density estimation curves is higher in the blue sources. This implies that the fraction of sources with the magnitude range is considerable higher in comparison with the red group. In conclusion the blue sources tends to be brighter than the red ones.

Middle panel of figure displays the $(r - i)$ distribution of the blue and red emission line objects. The peaks of the $(r - i)$ distributions are distinct for the blue and red sources. The peaks of the red sources at high red continuum, $(r - i) = 0.5$, compared to the value of the blue sample, $(r - i) = -0.9$. All these results are consistent because the $(r - i)$ color is an indicating of reddened sources. This is also consistent with previous works. For instance, Wevers et al. (2017) used different algorithms based on the $(r - i)$ color to successfully select blue outliers from the the Galactic Bulge Survey (GBS; Jonker et al. 2011).

Botton panel of Fig. 13 shows the $(r - J0660)$ color distribution of the blue and red objects. The fraction of objects selected as emitter rises drastically with $J0660$ excess, until at sufficiently large excesses. The peaks of the $(r - J0660)$ color distribution are relatively different for both groups of sources. Having the blue sources the peaks at $(r - J0660) = 0.5$ while for the red one the value peak is $(r - J0660) = 0.7$.

5 CONCLUSIONS

We have created an usefully and important sample of emission line objects. By identifying the locus of main-sequence and giant star and considering as $J0660$ -excess the objects that above of the locus, we have found the emission line sources in S-PLUS DR3. In agreement with the results after to find the coincidences with SIMBAD several type of emission objects are included in our list which including nebulae, binary systems, stars, emission line galaxies, quasars, globular clusters among other.

We also found that using the colors $g - r$ and $(z - g)$ is very efficient to separate the blue sources from the red ones.

We also found that using this colors as the input to implement unsupervised machine learning in better to group the source in the red or blue sources.

ACKNOWLEDGEMENTS

The S-PLUS project, including the T80-South robotic telescope and the S-PLUS scientific survey, was founded as a partnership between the Fundação de Amparo à Pesquisa do Estado de São Paulo (FAPESP), the Observatório Nacional (ON), the Federal University of Sergipe (UFS), and the Federal University of Santa Catarina (UFSC), with important financial and practical contributions from other collaborating institutes in Brazil, Chile (Universidad de La Serena), and Spain (Centro de Estudios de Física del Cosmos de Aragón, CEFCA). We further acknowledge financial support from the São Paulo Research Foundation (FAPESP), the Brazilian National Research Council (CNPq), the Coordination for the Improvement of Higher Education Personnel (CAPES), the Carlos Chagas Filho Rio de Janeiro State Research Foundation (FAPERJ), and the Brazilian Innovation Agency (FINEP).

Funding for the SDSS and SDSS-II has been provided by the Alfred P. Sloan Foundation, the Participating Institutions, the National Science Foundation, the U.S. Department of Energy, the National Aeronautics and Space Administration, the Japanese Monbukagakusho, the Max Planck Society, and the Higher Education Funding Council for England. The SDSS Web Site is <http://www.sdss.org/>.

The SDSS is managed by the Astrophysical Research Consortium for the Participating Institutions. The Participating Institutions are the American Museum of Natural History, Astrophysical Institute Potsdam, University of Basel, University of Cambridge, Case Western Reserve University, University of Chicago, Drexel University, Fermilab, the Institute for Advanced Study, the Japan Participation Group, Johns Hopkins University, the Joint Institute for Nuclear Astrophysics, the Kavli Institute for Particle Astrophysics and Cosmology, the Korean Scientist Group, the Chinese Academy of Sciences (LAMOST), Los Alamos National Laboratory, the Max-Planck-Institute for Astronomy (MPIA), the Max-Planck-Institute for Astrophysics (MPA), New Mexico State University, Ohio State University, University of Pittsburgh, University of Portsmouth, Princeton University, the United States Naval Observatory, and the University of Washington.

Guoshoujing Telescope (the Large Sky Area Multi-Object Fiber Spectroscopic Telescope LAMOST) is a National Major Scientific Project built by the Chinese Academy of Sciences. Funding for the project has been provided by the National Development and Reform Commission. LAMOST is operated and managed by the National Astronomical Observatories, Chinese Academy of Sciences.

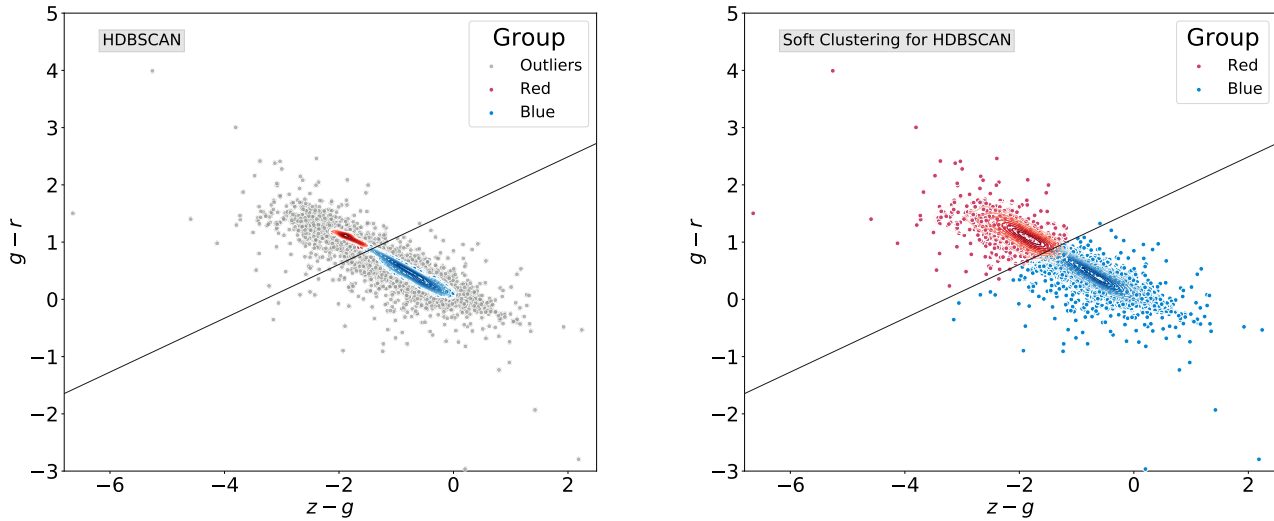


Figure 10. ($r - g$) versus ($g - z$) color-color diagram to separate the blue objects from the red ones.

DATA AVAILABILITY

REFERENCES

- Aggarwal C. C., 2015, Data Mining: The Textbook. Springer, Cham, doi:[10.1007/978-3-319-14142-8](https://doi.org/10.1007/978-3-319-14142-8)
- Ahumada R., et al., 2020, *ApJS*, **249**, 3
- Akras S., Guzman-Ramirez L., Gonçalves D. R., 2019, *MNRAS*, **488**, 3238
- Akras S., Guzman-Ramirez L., Leal-Ferreira M., Ramos-Larios G., 2019a, *ApJS*, **240**, 21
- Almeida-Fernandes F., et al., 2021, arXiv e-prints, p. [arXiv:2104.00020](https://arxiv.org/abs/2104.00020)
- Barentsen G., et al., 2014, *MNRAS*, **444**, 3230
- Campello R. J. G. B., Moulavi D., Sander J., 2013, in Pei J., Tseng V. S., Cao L., Motoda H., Xu G., eds, Advances in Knowledge Discovery and Data Mining. Springer Berlin Heidelberg, Berlin, Heidelberg, pp 160–172
- Campello R., Moulavi D., Zimek A., Sander J., 2015, *ACM Transactions on Knowledge Discovery from Data*, **10**, 1
- Casares J., 2015, *ApJ*, **808**, 80
- Casares J., 2016, *ApJ*, **822**, 99
- Cenarro A. J., et al., 2018, preprint, ([arXiv:1804.02667](https://arxiv.org/abs/1804.02667))
- Corradi R. L. M., Giannanco C., 2010, *A&A*, **520**, A99
- Corradi R. L. M., et al., 2008, *A&A*, **480**, 409
- Corradi R. L. M., Sabin L., Munari U., Cetrulo G., Englano A., Angeloni R., Greimel R., Mampaso A., 2011, *A&A*, **529**, A56
- Drew J. E., et al., 2005, *MNRAS*, **362**, 753
- Drew J. E., Greimel R., Irwin M. J., Sale S. E., 2008, *MNRAS*, **386**, 1761
- Drew J. E., et al., 2014, *MNRAS*, **440**, 2036
- Ester M., Kriegel H.-P., Sander J., Xu X., 1996, in Proc. of 2nd International Conference on Knowledge Discovery and Data Mining (KDD-96). pp 226–231
- Fukugita M., Ichikawa T., Gunn J. E., Doi M., Shimasaku K., Schneider D. P., 1996, *AJ*, **111**, 1748
- Geach J. E., 2012, *MNRAS*, **419**, 2633
- Gutiérrez-Soto L. A., et al., 2020, *A&A*, **633**, A123
- Horne K., Marsh T. R., 1986, *MNRAS*, **218**, 761
- Jain A. K., Murty M. N., Flynn P. J., 1999, *ACM Comput. Surv.*, **31**, 264
- Jayasinghe T., et al., 2019, *MNRAS*, **488**, 1141
- Jonker P. G., et al., 2011, *ApJS*, **194**, 18
- Malzer C., Baum M., 2021, *Sensors*, 21
- Mann A., Kaur N., 2013.
- Marín-Franch A., et al., 2012, in Navarro R., Cunningham C. R., Prieto E., eds, Society of Photo-Optical Instrumentation Engineers (SPIE) Conference Series Vol. 8450, Modern Technologies in Space- and Ground-based Telescopes and Instrumentation II. p. 84503S, doi:[10.1117/12.925430](https://doi.org/10.1117/12.925430)
- Martin G., Kaviraj S., Hocking A., Read S. C., Geach J. E., 2020, *MNRAS*, **491**, 1408
- McInnes L., Healy J., Astels S., 2017, *The Journal of Open Source Software*, **2**
- Mendes de Oliveira C., et al., 2019, *MNRAS*, **489**, 241
- Nakazono L., et al., 2021, *MNRAS*,
- Ntwaetsile K., Geach J. E., 2021, *MNRAS*, **502**, 3417
- Oke J. B., Gunn J. E., 1983, *ApJ*, **266**, 713
- Osterbrock D. E., Cohen R. D., 1982, *ApJ*, **261**, 64
- Osterbrock D. E., Ferland G. J., 2006, Astrophysics Of Gas Nebulae and Active Galactic Nuclei. Sausalito: University Science Books, <https://books.google.com.br/books?id=HgfrkDjBD98C>
- Parker Q. A., Bojićić I. S., Frew D. J., 2016, in Journal of Physics Conference Series. p. 032008 ([arXiv:1603.07042](https://arxiv.org/abs/1603.07042)), doi:[10.1088/1742-6596/728/3/032008](https://doi.org/10.1088/1742-6596/728/3/032008)
- Patterson J., 1984, *ApJS*, **54**, 443
- Pedregosa F., et al., 2011, *Journal of Machine Learning Research*, **12**, 2825
- Pickles A. J., 1998, *PASP*, **110**, 863
- Ratti E. M., Steeghs D. T. H., Jonker P. G., Torres M. A. P., Bassa C. G., Verbunt F., 2012, *MNRAS*, **420**, 75
- Sabin L., Zijlstra A. A., Wareing C., Corradi R. L. M., Mampaso A., Viironen K., Wright N. J., Parker Q. A., 2010, *Publ. Astron. Soc. Australia*, **27**, 166
- Scaringi S., Groot P. J., Verbeek K., Greiss S., Knigge C., Körding E., 2013, *MNRAS*, **428**, 2207
- Schwope A. D., Catalán M. S., Beuermann K., Metzner A., Smith R. C., Steeghs D., 2000, *MNRAS*, **313**, 533
- Steeghs D., Casares J., 2002, *ApJ*, **568**, 273
- Valenzuela L., Pichara K., 2018, *MNRAS*, **474**, 3259
- Viironen K., et al., 2009, *A&A*, **502**, 113
- Vink J. S., Drew J. E., Steeghs D., Wright N. J., Martin E. L., Gänsicke B. T., Greimel R., Drake J., 2008, *MNRAS*, **387**, 308

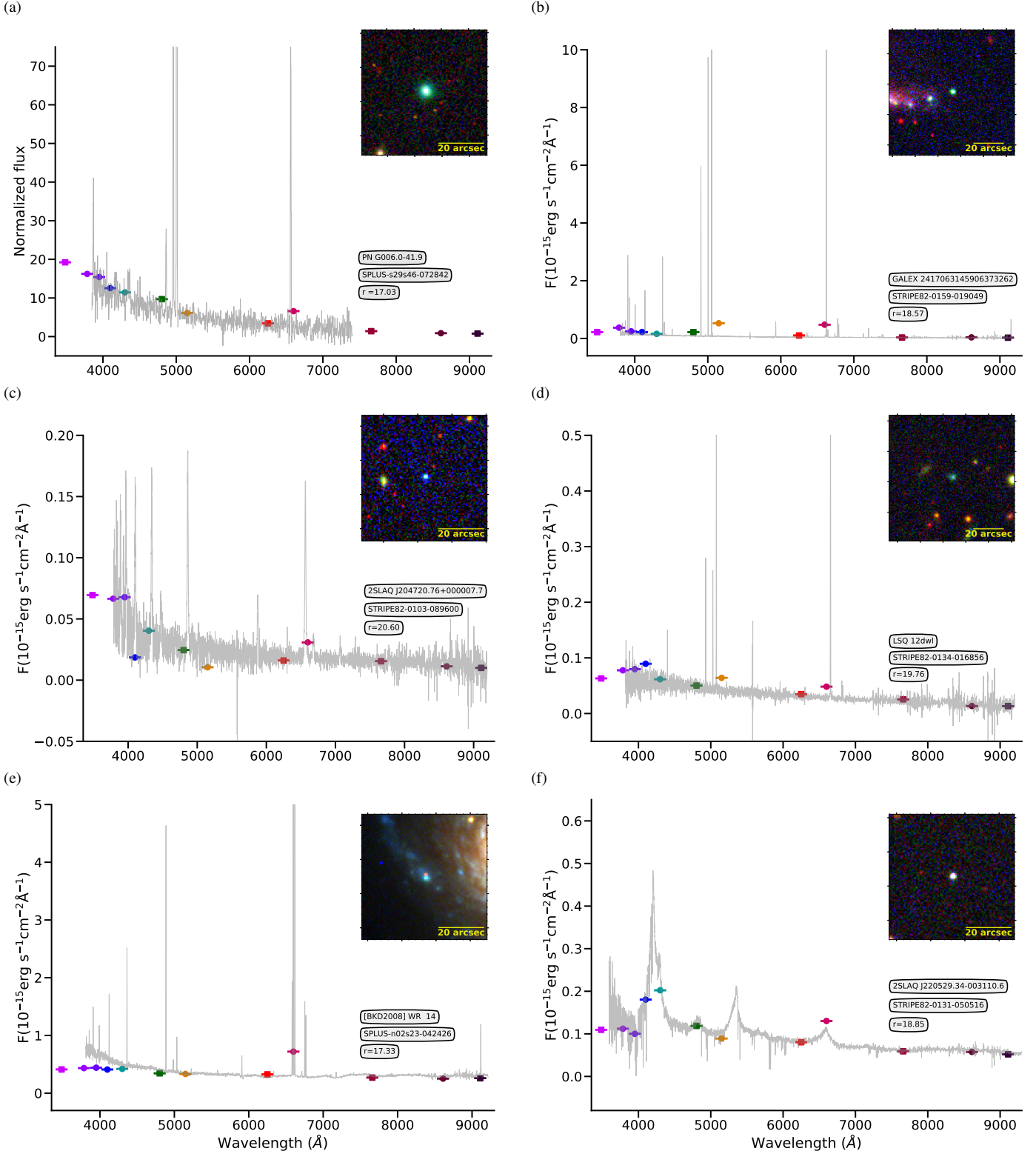


Figure 11. Summary of our selection results showing the spectrum (gray line in each panel) of different classes of emission line sources identified in our target list. A spectrum of a PN (a) from REF. The SDSS spectra of an external H II region (b), a cataclysmic variable star (c), a super nova (d), a WR in a galaxy (e) and a QSO (f) with red-shift of ~ 2.45 . As in Figure 3, coloured square and circles symbols represent the S-PLUS photometry. All these objects show a significance excesses on the $J0660$ filter in comparison with the broad-bands.

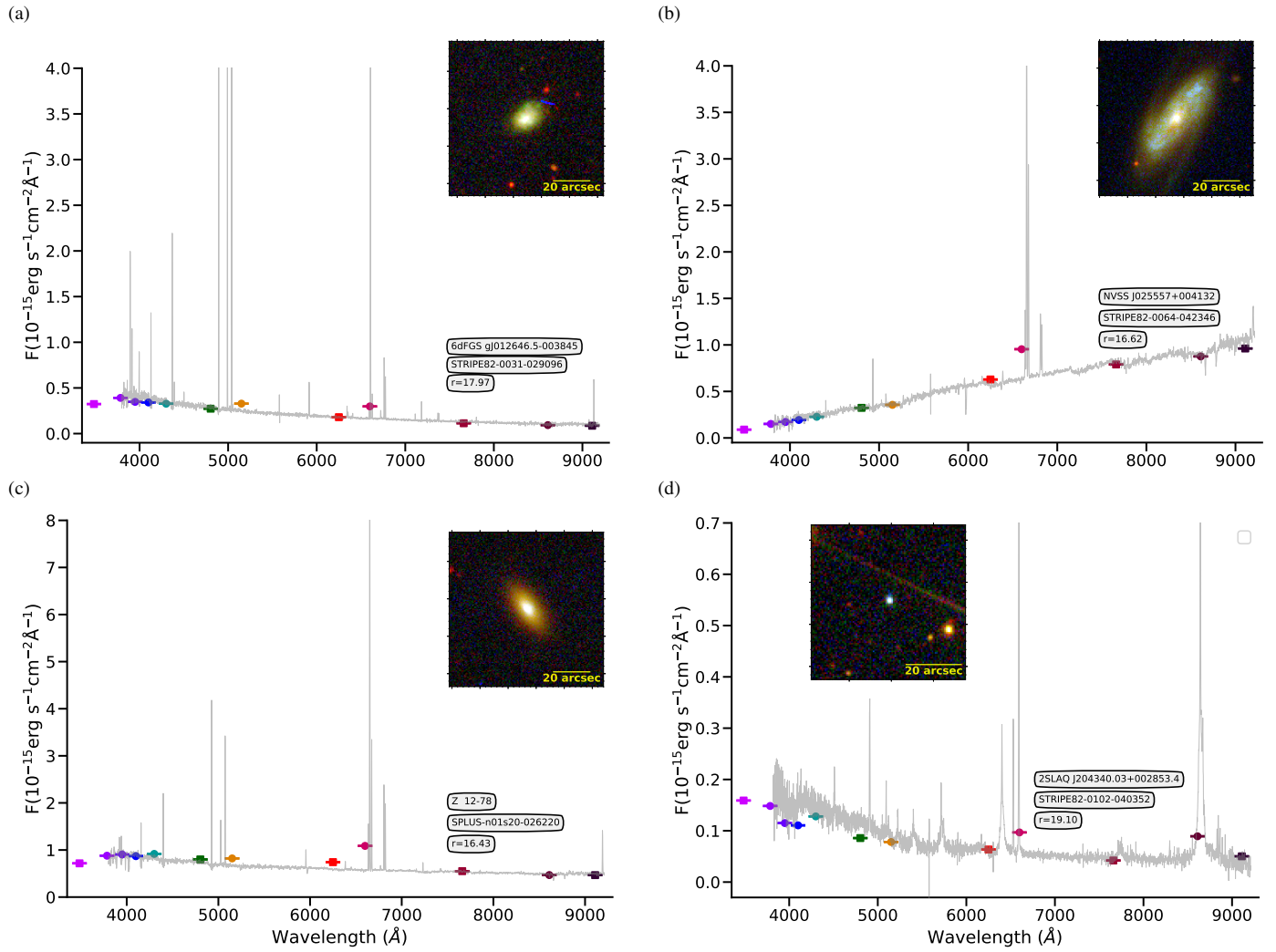


Figure 12. SDSS spectra of a H II galaxy with $z = 0.006$ (a), a radio galaxy with $z = 0.014$ (b), a star-forming galaxy with $z = 0.013$ (c). For this object, the H α line is responsible for the J0660 magnitude. And a Seyfert 1 with $z = 0.317$ (d). For this last object, the excess on the J0660 is due to the [O III] 4959, 5007 \AA emission lines (d). As in Figure 11 coloured symbols indicate the S-PLUS photometry.

- Webb S., et al., 2020, *MNRAS*, **498**, 3077
 Wevers T., et al., 2017, *MNRAS*, **466**, 163
 Witham A. R., et al., 2006, *MNRAS*, **369**, 581
 Witham A. R., et al., 2007, *MNRAS*, **382**, 1158
 Witham A. R., Knigge C., Drew J. E., Greimel R., Steeghs D., Gänsicke B. T., Groot P. J., Mampaso A., 2008, *MNRAS*, **384**, 1277
 Wu Y., et al., 2011, *Research in Astronomy and Astrophysics*, **11**, 924
 van Driel W., et al., 2016, *A&A*, **595**, A118
 van Spaandonk L., Steeghs D., Marsh T. R., Torres M. A. P., 2010, *MNRAS*, **401**, 1857

APPENDIX B: SIMBAD OBJECTS

APPENDIX A: CONDENSED TREES

The question now is what does the cluster hierarchy look like - which clusters are near each other, or could perhaps be merged, and which are far apart. We can access the basic hierarchy via the `condensed_tree_` attribute of the `clusterer` object. It is possible to see that HDBSCAN has found two cluster that in agreement with previous results are the blue and red sources.

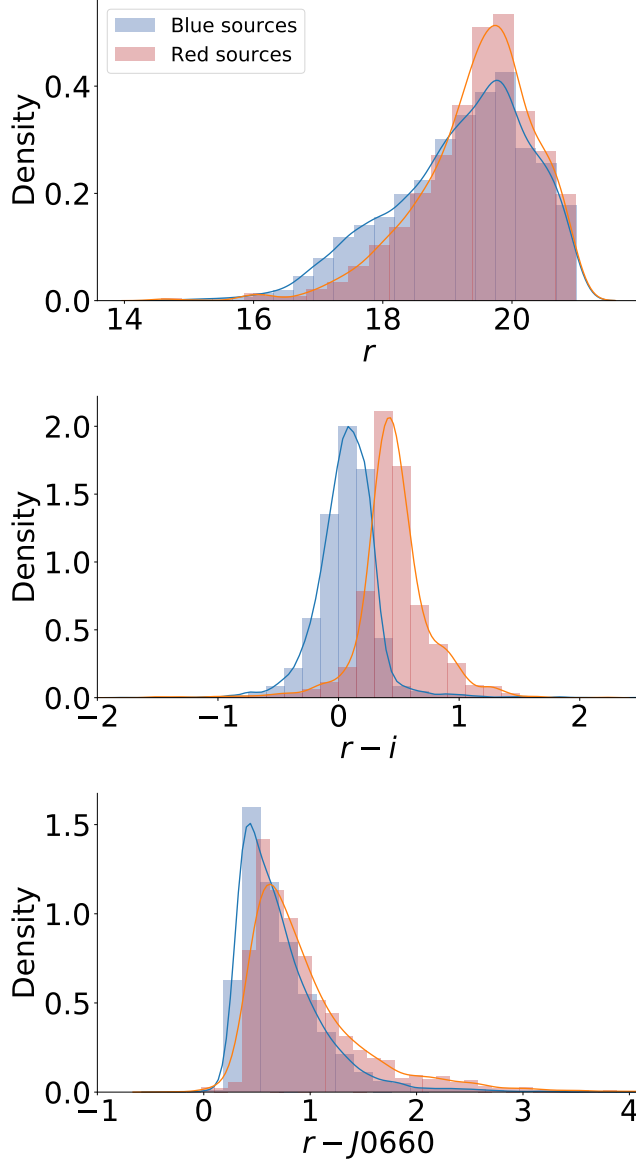


Figure 13. Distribution of r magnitude (left panel), $(r-i)$ color (middle panel), and $(r-J0660)$ color (right panel) for the blue and red sources of the sample of H α emitters. Both sample are normalized to their maximum counts, xx and xx objects for blue and red sources, respectively. The smooth curves represent a Kernel density estimation for both samples.

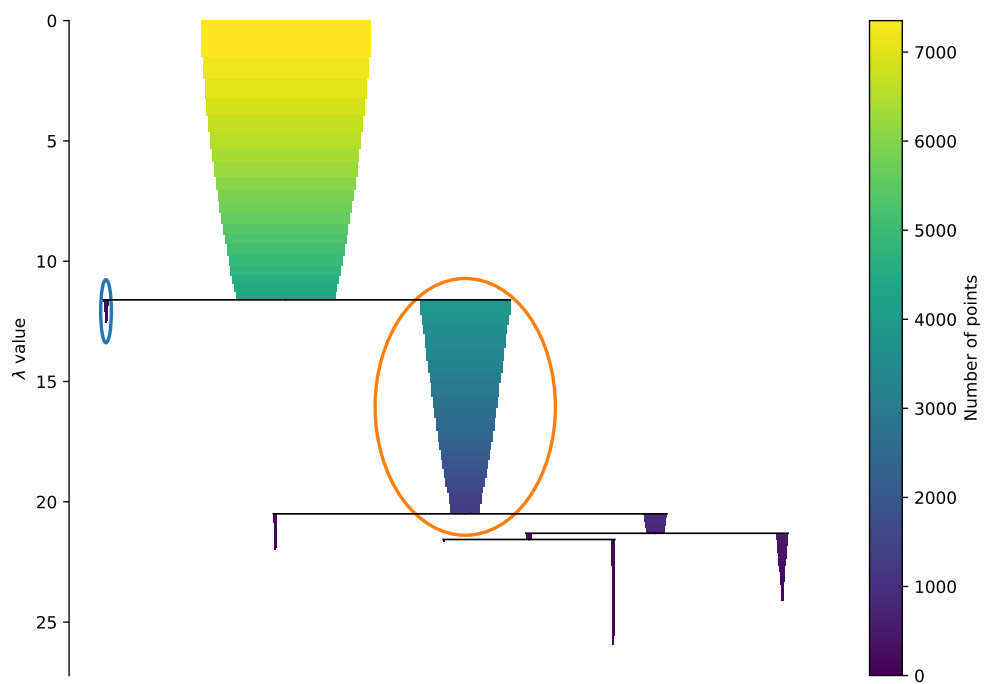


Figure A1. Branches were selected by the HDBSCAN* algorithm.

Table B1: Simbad sources.

Id Object	RA	Dec	Type	Redshift	Group	P(Blue)	P(Red)
						HAC	HDBSCAN
CTLGD 9478	00:01:59.25	-29:18:40.4	Star	–	Blue	0.98	0.02
QSO B2359+005	00:02:30.71	00:49:59.2	QSO	1.354	Blue	0.74	0.08
[GMB2011] 1808	00:02:47.58	-00:22:23.5	CIG	0.351	–	–	–
CTLGD 2037	00:05:08.77	-30:51:04.2	Star	–	Red	0.15	0.73
SDSS J000637.99-003656.2	00:06:37.99	-00:36:56.2	QSO	4.435	–	–	–
LBQS 0004+0036	00:07:10.00	00:53:29.1	QSO	0.316	Blue	0.61	0.11
SDSS J000809.34+004935.5	00:08:09.34	00:49:35.3	QSO	3.293	–	–	–
2SLAQ J000918.74-003907.2	00:09:18.76	-00:39:07.0	Galaxy	–	Blue	0.71	0.07
[VV2006] J001040.1-294428	00:10:40.08	-29:44:27.3	QSO	1.361	Blue	0.71	0.14
CTLGD 7291	00:10:48.73	-29:47:28.8	Star	–	Red	0.29	0.35
2QZ J001055.3-304423	00:10:55.37	-30:44:23.5	Galaxy	0.307	Blue	0.58	0.07
[VV2006] J001228.8-310241	00:12:28.78	-31:02:40.0	QSO	1.360	Blue	0.49	0.07
LBQS 0010+0035	00:13:27.32	00:52:32.2	Seyfert 1	0.363	Blue	0.77	0.08
[GPM2009] J0014-0044 2	00:14:28.79	-00:44:43.8	EmG	0.014	Blue	0.15	0.06
2SLAQ J001455.99+001903.5	00:14:55.99	00:19:03.7	Star	–	Blue	0.79	0.07
2SLAQ J001526.52+001813.2	00:15:26.52	00:18:13.4	QSO	1.362	Blue	0.51	0.09
[VV2006] J001535.5+005355	00:15:35.55	00:53:56.1	QSO	1.358	Blue	0.77	0.03
SDSS J001628.25+010801.9	00:16:28.24	01:08:02.0	Galaxy	0.010	Blue	0.70	0.13
[VV2006] J001641.9-312657	00:16:41.87	-31:26:56.6	QSO	0.360	Blue	0.74	0.09
2SLAQ J001731.27-004859.3	00:17:31.26	-00:48:59.2	QSO	1.357	Blue	0.76	0.11
LEDA 1156	00:17:39.97	00:30:22.5	StarburstG	0.017	Blue	0.94	0.01
SDSS J001753.82+005057.6	00:17:53.82	00:50:57.7		1.358	–	–	–
2SLAQ J001912.39+000319.6	00:19:12.39	00:03:19.8	QSO	1.372	Blue	0.75	0.07
2SLAQ J001940.23-005435.9	00:19:40.24	-00:54:35.8	QSO	1.374	Blue	0.70	0.05
[VV2006] J001950.1-004040	00:19:50.06	-00:40:40.7	QSO	4.340	–	–	–
2SLAQ J002237.90+000519.0	00:22:37.90	00:05:19.2	QSO	1.373	Blue	0.56	0.03
UM 240	00:25:07.40	00:18:45.2	EmObj	0.011	Blue	0.74	0.12
2MASX J00251994+0031312	00:25:19.92	00:31:31.7	Seyfert 1	0.014	Blue	0.82	0.03
LEDA 3107905	00:27:53.84	-00:58:00.2	Galaxy	0.014	Blue	0.96	0.02
SDSS J002916.79-010021.5	00:29:16.81	-01:00:23.1	Galaxy	0.013	Blue	1.00	0.00
SDSS J002940.01+010528.5	00:29:40.02	01:05:28.7	QSO	1.387	Blue	0.55	0.05
[VV2010c] J002951.5+004159	00:29:51.45	00:42:00.0	AGN	0.315	Red	0.34	0.18
SDSS J003117.70+001705.0	00:31:17.69	00:17:05.1	QSO	4.335	–	–	–
2QZ J003137.5-292815	00:31:37.50	-29:28:15.3	Unknown	–	Blue	0.67	0.03
2dFGRS TGS283Z142	00:31:50.70	-28:55:36.7		0.013	Blue	0.90	0.01
2QZ J003152.5-293534	00:31:52.56	-29:35:33.3	Galaxy	0.313	Blue	0.86	0.07
2SLAQ J003208.53-005303.7	00:32:08.53	-00:53:03.6	QSO	1.344	Blue	0.36	0.06
SDSS J003234.62-001557.1	00:32:34.62	-00:15:57.1	QSO	3.243	Blue	0.41	0.08
LEDA 559945	00:32:34.69	-42:40:10.4	Galaxy	–	Blue	0.70	0.04
[VV2006] J003242.7+003111	00:32:42.74	00:31:11.1	QSO	0.360	Blue	0.21	0.07
2dFGRS TGS365Z059	00:33:54.71	-29:56:12.7	Galaxy	0.006	Blue	0.78	0.02
SWIRE J003517.14-420518.6	00:35:17.11	-42:05:19.0	AGN	0.320	Red	0.03	0.66
[VV2006] J003545.9+002306	00:35:45.86	00:23:06.0	QSO	3.237	Blue	0.82	0.02
2MASS J00362543-0029075	00:36:25.39	-00:29:07.1	AGN	0.308	Red	0.16	0.75
2dFGRS TGS440Z027	00:36:38.44	-32:34:44.7	Galaxy	0.006	Blue	0.28	0.08
[VV2006] J003714.1-005602	00:37:14.11	-00:56:04.0	QSO	4.361	–	–	–
[VV2006] J003722.2-001140	00:37:22.17	-00:11:40.6	QSO	1.370	Blue	0.70	0.04
UM 260	00:37:41.13	00:33:20.0	EmObj	0.014	Blue	0.70	0.08
SDSS J003859.34-004252.2	00:38:59.35	-00:42:52.0	QSO	2.502	Blue	0.12	0.04
SDSS J003930.30+012021.6	00:39:30.28	01:20:20.9	BlueCompG	0.015	Blue	0.31	0.06
IRAS 00370+0035	00:39:34.78	00:51:36.9	FIR	–	Blue	0.82	0.04
IRAS 00370+0035	00:39:34.78	00:51:36.9	FIR	–	Blue	0.82	0.04
2QZ J004215.6-321257	00:42:15.62	-32:12:57.2	Galaxy	0.317	Blue	0.91	0.03
GALEX 2673249256393934953	00:42:43.87	01:17:02.2	QSO	1.366	Blue	0.75	0.08
2dFGRS TGS501Z235	00:43:21.88	-33:19:02.9	Galaxy	0.015	Blue	0.58	0.14
2SLAQ J004335.13-003729.7	00:43:35.16	-00:37:29.6	Catacly*V	–	Blue	0.55	0.14
SDSS J004415.83-004303.1	00:44:15.81	-00:43:03.1	QSO	3.248	–	–	–

Table B1: –continued

Id Object	RA	Dec	Type	Redshift	Group	P(Blue)	P(Red)
						HAC	HDBSCAN
[VV2006] J004544.4-315729	00:45:44.35	-31:57:29.2	QSO	1.344	Blue	0.78	0.09
2SLAQ J004626.30-011417.0	00:46:26.30	-01:14:16.8	Galaxy	–	Blue	0.86	0.03
[VV98] J004826.9-341340	00:48:26.97	-34:13:38.7	QSO	1.910	Blue	0.70	0.11
SDSS J004918.52+011308.9	00:49:18.52	01:13:09.1	QSO	1.339	Blue	0.59	0.09
LEDA 3034	00:51:49.42	00:33:53.8	Seyfert 1	0.015	Blue	0.85	0.02
QSO B0049-272	00:51:55.64	-26:57:43.3	QSO	2.484	Blue	0.21	0.05
[BKD2008] WR 353	00:51:59.72	-00:29:20.8	PartofG	0.005	Blue	0.54	0.08
ESO 411-27	00:52:51.61	-27:19:32.8	Galaxy	0.006	Blue	0.98	0.02
SDSS J005343.78+012147.6	00:53:43.76	01:21:47.5	QSO	1.358	Blue	0.60	0.07
RESOLVE rf554	00:54:15.54	-01:04:56.0	Galaxy	0.015	Blue	0.97	0.03
2QZ J005440.1-320042	00:54:40.12	-32:00:42.2	EmG	0.324	Blue	0.56	0.04
QSO B0052-307	00:54:43.95	-30:30:54.1	QSO	2.450	Blue	0.67	0.10
[VV2006] J005532.1-311538	00:55:32.08	-31:15:37.8	QSO	1.350	Blue	0.77	0.08
[TYZ2012] II 11	00:55:41.32	-00:56:30.6	Galaxy	0.015	Blue	0.80	0.02
[CT83] 219	00:55:51.35	-30:56:42.8	UV	–	Blue	0.58	0.07
RGO 8439	00:55:53.16	-28:54:57.3	Star	–	Blue	0.99	0.01
2dFGRS TGS502Z028	00:55:53.31	-33:39:01.5	Galaxy	0.325	Blue	0.70	0.14
[VV2006] J005609.9-312209	00:56:09.93	-31:22:08.6	QSO	2.460	Blue	0.33	0.07
[VV2006] J005639.0-315759	00:56:39.05	-31:57:58.6	QSO	1.350	Blue	1.00	0.00
[GPM2009] 0057-0022	00:57:12.60	-00:21:57.7	Galaxy	0.010	Blue	0.78	0.13
[VV2000] J005840.5-300203	00:58:40.42	-30:02:00.1	QSO	1.361	Blue	0.35	0.06
LEDA 3530	00:59:04.10	01:00:04.2	GinCl	0.018	Blue	0.97	0.03
2dFGRS TGS503Z245	00:59:13.57	-34:19:15.7	Galaxy	0.012	Blue	0.97	0.03
2MASX J00593609-3020390	00:59:36.09	-30:20:39.0	Galaxy	0.155	Red	0.05	0.75
LBQS 0057-0135	00:59:48.81	-01:19:05.2	QSO	0.325	Blue	0.44	0.08
QSO B0057-3948	00:59:53.21	-39:31:57.3	QSO	3.240	Blue	0.85	0.05
CAIRNS J005959.59-005157.2	00:59:59.58	-00:51:57.1	GinCl	0.166	Red	0.00	1.00
SCMS 679	01:00:04.44	-33:39:32.5	Star	–	Blue	0.53	0.05
2QZ J010009.9-320131	01:00:09.94	-32:01:31.1	Unknown	–	Blue	1.00	0.00
2dFGRS TGS561Z059	01:00:16.17	-34:57:40.6	Galaxy	0.113	Blue	0.52	0.06
2SLAQ J010121.76-000301.7	01:01:21.76	-00:03:01.8	Galaxy	–	Blue	0.14	0.05
QSO B0059-304B	01:02:14.65	-30:07:53.8	QSO	3.240	Blue	0.88	0.01
2SLAQ J010230.03-003206.8	01:02:30.02	-00:32:06.8	Seyfert 1	0.343	Blue	0.50	0.08
2MASX J01023175+0120363	01:02:31.78	01:20:36.1	GinCl	0.016	Blue	0.85	0.02
[VV2006] J010336.4-005508	01:03:36.39	-00:55:08.8	QSO	2.443	Blue	0.55	0.06
SDSS J010413.86-011552.1	01:04:13.86	-01:15:52.0	QSO	1.366	Blue	0.96	0.04
QSO B0103+000	01:06:19.23	00:48:23.4	QSO	4.435	Red	0.03	0.04
6dFGS gJ010653.4-324342	01:06:53.44	-32:43:41.9	AGN	0.371	Blue	0.64	0.03
LIRAS J010658.95+010438.3	01:06:58.93	01:04:38.2	AGN	0.327	Red	0.12	0.74
[VV2006] J010705.6+000609	01:07:05.55	00:06:09.0	QSO	1.357	Blue	0.74	0.08
UGC 695	01:07:46.47	01:03:50.3	LSB G	0.002	Blue	0.88	0.07
SDSS J010748.62+004453.5	01:07:48.62	00:44:53.7	BCIG	0.266	Red	0.14	0.44
MCG+00-04-011	01:09:01.58	01:22:41.5	GinCl	0.018	Blue	0.74	0.07
MCG+00-04-011	01:09:01.58	01:22:41.5	GinCl	0.018	Blue	0.74	0.07
2SLAQ J010907.59+000649.8	01:09:07.59	00:06:50.0	QSO	1.372	Blue	0.55	0.07
LEDA 1185205	01:09:07.95	01:07:15.5	HII G	0.004	Blue	0.75	0.13
SDSS J010918.56+005419.3	01:09:18.56	00:54:19.4	QSO	1.356	Blue	0.64	0.08
2SLAQ J010925.95-003739.0	01:09:25.96	-00:37:39.0	QSO	1.360	Blue	0.69	0.04
2QZ J011014.0-302445	01:10:13.97	-30:24:44.5	EmG	0.313	Blue	0.60	0.05
2QZ J011119.0-300019	01:11:19.02	-30:00:18.2	EmG	0.309	Blue	0.83	0.05
SDSS J011128.38+000143.7	01:11:28.35	00:01:43.3	QSO	0.765	Blue	0.13	0.10
2dFGRS TGS505Z356	01:12:12.64	-33:56:31.1	Galaxy	0.333	Red	0.43	0.13
2SLAQ J011230.55+001441.5	01:12:30.55	00:14:41.7	QSO	3.259	Blue	0.84	0.03
PB 6318	01:12:58.01	00:58:37.0	Star	–	Blue	0.65	0.04
2dFGRS TGS447Z027	01:13:13.03	-32:26:09.9	Galaxy	0.017	Blue	0.86	0.05
UGC 772	01:13:40.42	00:52:39.0	LSB G	0.004	–	–	–
2SLAQ J011402.35-004750.9	01:14:02.35	-00:47:50.8	Seyfert 1	0.350	Blue	0.55	0.07
[VV2006] J011405.3-310903	01:14:05.25	-31:09:02.8	QSO	1.333	Blue	0.21	0.05

Table B1: –continued

Id Object	RA	Dec	Type	Redshift	Group	P(Blue)	P(Red)
						HAC	HDBSCAN
2dFGRS TGS505Z120	01:14:36.11	-32:38:41.0	Galaxy	0.020	Blue	0.79	0.09
SDSS J011531.90-005144.5	01:15:31.89	-00:51:44.3	HII G	0.005	Blue	0.89	0.06
2SLAQ J011533.07-005134.9	01:15:33.06	-00:51:34.8	Galaxy	–	Blue	0.56	0.08
[BKD2008] WR 354	01:15:33.79	-00:51:31.5	HII G	0.006	Blue	0.22	0.07
[BKD2008] WR 354	01:15:33.79	-00:51:31.5	HII G	0.006	Blue	0.22	0.07
2SLAQ J011542.18+002300.2	01:15:42.18	00:23:00.4	QSO	1.373	Blue	0.69	0.04
2dFGRS TGS505Z064	01:16:38.40	-32:55:39.1	Galaxy	0.018	Blue	0.94	0.02
2dFGRS TGS505Z018	01:17:40.21	-33:04:40.7	Galaxy	0.018	Blue	0.67	0.08
2dFGRS TGS377Z137	01:17:56.44	-30:26:25.8	Galaxy	0.018	Blue	0.87	0.08
2dFGRS TGS506Z276	01:18:05.71	-33:03:09.1	Galaxy	0.012	Blue	0.88	0.07
2SLAQ J011818.13+001455.2	01:18:18.12	00:14:55.5	QSO	1.372	Blue	0.62	0.03
2SLAQ J011829.63+004549.4	01:18:29.62	00:45:49.4	Seyfert 1	0.314	Blue	0.67	0.14
2dFGRS TGS506Z243	01:18:49.15	-33:20:13.1	Galaxy	0.012	Blue	0.83	0.07
2MASX J01195427-3414599	01:19:54.23	-34:15:00.0	EmG	0.019	Blue	0.99	0.01
2dFGRS TGS506Z158	01:20:09.99	-33:14:10.7	Galaxy	0.011	Blue	1.00	0.00
2SLAQ J012110.74-005037.2	01:21:10.74	-00:50:37.1	QSO	1.352	Blue	0.71	0.02
[HB93] 0119-341B	01:21:52.19	-33:56:15.8	Star	–	Red	0.33	0.18
SDSS J012213.85+005731.4	01:22:13.87	00:57:31.6	HII G	0.008	Blue	1.00	0.00
2dFGRS TGS565Z149	01:22:17.09	-34:02:41.6	Galaxy	0.012	Blue	0.87	0.05
2SLAQ J012226.76+000327.5	01:22:26.75	00:03:27.9	QSO	2.480	Blue	0.86	0.04
QSO B0120-002	01:23:01.78	00:03:23.6	QSO	1.356	Blue	0.81	0.08
2dFGRS TGS297Z222	01:23:50.87	-29:11:46.4	Galaxy	0.000	Blue	0.05	0.03
MCG+00-04-113	01:23:54.75	00:16:56.4	GinCl	0.018	Blue	0.70	0.05
SDSS J012356.34+001230.6	01:23:56.35	00:12:31.0	Galaxy	–	Blue	0.99	0.01
ESO 352-67	01:23:57.47	-33:48:07.5	Galaxy	0.005	Blue	0.89	0.06
SDSS J012405.73+005905.0	01:24:05.73	00:59:04.9	Galaxy	0.007	–	–	–
QSO B0121-324	01:24:16.18	-32:12:21.7	QSO	1.358	Blue	0.61	0.08
2dFGRS TGS507Z113	01:24:30.16	-33:38:45.5	Galaxy	0.305	Red	0.45	0.39
QSO B0122-3232	01:25:04.59	-32:17:14.6	QSO	2.450	Blue	0.41	0.09
2QZ J012526.2-304433	01:25:26.24	-30:44:32.8	EmG	0.311	Blue	0.57	0.07
2QZ J012549.3-280944	01:25:49.29	-28:09:43.6	Galaxy	0.324	–	–	–
LEDA 1180903	01:26:27.03	00:58:51.9	Galaxy	0.008	Blue	0.98	0.02
2dFGRS TGS566Z338	01:26:37.73	-34:35:13.8	Galaxy	0.012	Blue	0.89	0.02
6dFGS gJ012646.5-003845	01:26:46.51	-00:38:44.7	HII G	0.006	Blue	0.54	0.08
ESO 413-7	01:27:59.31	-29:05:12.0	GinCl	0.005	Blue	1.00	0.00
6dFGS gJ012926.6-011159	01:29:26.54	-01:11:59.0	GinCl	0.016	Red	0.42	0.24
SDSS J013034.18-002106.6	01:30:34.17	-00:21:06.5	QSO	3.234	Blue	0.64	0.04
2dFGRS TGS509Z295	01:31:21.84	-33:06:06.2	Galaxy	0.017	Blue	0.81	0.07
2dFGRS TGS508Z142	01:31:45.65	-32:56:56.8	Galaxy	0.017	Blue	0.96	0.02
LEDA 679811	01:31:47.24	-33:10:55.1	Galaxy	–	Blue	1.00	0.00
2dFGRS TGS509Z242	01:32:53.43	-33:26:42.7	Galaxy	0.017	Blue	0.62	0.12
2MASS J01330450+0003553	01:33:04.52	00:03:56.1	low-mass*	0.000	Red	0.13	0.47
2SLAQ J013400.41-010358.2	01:34:00.46	-01:03:59.2		–	Blue	0.99	0.01
RESOLVE rf246	01:34:52.04	-00:38:55.2	Galaxy	0.017	Blue	0.66	0.12
[VV2006] J013500.8-004054	01:35:00.83	-00:40:54.2	QSO	1.007	Blue	0.17	0.04
FBQS J0135-0019	01:35:17.53	-00:19:39.0	Seyfert 1	0.312	Blue	0.45	0.11
2QZ J013531.1-313651	01:35:31.16	-31:36:51.0	Galaxy	0.320	Blue	0.46	0.07
SDSS J013701.72-012059.3	01:37:01.71	-01:20:59.1	QSO	2.496	Blue	0.85	0.07
[VV2006] J013729.4-320715	01:37:29.40	-32:07:15.7	QSO	1.368	Blue	0.56	0.05
[VV2006] J013837.3+002818	01:38:37.28	00:28:18.5	QSO	1.348	Blue	0.82	0.08
2SLAQ J013951.07+002537.9	01:39:51.07	00:25:38.0	QSO	1.342	Blue	0.96	0.04
2E 458	01:40:17.06	-00:50:03.0	Seyfert 1	0.334	Blue	0.27	0.05
SDSS J014125.63+000755.6	01:41:25.64	00:07:55.8	QSO	0.322	Red	0.04	0.85
[VV2006] J014224.7-320414	01:42:24.73	-32:04:13.7	QSO	2.460	Blue	0.55	0.09
[VV2006] J014303.6-295255	01:43:03.49	-29:52:54.8	QSO	2.450	Blue	0.45	0.07
ESO 353-36	01:43:18.29	-34:12:22.4	EmG	0.013	Red	0.06	0.37
SDSS J014721.12-004505.3	01:47:21.12	-00:45:05.3	QSO	1.348	Red	0.33	0.35
[VV2006] J014739.2-285259	01:47:39.21	-28:52:59.2	QSO	0.360	Blue	0.75	0.05

Table B1: –continued

Id Object	RA	Dec	Type	Redshift	Group	P(Blue)	P(Red)
						HAC	HDBSCAN
[VV2006] J014739.2-285259	01:47:39.21	-28:52:59.3	QSO	0.360	Blue	0.84	0.05
SDSS J014806.25-002841.6	01:48:06.25	-00:28:41.6	Galaxy	0.215	Blue	0.70	0.04
[VV2006] J014812.2+000154	01:48:12.24	00:01:53.5	QSO	1.712	Blue	0.07	0.03
2QZ J014844.1-275610	01:48:44.17	-27:56:11.0	Star	–	Blue	0.73	0.07
IC 1734	01:49:17.03	-32:44:33.1	Galaxy	0.017	Blue	0.59	0.06
[VV2006] J014921.5-003220	01:49:21.53	-00:32:20.9	QSO	1.379	Blue	0.81	0.08
[RGD2013] J015239.744+010557.768	01:52:39.74	01:05:57.9	Galaxy	0.331	Red	0.15	0.63
[RGD2013] J015253.854+011215.480	01:52:53.85	01:12:15.5	Galaxy	0.184	Red	0.05	0.87
2QZ J015257.7-284838	01:52:57.76	-28:48:37.8	Seyfert 1	0.326	Blue	0.52	0.08
2SLAQ J015331.85+002252.8	01:53:31.85	00:22:53.0	QSO	1.367	Blue	0.91	0.02
SDSS J015400.48-004509.5	01:54:00.50	-00:45:10.0	HII G	0.016	Blue	0.66	0.04
2SLAQ J015409.27+002645.2	01:54:09.27	00:26:45.3	QSO	1.355	Blue	0.72	0.05
[VV2006] J015410.9-285214	01:54:10.94	-28:52:14.6	QSO	1.356	Blue	0.54	0.07
[VV2006] J015415.4-285254	01:54:15.48	-28:52:54.9	QSO	1.344	Blue	0.61	0.07
SDSS J015440.44-000643.9	01:54:40.45	-00:06:43.6	EmG	0.019	Blue	0.35	0.08
2SLAQ J015526.89+000615.4	01:55:26.87	00:06:15.8	Galaxy	0.016	Blue	0.79	0.02
2SLAQ J015529.12-003927.3	01:55:29.07	-00:39:27.1	Galaxy	–	Blue	0.70	0.07
SDSS J015813.75+010143.5	01:58:13.75	01:01:43.4	RRLyr	–	Blue	0.94	0.01
[VV2006] J015832.1-301703	01:58:32.15	-30:17:02.8	QSO	1.380	Blue	0.76	0.09
[VV2006] J015832.1-301703	01:58:32.16	-30:17:02.7	QSO	1.380	Blue	0.61	0.04
[VV2006] J015850.2-300438	01:58:50.22	-30:04:38.1	QSO	1.351	–	–	–
[VV2006] J015935.4+000401	01:59:35.48	00:04:01.5	QSO	3.277	Blue	0.63	0.08
SDSS J020025.40+002916.5	02:00:25.40	00:29:16.8	QSO	0.313	Red	0.05	0.68
[VV2006] J020055.0-293527	02:00:55.02	-29:35:26.5	QSO	1.349	Blue	0.64	0.05
ESO 414-22	02:01:14.49	-31:43:42.9	GinGroup	0.019	Blue	0.66	0.09
[VV98] J020115.4+003136	02:01:15.53	00:31:35.1		0.362	Blue	0.34	0.06
2SLAQ J020200.06-000921.2	02:02:00.06	-00:09:21.2	QSO	1.359	Blue	0.59	0.04
[VV96] J020435.5-455923	02:04:35.46	-45:59:24.0	QSO	3.240	Blue	0.73	0.05
LEDA 1193771	02:05:00.83	01:24:03.7	Galaxy	–	Blue	0.59	0.06
2dFGRS TGS514Z164	02:07:20.33	-33:01:54.3	Galaxy	0.011	–	–	–
2SLAQ J020804.48-000023.2	02:08:04.49	-00:00:23.0	QSO	1.339	Blue	0.53	0.04
2SLAQ J020827.06-005208.1	02:08:27.07	-00:52:07.9	QSO	1.341	Blue	0.77	0.06
SDSS J020921.99-005455.5	02:09:22.00	-00:54:55.4	QSO	1.367	Blue	0.97	0.03
2dFGRS TGS515Z070	02:12:25.05	-33:04:59.0	Galaxy	0.106	–	–	–
2dFGRS TGS515Z311	02:14:24.22	-33:14:52.0	Galaxy	0.012	Blue	0.86	0.09
2dFGRS TGS461Z092	02:14:47.63	-32:42:35.2	Galaxy	0.012	Blue	0.82	0.06
2SLAQ J021529.02-005314.8	02:15:29.02	-00:53:14.9	QSO	1.369	Blue	0.63	0.05
2dFGRS TGS460Z130	02:16:01.62	-31:36:51.8	Galaxy	0.012	Blue	0.92	0.02
2dFGRS TGS387Z025	02:16:13.75	-30:50:56.8	Galaxy	0.012	Blue	1.00	0.00
SDSS J021617.19-011046.9	02:16:17.19	-01:10:46.7	QSO	3.264	Blue	0.96	0.01
2SLAQ J021810.52-010147.4	02:18:10.52	-01:01:47.2	QSO	1.353	Blue	0.68	0.06
V* AX For	02:19:28.00	-30:45:46.0	CataclyV*	–	Blue	0.45	0.07
2QZ J022112.5-302559	02:21:12.54	-30:25:59.0		0.315	Blue	0.80	0.08
2SLAQ J022316.91-010049.7	02:23:16.93	-01:00:49.6	Galaxy	–	Blue	0.85	0.06
SHOC 120	02:24:17.14	00:06:26.1	Seyfert 1	0.060	–	–	–
LEDA 667000	02:24:52.74	-34:06:34.3	Galaxy	–	Blue	0.78	0.06
SDSS J022530.93-005007.0	02:25:30.92	-00:50:07.1	Galaxy	0.059	Blue	0.61	0.07
[BKD2008] WR 346	02:26:28.28	01:09:37.6	PartofG	0.005	Blue	1.00	0.00
[BKD2008] WR 346	02:26:28.28	01:09:37.6	PartofG	0.005	Blue	1.00	0.00
LEDA 546974	02:26:46.27	-43:35:29.6	Galaxy	–	Blue	0.65	0.07
SDSS J022714.48+010536.1	02:27:14.47	01:05:36.3	EmG	0.349	Blue	0.66	0.07
RESOLVE rf668	02:27:19.29	01:01:32.2	Galaxy	0.015	Blue	0.98	0.02
[VV2006] J022738.3-313627	02:27:38.28	-31:36:26.4	QSO	1.350	Blue	0.46	0.06
[VV2006] J022758.2+000226	02:27:58.20	00:02:25.6	QSO	1.066	–	–	–
LCRS B022613.7-392927	02:28:14.52	-39:16:04.0	Galaxy	–	Blue	0.68	0.05
[BKD2008] WR 315	02:28:28.73	-01:08:58.6	PartofG	0.005	Blue	0.91	0.01
2SLAQ J022945.34+000856.2	02:29:45.34	00:08:56.4	Star	–	Blue	0.54	0.09
2QZ J022954.6-303558	02:29:54.69	-30:35:58.4	Seyfert 1	0.372	Blue	0.34	0.06

Table B1: –continued

Id Object	RA	Dec	Type	Redshift	Group	P(Blue)	P(Red)
						HAC	HDBSCAN
Pul -3 180355	02:29:57.00	-01:00:32.3	Star	–	Red	0.04	0.06
2dFGRS TGS463Z130	02:30:09.77	-31:36:18.2	Galaxy	0.015	Blue	1.00	0.00
SDSS J023020.93+001355.5	02:30:20.93	00:13:55.8	Seyfert 1	0.335	Blue	0.20	0.06
UGC 2009	02:32:09.34	-01:23:10.3	Galaxy	0.015	Red	0.03	0.88
2dFGRS TGS518Z089	02:32:18.08	-33:50:43.0	Galaxy	0.016	Blue	0.59	0.14
SDSS J023230.63-011654.5	02:32:30.63	-01:16:54.5	QSO	1.364	Blue	0.61	0.05
6dFGS gJ023241.8-391744	02:32:41.88	-39:17:42.8	Galaxy	0.005	Blue	0.51	0.08
SDSS J023248.71+005138.8	02:32:48.71	00:51:38.8	Galaxy	0.344	Blue	0.57	0.06
V* HP Cet	02:33:22.62	00:50:59.4	Nova	-0.000	Blue	0.54	0.09
NGC 986	02:33:34.29	-39:02:40.9	EmG	0.007	Blue	0.93	0.07
[VV2006] J023335.4-010744	02:33:35.37	-01:07:44.6	QSO	0.367	Blue	0.50	0.06
SDSS J023628.77-005829.7	02:36:28.75	-00:58:30.0	Galaxy	0.008	Blue	0.78	0.08
[VV2006] J023635.7-003203	02:36:35.69	-00:32:03.4	QSO	1.362	–	–	–
SDSS J024059.15+004545.8	02:40:59.14	00:45:45.9	QSO	3.233	Blue	0.99	0.01
[VV2006] J024235.0-010351	02:42:34.91	-01:03:51.9	QSO	1.373	Blue	0.56	0.03
[EKS96] NGC 1068 91	02:42:46.94	00:01:26.2	HII	–	Blue	0.14	0.06
[ZBF2015] NGC1073 1	02:43:35.61	01:22:37.9	HII	–	Blue	0.27	0.06
[ZBF2015] NGC1073 16	02:43:37.69	01:22:22.5	HII	–	Blue	0.94	0.06
[ZBF2015] NGC1073 21	02:43:42.74	01:21:34.4	HII	–	Blue	0.50	0.07
[ZBF2015] NGC1073 10	02:43:44.03	01:22:40.5	HII	–	Blue	0.80	0.05
6dFGS gJ024605.3-330500	02:46:05.28	-33:04:59.4	Galaxy	0.017	Blue	0.83	0.01
2MASS J02462415-0029539	02:46:24.14	-00:29:52.9	Star	–	Blue	0.76	0.03
Gaia DR2 249776434864940160	02:46:24.75	-00:30:16.3	QSO	–	Blue	0.53	0.07
[BKD2008] WR 316	02:46:25.42	-00:30:09.8	PartofG	0.005	Blue	0.57	0.04
2SLAQ J024626.59-003000.2	02:46:26.57	-00:30:00.4	Star	–	Blue	1.00	0.00
2SLAQ J025100.64+001707.2	02:51:00.64	00:17:07.3	QSO	2.466	Blue	0.70	0.07
2SLAQ J025216.75+001741.2	02:52:16.73	00:17:41.2	Galaxy	0.005	Blue	0.89	0.06
2SLAQ J025252.02-002211.7	02:52:52.00	-00:22:11.6	QSO	1.370	Blue	0.85	0.05
SHOC 143	02:54:26.13	-00:41:22.7	Seyfert 1	0.015	Blue	0.88	0.08
NVSS J025557+004132	02:55:57.24	00:41:33.5	RadioG	0.014	Red	0.12	0.32
QSO B0253+0058	02:56:07.25	01:10:38.8	QSO	1.349	Blue	0.66	0.08
HBQS 0253+0022	02:56:25.32	00:34:29.4	HII	0.013	Blue	0.99	0.01
LEDA 1170514	02:56:28.43	00:36:28.2	Galaxy	0.009	Blue	0.64	0.05
2dFGRS TGS522Z138	02:57:45.54	-33:28:55.5	Galaxy	0.335	Red	0.43	0.28
2MASSI J0259103-002239	02:59:10.38	-00:22:39.8	Seyfert 1	0.360	Blue	0.54	0.09
2SLAQ J030309.82+001337.5	03:03:09.83	00:13:37.8	Galaxy	–	–	–	–
UGC 2517	03:04:12.47	-01:11:33.8	Galaxy	0.013	Red	0.53	0.20
2SLAQ J030417.77-004931.7	03:04:17.77	-00:49:31.5	Galaxy	–	Blue	0.62	0.11
LEDA 1142424	03:04:34.76	-00:28:30.7	Seyfert 1	0.006	Blue	0.98	0.02
LBQS 0302-0019	03:04:49.85	-00:08:13.4	QSO	3.295	Blue	0.95	0.02
2MASS J03045799+0057131	03:04:57.98	00:57:14.0	Blue	0.012	Blue	0.99	0.01
MCG+00-08-089	03:05:18.24	-00:09:34.1	Galaxy	0.009	Blue	0.72	0.04
LBQS 0303+0110	03:06:12.72	01:21:57.3	QSO	1.335	Blue	0.70	0.07
WISE J030629.21-335332.3	03:06:29.22	-33:53:32.3	AGN	0.780	Blue	0.67	0.11
SDSS J030630.33-000622.9	03:06:30.33	-00:06:22.9	Galaxy	0.106	Red	0.12	0.72
SDSS J030715.63+004352.1	03:07:15.60	00:43:52.6	Galaxy	0.010	Blue	1.00	0.00
2SLAQ J030757.55+000712.0	03:07:57.55	00:07:12.1	QSO	1.343	Blue	0.74	0.04
2SLAQ J031129.69-001701.4	03:11:29.70	-00:17:01.5	QSO	1.357	Blue	0.72	0.05
2QZ J031130.9-315250	03:11:30.92	-31:52:51.1	WD*	–	Blue	0.58	0.13
ESO 417-20	03:12:48.61	-31:29:10.7	GinGroup	0.013	Blue	0.96	0.03
SDSS J031258.36-000453.6	03:12:58.36	-00:04:53.6	Galaxy	0.117	Blue	0.76	0.02
2dFGRS TGS398Z109	03:13:56.08	-31:28:12.6	Galaxy	0.014	Blue	0.32	0.09
2SLAQ J031428.25+004506.6	03:14:28.25	00:45:07.0	Galaxy	–	Blue	1.00	0.00
2dFGRS TGS471Z114	03:16:15.31	-31:12:33.3	Galaxy	0.004	Blue	0.81	0.04
2SLAQ J031618.00-003025.2	03:16:18.01	-00:30:24.9	Galaxy	–	Blue	1.00	0.00
2dFGRS TGS524Z054	03:16:50.65	-33:18:03.8	Galaxy	0.006	Blue	0.94	0.02
2dFGRS TGS524Z054	03:16:50.66	-33:18:04.0	Galaxy	0.006	Blue	0.96	0.04
2SLAQ J031829.06-000040.3	03:18:29.06	-00:00:40.5	Galaxy	–	Blue	0.65	0.04

Table B1: –continued

Id Object	RA	Dec	Type	Redshift	Group	P(Blue)	P(Red)
						HAC	HDBSCAN
[VV2006] J031845.2-001844	03:18:45.17	-00:18:45.3	QSO	3.224	Blue	0.97	0.03
2SLAQ J031937.30-002641.1	03:19:37.29	-00:26:41.0	QSO	1.371	Blue	0.37	0.08
SDSS J032244.90+004442.4	03:22:44.90	00:44:42.3	QSO Candidate	0.304	Blue	0.94	0.03
6dFGS gJ032504.2-365540	03:25:04.15	-36:55:39.9	GinPair	0.006	Blue	0.64	0.08
6dFGS gJ032512.9-362210	03:25:13.07	-36:22:09.7	Galaxy	0.004	Blue	0.75	0.12
[JPB2015] 051.4803133-32.8829964	03:25:55.27	-32:52:58.9	GICl	–	Blue	0.83	0.08
SDSS J033226.29-011126.2	03:32:26.29	-01:11:26.0	QSO	1.361	Blue	0.52	0.07
SDSS J033226.29-011126.2	03:32:26.30	-01:11:26.3	QSO	1.361	Blue	0.53	0.05
SDSS J033310.10+000849.1	03:33:10.08	00:08:49.2	Seyfert 2	0.327	Red	0.13	0.37
[VV2006] J033458.5-000744	03:34:58.48	-00:07:43.9	QSO	1.357	Blue	0.77	0.02
[VV2006] J033821.6+003106	03:38:21.51	00:31:06.6	QSO	1.349	Blue	0.64	0.04
2XMM J033841.3-353134	03:38:41.36	-35:31:34.4	BLLac	0.360	Blue	0.26	0.06
2XMM J033841.3-353134	03:38:41.37	-35:31:34.2	BLLac	0.360	Blue	0.25	0.05
[VV2006] J033927.5-344707	03:39:27.45	-34:37:07.0	QSO	1.364	Blue	0.55	0.04
CXO J034012.4-353740	03:40:12.39	-35:37:40.1	HMXB	–	Blue	0.18	0.05
SDSS J034019.89+010330.7	03:40:19.89	01:03:30.7	EmG	0.322	Blue	0.72	0.11
[VV2006] J034023.0-351606	03:40:22.99	-35:16:07.0	QSO	1.372	Blue	0.55	0.08
2XMM J034050.4-352620	03:40:50.48	-35:26:21.7	AGN	1.366	Blue	0.59	0.08
ESO 358-51	03:41:32.55	-34:53:19.0	GinGroup	0.006	Blue	0.88	0.07
2MASS J03424773+0109331	03:42:47.72	01:09:33.0	Seyfert 1	0.360	Blue	0.16	0.07
2SLAQ J034304.64+002512.1	03:43:04.65	00:25:12.3	Star	–	Blue	0.43	0.09
LCRS B034214.4-381736	03:44:04.68	-38:08:11.9	Galaxy	–	Red	0.00	1.00
[VV2006] J034408.3-003106	03:44:08.25	-00:31:05.8	QSO	1.646	Blue	0.93	0.03
SDSS J034427.73-002740.4	03:44:27.73	-00:27:40.2	Galaxy	0.041	Red	0.53	0.25
SDSS J034517.02-001549.8	03:45:17.01	-00:15:49.7	QSO	1.335	Blue	1.00	0.00
6dFGS gJ034545.4-362046	03:45:45.38	-36:20:46.1	GinCl	0.004	Blue	0.84	0.02
SDSS J034602.53-000058.7	03:46:02.53	-00:00:58.6	Seyfert 2	0.308	Red	0.18	0.50
2MASX J03472195-3251054	03:47:21.94	-32:51:05.2	GinCl	0.116	Red	0.29	0.56
SDSS J034907.92+010943.3	03:49:07.93	01:09:43.2	LSB G	0.014	Blue	0.96	0.04
MCG+00-10-021	03:49:08.87	01:09:46.3	LSB G	0.014	Blue	0.85	0.05
FASTT 83	03:51:19.36	00:32:16.6	EB*	–	Red	0.12	0.54
LEDA 607287	03:55:02.55	-38:35:40.2	Galaxy	–	Red	0.17	0.75
Gaia DR2 4857261601188886016	03:55:16.01	-37:29:44.7	Candidate WD*	–	–	–	–
[ZJM2003] SA 95-2230	03:55:38.45	00:28:34.9		–	Blue	0.98	0.02
2dFGRS TGS817Z154	03:56:05.58	-49:28:40.7	Galaxy	0.003	Blue	0.98	0.01
SDSSCGB 74387.1	03:56:50.79	-00:14:34.9	Galaxy	–	Red	0.37	0.27
2dFGRS TGS848Z501	03:57:22.10	-37:01:54.1	Galaxy	0.016	Blue	0.97	0.03
6dFGS gJ035732.5-000047	03:57:32.27	-00:00:47.6	Galaxy	0.017	Blue	0.69	0.06
UGC 2913	03:59:03.91	01:21:33.6	Galaxy	0.013	Blue	0.55	0.09
UGC 2913	03:59:03.91	01:21:33.6	Galaxy	0.013	Blue	0.55	0.09
ESO 201-14	04:00:29.38	-49:01:48.4	EmG	0.004	Blue	0.78	0.05
2MASS J04004608-3424277	04:00:46.07	-34:24:27.7	AGN Candidate	–	Blue	0.53	0.11
6dFGS gJ040053.2-351416	04:00:53.13	-35:14:16.2		Galaxy	0.015	Blue	0.80
QSO B0401-3505	04:03:10.56	-34:56:56.8	QSO	3.251	Blue	0.67	0.04
LCRS B040209.0-382209	04:03:56.75	-38:13:58.5	Galaxy	–	Blue	0.54	0.14
6dFGS gJ040441.2-345756	04:04:41.14	-34:57:55.8	Galaxy	0.008	Blue	0.80	0.07
6dFGS gJ040520.4-364859	04:05:20.40	-36:48:59.0	Galaxy	0.003	Blue	0.39	0.11
6dFGS gJ040520.4-364859	04:05:20.40	-36:48:58.8	Galaxy	0.003	Blue	0.40	0.12
Gaia DR2 4845009910624639232	04:05:27.97	-38:11:22.1	Star	–	Blue	0.99	0.01
[VV96] J041130.5-335331	04:11:30.51	-33:53:31.1	QSO	1.350	Blue	0.76	0.04
2dFGRS TGS894Z351	04:11:58.37	-37:58:44.0	Galaxy	0.013	Blue	0.96	0.04
ESO 420-11	04:12:53.30	-31:18:30.2	GinGroup	0.005	Blue	0.97	0.03
2dFGRS TGS894Z291	04:13:00.00	-38:19:42.5		Galaxy	0.012	Blue	0.98
Gaia DR2 4872129059981617536	04:20:06.78	-32:51:20.0	Candidate WD*	–	–	–	–
LEDA 685147	04:20:56.84	-32:50:42.8		–	–	–	–
2MASX J04255940-4316225	04:25:59.40	-43:16:22.6	Galaxy	0.078	Blue	0.98	0.02
LEDA 579779	04:26:32.58	-41:01:56.6	Galaxy	–	Blue	1.00	0.00
LEDA 125483	04:26:44.34	-42:15:41.2	Galaxy	0.015	Blue	1.00	0.00

Table B1: –continued

Id Object	RA	Dec	Type	Redshift	Group	P(Blue)	P(Red)
						HAC	HDBSCAN
LEDA 568379	04:26:44.87	-42:05:40.5	Galaxy	–	Blue	0.98	0.01
LEDA 554934	04:26:44.91	-42:58:38.4	Galaxy	–	Blue	0.90	0.03
MCG-07-10-009	04:27:42.24	-42:38:20.4	Galaxy	0.016	Blue	0.83	0.06
2MASX J04282877-4314283	04:28:28.71	-43:14:29.1	Galaxy	0.015	Blue	0.70	0.04
6dFGS gJ043139.6-301514	04:31:39.57	-30:15:14.1	CataclyV*	-0.000	Blue	0.27	0.08
LEDA 697927	04:32:44.32	-32:01:20.1	Galaxy	–	Red	0.10	0.85
ESO 251-12	04:33:09.79	-43:46:13.6	Galaxy	0.010	Blue	0.82	0.05
ESO 304-2	04:35:19.80	-42:12:11.8	Galaxy	0.007	Blue	1.00	0.00
LEDA 494343	04:35:41.79	-47:52:43.9	Galaxy	–	Blue	0.89	0.05
[HM2015b] 236 3	04:37:11.17	-46:41:06.8	Galaxy	–	Blue	0.38	0.06
LEDA 692923	04:37:18.21	-32:22:10.3	Galaxy	–	Blue	1.00	0.00
Gaia DR2 4790561549357871744	04:37:35.04	-44:20:28.8	Candidate RRLyr	–	Blue	0.99	0.01
LEDA 681270	04:38:23.53	-33:05:08.6		Galaxy	–	Blue	0.83
6dFGS gJ043927.4-425912	04:39:27.45	-42:59:11.8	Galaxy	0.362	Blue	0.41	0.06
LEDA 606705	04:45:44.98	-38:38:48.7	Galaxy	–	Blue	1.00	0.00
LEDA 88363	04:48:23.05	-44:52:57.7	Galaxy	–	Blue	0.97	0.03
2dFGRS TGS880Z325	04:50:02.35	-47:28:39.0	Galaxy	0.010	Blue	0.68	0.10
LEDA 512705	04:51:48.86	-46:37:36.8	Galaxy	–	Blue	1.00	0.00
Gaia DR2 4811451372635865984	04:52:31.12	-44:11:04.3	Star	–	Blue	0.48	0.11
LEDA 686311	04:53:19.46	-32:46:32.8	Galaxy	–	Blue	0.85	0.04
[VV98] J045444.5-481300	04:54:43.04	-48:13:20.2	Seyfert 1	0.363	Blue	0.68	0.06
SN 2012at	04:54:52.74	-37:19:15.5	SN	–	Blue	0.56	0.13
2MASX J04550020-3715351	04:55:00.19	-37:15:35.4	GinPair	0.008	Blue	0.88	0.05
LEDA 715392	04:55:26.51	-30:35:28.6	Galaxy	–	Blue	0.20	0.07
ESO 499-24	09:57:01.69	-26:29:28.5	Galaxy	0.015	Blue	0.89	0.03
LEDA 859547	09:57:06.62	-19:07:06.1	Galaxy	–	Blue	0.84	0.08
LEDA 1022680	09:57:23.46	-07:12:51.4	Galaxy	–	Blue	0.18	0.06
2MASX J09583711-4704597	09:58:37.10	-47:05:00.4	Galaxy	0.012	Blue	0.63	0.07
[CMI2006b] H42-f02-1939	09:59:46.82	-19:28:00.0	Galaxy	0.265	Blue	0.99	0.01
CRTS J095950.7-383024	09:59:50.88	-38:30:22.9	RRLyr	–	Blue	0.97	0.03
LEDA 605183	10:00:05.44	-38:47:28.7	Galaxy	–	Blue	0.57	0.08
NGC 3095	10:00:05.83	-31:33:10.8	GinGroup	0.009	Red	0.08	0.49
LEDA 154528	10:00:49.12	-30:32:41.9	Galaxy	–	Blue	0.75	0.07
SDSS J100059.08+032751.4	10:00:59.07	03:27:51.5	Galaxy	0.007	Blue	0.74	0.08
ESO 567-3	10:01:09.07	-19:26:29.7	LSB G	0.012	Blue	0.99	0.01
LEDA 1011555	10:01:34.08	-07:52:55.7	Galaxy	–	Blue	0.90	0.08
Gaia DR2 5670829935783719936	10:02:11.73	-19:25:37.1	Star	–	Blue	0.32	0.06
2QZ J100215.7-001056	10:02:15.83	-00:10:55.8	QSO	0.353	Blue	0.63	0.09
VVDS 100108471	10:02:25.38	01:19:36.8	Galaxy	0.123	Blue	1.00	0.00
ESO 262-15	10:02:38.71	-45:29:53.9	GinGroup	0.012	Red	0.17	0.48
[BCP93] F2 H6	10:02:51.82	-26:09:23.9		HII	–	Blue	1.00
[EBU2007] 7	10:02:54.69	-26:08:59.6	BlueSG*	0.001	Blue	0.24	0.09
[H69] NGC 3109 12	10:02:56.31	-26:08:58.5	HII	–	Blue	0.26	0.09
[PRS2007] HII 44	10:02:59.47	-26:08:46.4	HII	–	Blue	0.43	0.11
[PRS2007] HII 44	10:02:59.48	-26:08:46.4	HII	–	Blue	0.48	0.10
PSO J150.7588-26.1494	10:03:02.10	-26:08:58.7	AGN Candidate	–	Blue	0.67	0.08
2MASX J10030450-1949377	10:03:04.51	-19:49:38.1	Galaxy	0.012	Blue	0.84	
2dFGRS TGN094Z280	10:03:15.05	-05:54:32.8	Galaxy	0.013	Blue	0.96	0.04
[EBU2007] 3	10:03:17.64	-26:10:01.7	BlueSG*	0.001	Blue	0.26	0.08
[VV98] J100342.1-150808	10:03:41.93	-15:08:08.9	QSO	0.342	Blue	0.43	0.07
2MASX J10035230-3124480	10:03:52.32	-31:24:48.5	Galaxy	0.009	Blue	0.99	0.01
2MASX J10041992-4425311	10:04:19.86	-44:25:32.6	Galaxy	0.012	Blue	0.90	0.07
2MASX J10050765-1951299	10:05:07.68	-19:51:30.2	Galaxy	–	Blue	0.64	0.06
2dFGRS TGN421Z115	10:05:17.31	01:38:21.7	Galaxy	0.004	Blue	0.88	0.05
2MFGC 7816	10:05:28.51	-38:07:30.1	Galaxy	–	Blue	1.00	0.00
[VV2006] J100539.9+040914	10:05:39.88	04:09:14.7	QSO	1.355	Blue	0.59	0.07
CRTS J100548.9-254146	10:05:48.99	-25:41:47.1	RRLyr	–	Blue	0.99	0.01
2MASX J10061715-0634276	10:06:17.20	-06:34:27.7	Galaxy	0.011	Blue	0.95	0.05

Table B1: –continued

Id Object	RA	Dec	Type	Redshift	Group	P(Blue)	P(Red)
						HAC	HDBSCAN
6dFGS gJ100622.2-264958	10:06:22.20	-26:49:57.2	Galaxy	0.015	Blue	0.99	0.01
6dFGS gJ100631.4-320236	10:06:31.39	-32:02:35.9	GinGroup	0.008	Red	0.42	0.24
NGC 3125	10:06:33.37	-29:56:07.8	HII G	0.004	Blue	0.53	0.10
1RXH J100633.9-295612	10:06:33.90	-29:56:11.6	X	–	Blue	0.73	0.07
2MASX J10071106-1904039	10:07:11.07	-19:04:04.6	Galaxy	0.012	Blue	0.87	0.05
LEDA 699275	10:07:27.24	-31:55:26.9	Galaxy	–	Blue	0.94	0.06
CRTS J100733.7-301921	10:07:33.84	-30:19:19.4	EB*	–	Blue	0.80	0.03
RX J1007.5-2017	10:07:34.65	-20:17:32.4	CataclyV*	–	Blue	0.48	0.11
RX J1007.5-2017	10:07:34.66	-20:17:32.5	CataclyV*	–	Blue	0.18	0.08
2MASX J10081071-3331017	10:08:10.76	-33:31:02.2	Galaxy	0.010	Red	0.54	0.20
2MASX J10082199-1448362	10:08:22.01	-14:48:36.1	Galaxy	0.008	Blue	0.75	0.06
LEDA 768685	10:08:30.09	-26:21:33.0	Galaxy	–	Blue	0.97	0.03
2MASX J10091380-4300089	10:09:13.81	-43:00:09.0	GinGroup	0.015	Red	0.21	0.33
LEDA 648630	10:09:50.26	-35:27:43.3	Galaxy	–	Blue	0.97	0.03
LEDA 3094360	10:09:58.73	-20:30:59.5	Galaxy	–	Blue	0.84	0.06
ESO 435-50	10:10:50.41	-30:25:24.4	Galaxy	0.009	Blue	0.73	0.06
LEDA 654529	10:10:51.81	-35:00:28.1	Galaxy	–	Blue	1.00	0.00
NGC 3146	10:11:09.90	-20:52:14.0	EmG	0.013	Blue	0.75	0.06
LEDA 729120	10:11:13.49	-29:27:27.9	Galaxy	–	Blue	0.65	0.13
CRTS J101200.8-365725	10:12:00.81	-36:57:25.2	EB*	–	Red	0.32	0.28
LEDA 691325	10:12:03.36	-32:28:06.8	Galaxy	–	Blue	1.00	0.00
Gaia DR2 5407412036686860672	10:12:47.58	-47:33:51.1	Star	–	Blue	0.63	0.10
LEDA 655538	10:12:59.65	-34:56:06.6	Galaxy	–	Blue	0.99	0.01
2MASX J10134201-3451194	10:13:41.91	-34:51:18.3	EmG	0.015	Blue	0.72	0.08
LEDA 658182	10:13:54.08	-34:44:23.0	Galaxy	–	Blue	0.85	0.04
LEDA 713928	10:14:25.56	-30:42:30.1	Galaxy	–	Blue	0.67	0.03
2MASX J10142679-2329036	10:14:26.81	-23:29:04.9	Galaxy	0.012	Blue	0.99	0.01
ESO 263-21	10:14:41.74	-44:51:14.1	EmG	0.004	Blue	0.80	0.03
IC 2559	10:14:45.36	-34:03:33.0	EmG	0.010	Red	0.29	0.36
ESO 263-22	10:14:48.13	-43:31:49.5	Galaxy	0.010	Blue	0.69	0.06
ESO 263-23	10:14:57.32	-43:37:09.2	Galaxy	0.010	Red	0.35	0.23
ESO 567-32	10:15:44.54	-20:17:44.0	EmG	0.012	Red	0.06	0.34
Gaia DR2 5407327747940309248	10:15:58.31	-47:58:09.1	Star	–	Blue	0.32	0.08
IC 2560	10:16:18.68	-33:33:49.8	Seyfert 2	0.010	Red	0.33	0.28
ESO 567-39	10:17:13.15	-21:04:00.3	EmG	0.012	Blue	0.72	0.04
LEDA 702814	10:18:05.73	-31:38:49.0	Galaxy	–	Blue	0.64	0.07
[VV96] J101821.7-214008	10:18:21.76	-21:40:07.7	QSO	2.470	Blue	0.48	0.08
CRTS SSS120320 J101854-400644	10:18:53.51	-40:06:43.7	Candidate CV*	–	Blue	0.29	0.10
ESO 375-7	10:19:01.23	-37:40:19.2	Galaxy	0.016	Blue	1.00	0.00
CTS 1011	10:19:21.17	-22:08:33.4	HII G	0.012	Blue	0.43	0.12
CTS 1011	10:19:21.28	-22:08:35.9	HII G	0.012	Blue	0.58	0.14
NGC 3208	10:19:41.31	-25:48:52.9	EmG	0.010	Blue	0.62	0.06
6dFGS gJ102028.5-232845	10:20:28.52	-23:28:45.3	Galaxy	0.012	Blue	1.00	0.00
LEDA 800754	10:20:32.72	-23:26:54.0	Galaxy	–	Blue	0.48	0.09
CRTS SSS120215 J102042-335002	10:20:42.16	-33:50:02.4	Candidate CV*	–	Blue	0.61	0.08
Gaia DR2 5668001579559758720	10:20:43.31	-20:47:54.6	Star	–	Blue	0.54	0.07
ESO 500-30	10:20:48.90	-23:27:57.1	EmG	0.012	Red	0.63	0.18
6dFGS gJ102109.3-325140	10:21:09.27	-32:51:39.9	Galaxy	0.010	Blue	0.96	0.04
6dFGS gJ102121.0-213628	10:21:21.03	-21:36:27.7	Galaxy	0.011	Blue	0.99	0.01
LEDA 592969	10:22:02.22	-39:52:45.9	Galaxy	–	Blue	0.89	0.06
6dFGS gJ102239.9-302931	10:22:39.94	-30:29:30.6	AGN Candidate	0.317	Blue	0.45	0.08
ESO 263-30	10:22:59.54	-42:49:38.9	Galaxy	0.009	Blue	0.83	0.03
ESO 317-19	10:23:02.34	-39:09:59.8	GinGroup	0.010	Blue	0.84	0.06
ESO 375-18	10:23:40.27	-35:49:33.5	EmG	0.015	Red	0.40	0.39
ESO 375-18	10:23:40.27	-35:49:33.5	EmG	0.015	Red	0.29	0.45
ESO 263-32	10:24:21.47	-43:55:01.6	Galaxy	–	Blue	0.85	0.02
ESO 500-34	10:24:31.43	-23:33:09.6	Seyfert 2	0.012	Red	0.05	0.52
CRTS J102513.4-354014	10:25:13.46	-35:40:16.7	EB*	–	Blue	0.99	0.01

Table B1: –continued

Id Object	RA	Dec	Type	Redshift	Group	P(Blue)	P(Red)
						HAC	HDBSCAN
6dFGS gJ102607.5-243321	10:26:07.41	-24:33:20.2	Galaxy	0.013	Blue	0.75	0.08
ESO 436-21	10:26:21.70	-29:11:57.8	GinCl	–	Blue	0.96	0.01
NAME OT J102706-434341	10:27:05.83	-43:43:41.3	CataclyV*	–	Blue	0.75	0.05
ESO 500-42	10:27:20.27	-23:48:19.6		0.012	Blue	0.97	0.01
SN 2001db	10:27:50.35	-43:54:20.8	SN	–	Red	0.57	0.34
SN 2001db	10:27:50.37	-43:54:20.8	SN	–	Red	0.40	0.30
[LWZ2002] 5	10:27:51.28	-43:53:58.5	X	–	Blue	0.70	0.11
NGC 3256	10:27:51.29	-43:54:14.0	IG	0.009	Red	0.35	0.40
NGC 3256	10:27:51.30	-43:54:13.7	IG	0.009	Red	0.37	0.38
[LDT2000] R02	10:27:51.73	-43:54:13.6	X	–	Blue	0.94	0.06
[LDT2000] R02	10:27:51.73	-43:54:13.3	X	–	Blue	0.94	0.06
[EF2003] B3	10:27:52.88	-43:54:11.5	HII	0.010	Blue	0.45	0.07
[EF2003] B3	10:27:52.89	-43:54:11.2	HII	0.010	Blue	0.46	0.07
[EF2003] B3	10:27:52.89	-43:54:11.2	HII	0.010	Blue	0.46	0.07
ESO 436-26	10:28:42.96	-31:02:17.7	AGN	0.014	Red	0.33	0.27
CRTS CSS140309 J102844-161303	10:28:43.86	-16:13:03.3	CataclyV*	–	Blue	0.13	0.07
[SHM2017] J157.24190-30.14112	10:28:58.05	-30:08:27.7		–	Blue	0.19	0.04
ESO 317-34	10:29:00.71	-40:04:57.9	GinGroup	0.009	Blue	0.97	0.03
IC 2582	10:29:11.07	-30:20:32.7	EmG	0.014	Blue	0.79	0.05
LEDA 636268	10:30:30.59	-36:28:47.1	Galaxy	–	Blue	0.76	0.08
LEDA 636268	10:30:30.59	-36:28:47.1	Galaxy	–	Blue	0.65	0.05
LEDA 83158	10:30:57.69	-34:42:28.5	GinGroup	–	Blue	0.74	0.05
ESO 317-39	10:31:00.18	-40:10:42.5	Galaxy	0.015	Red	0.13	0.29
ESO 436-32	10:31:29.90	-32:42:47.1	EmG	0.013	Blue	0.51	0.11
NGC 3281	10:31:52.11	-34:51:13.0	Seyfert 2	0.011	Red	0.05	0.36
LEDA 571751	10:31:57.37	-41:48:41.1	Galaxy	–	Blue	0.62	0.02
[BM98] 2	10:32:59.22	-27:32:36.9	GinCl	0.016	Blue	0.95	0.02
6dFGS gJ103317.5-430444	10:33:17.40	-43:04:43.1	Galaxy	0.010	Blue	0.64	0.07
ESO 375-64	10:34:00.75	-35:16:57.6	GinGroup	0.009	Blue	0.62	0.07
ESO 375-64	10:34:00.75	-35:16:57.3	GinGroup	0.009	Blue	0.64	0.07
LEDA 754029	10:34:26.74	-27:30:04.0	GinCl	0.012	Blue	0.98	0.02
ESO 436-42	10:34:38.75	-28:35:00.1	EmG	0.012	Blue	0.76	0.04
ESO 568-18	10:34:54.59	-20:32:55.6	EmG	0.012	Blue	0.98	0.01
2MASX J10345852-4054438	10:34:58.52	-40:54:43.3	Galaxy	0.016	Blue	0.73	0.06
6dFGS gJ103502.9-293024	10:35:02.88	-29:30:23.8	GinCl	0.012	Blue	0.97	0.03
ESO 437-3	10:35:07.72	-27:59:28.7	EmG	0.008	Blue	0.70	0.04
ESO 375-69	10:35:18.72	-36:52:42.5	EmG	0.011	Blue	0.95	0.05
ESO 501-22	10:35:21.68	-27:41:44.5	GinCl	0.010	Blue	0.96	0.04
LEDA 712419	10:35:31.70	-30:50:00.0	Galaxy	–	Blue	0.62	0.03
LEDA 535830	10:35:34.16	-44:34:41.1	Galaxy	–	Blue	0.77	0.08
LEDA 784823	10:36:02.66	-24:54:24.1	Galaxy	–	Blue	0.81	0.03
LEDA 743415	10:36:06.94	-28:17:45.0	Galaxy	–	Blue	0.87	0.06
ESO 501-32	10:36:22.11	-25:22:35.4	EmG	0.013	Blue	0.81	0.05
[CZ2003] 1060C-393 25	10:36:30.34	-27:54:04.0	GinCl	0.008	Blue	0.82	0.06
6dFGS gJ103645.4-281005	10:36:45.48	-28:10:02.7	GinCl	0.012	Blue	0.90	0.03
LEDA 769967	10:36:54.86	-26:14:26.0	HII G	0.012	Blue	0.14	0.05
6dFGS gJ103656.1-265414	10:36:56.08	-26:54:13.6	Galaxy	0.096	Blue	0.99	0.01
LEDA 742546	10:37:01.84	-28:22:01.7	GinCl	–	Blue	0.87	0.05
6dFGS gJ103704.4-312157	10:37:04.45	-31:21:57.3	Galaxy	0.010	Blue	0.81	0.03
NGC 3314	10:37:12.87	-27:41:02.2	EmG	0.009	Blue	0.64	0.11
6dFGS gJ103719.9-281420	10:37:19.89	-28:14:19.9	GinCl	0.012	Blue	1.00	0.00
LEDA 753354	10:37:22.21	-27:32:41.9	Galaxy	–	Blue	0.70	0.08
WISE J103754.92-242544.5	10:37:54.92	-24:25:44.6	MIR	–	Red	0.14	0.47
ESO 501-61	10:38:05.84	-25:05:40.1	IG	0.012	Blue	0.94	0.02
[WLH83] 1036-378A	10:38:14.37	-38:05:25.5	HII	–	Blue	0.93	0.03
LEDA 740766	10:38:28.68	-28:30:55.0	GinCl	–	Blue	0.97	0.03
2MASX J10383034-2332546	10:38:30.34	-23:32:54.7	Galaxy	–	Blue	0.91	0.05
ESO 501-65	10:38:33.42	-27:44:13.8	EmG	0.015	Blue	0.86	0.06

Table B1: –continued

Id Object	RA	Dec	Type	Redshift	Group	P(Blue)	P(Red)
						HAC	HDBSCAN
WPVS 78	10:38:41.50	-25:35:32.2	EmG	0.010	Blue	0.49	0.12
6dFGS gJ103857.2-200242	10:38:57.24	-20:02:41.8	Galaxy	0.007	Blue	0.91	0.02
LEDA 838980	10:39:13.02	-20:38:12.5	Galaxy	–	Blue	0.64	0.04
MCG-04-25-054	10:39:26.01	-23:45:16.8	EmG	0.013	Blue	0.60	0.06
2MASS J10395999-4701261	10:39:59.97	-47:01:26.3	CataclyV*	–	Blue	0.55	0.12
2MASS J10395999-4701261	10:39:59.97	-47:01:26.3	CataclyV*	–	Blue	0.55	0.12
ESO 437-37	10:40:31.01	-29:16:10.5	IG	0.012	Blue	0.90	0.03
ESO 568-20	10:40:58.70	-21:47:04.3	EmG	0.012	Red	0.22	0.50
6dFGS gJ104102.1-304740	10:41:02.12	-30:47:40.1	Galaxy	0.011	Blue	0.82	0.05
CRTS J104104.0-341120	10:41:03.86	-34:11:23.4	RRLyr	–	Blue	1.00	0.00
ESO 568-21	10:41:15.17	-21:01:22.9	Seyfert 1	0.012	Blue	0.95	0.03
ESO 437-42	10:41:27.71	-31:46:49.1	Galaxy	0.009	Blue	0.82	0.05
ESO 437-42	10:41:27.71	-31:46:49.1	Galaxy	0.009	Blue	0.82	0.05
LEDA 3081775	10:41:35.15	-37:28:09.5	Galaxy	–	Blue	0.81	0.05
6dFGS gJ104139.4-274638	10:41:39.43	-27:46:38.2	Galaxy	0.014	Blue	0.66	0.07
ESO 568-22	10:42:06.62	-22:06:20.1	IG	0.007	Blue	0.74	0.05
LEDA 31904	10:42:19.50	-36:19:13.7	Galaxy	–	Blue	0.97	0.03
6dFGS gJ104238.0-235609	10:42:37.99	-23:56:08.4	Galaxy	0.003	Blue	0.90	0.02
ESO 437-50	10:43:31.00	-30:46:20.0	EmG	0.013	Blue	0.76	0.03
ESO 437-50	10:43:31.00	-30:46:20.0	EmG	0.013	Blue	0.76	0.03
6dFGS gJ104409.7-204909	10:44:09.71	-20:49:09.5	Galaxy	0.013	Blue	0.82	0.04
ESO 569-2	10:45:00.21	-22:09:08.2	IG	0.010	Blue	1.00	0.00
6dFGS gJ104534.8-241702	10:45:34.75	-24:17:01.3	Galaxy	0.012	Blue	0.80	0.07
6dFGS gJ104617.1-282524	10:46:17.11	-28:25:23.6	EmG	0.012	Blue	0.73	0.04
LEDA 718607	10:46:30.26	-30:19:17.8	Galaxy	–	Blue	0.83	0.04
ESO 376-20	10:46:38.45	-36:21:11.9	EmG	0.014	Blue	0.69	0.07
ESO 501-96	10:46:47.54	-23:19:39.8	Galaxy	0.011	Blue	0.94	0.06
Gaia DR2 5391507429181636352	10:47:23.91	-41:59:49.3	Star	–	Blue	0.56	0.07
EC 10453-2041	10:47:44.36	-20:57:48.8	EmG	0.012	Blue	0.53	0.09
2MASX J10475221-2004542	10:47:52.11	-20:04:53.3	HII G	0.013	Blue	0.87	0.02
2MASX J10475221-2004542	10:47:52.13	-20:04:53.5	HII G	0.013	Blue	1.00	0.00
[KRB2015] A	10:48:23.47	-25:09:43.6	Radio	–	Red	0.62	0.19
2MASX J10482527-2151000	10:48:25.30	-21:51:00.5	Galaxy	0.015	Blue	0.73	0.04
SN 2018aqi	10:48:25.45	-25:09:36.1	SN	0.012	Red	0.20	0.07
LEDA 688498	10:48:42.32	-32:38:37.4	Galaxy	–	Blue	1.00	0.00
LEDA 738826	10:49:46.88	-28:40:37.1	Galaxy	–	Blue	0.50	0.08
2MASX J10503963-1832342	10:50:39.64	-18:32:34.4	Galaxy	0.014	Red	0.43	0.22
LEDA 844461	10:51:00.37	-20:14:21.3	Galaxy	–	Blue	1.00	0.00
6dFGS gJ105101.9-282017	10:51:01.81	-28:20:16.5	Galaxy	0.011	Blue	0.85	0.03
LEDA 851789	10:51:27.40	-19:41:37.0	Galaxy	–	Blue	0.99	0.01
6dFGS gJ105149.2-215323	10:51:49.07	-21:53:17.5	Galaxy	0.010	Blue	0.67	0.05
6dFGS gJ105233.0-230900	10:52:33.04	-23:08:59.6	Galaxy	0.318	Blue	0.29	0.08
MASTER OT J105440.86-391319.0	10:54:40.84	-39:13:19.0	Candidate SN*	–	Blue	0.76	0.08
6dFGS gJ105521.6-232527	10:55:21.62	-23:25:27.3	Galaxy	0.012	Blue	0.87	0.06
6dFGS gJ105521.6-232527	10:55:21.63	-23:25:27.3	Galaxy	0.012	Blue	0.90	0.04
2MASX J10563839-2047119	10:56:38.39	-20:47:12.2	Galaxy	0.012	Blue	0.87	0.03
LEDA 849870	10:56:48.51	-19:50:00.4	Galaxy	–	Blue	0.85	0.08
ESO 376-28	10:57:04.32	-33:09:20.3	Galaxy	0.013	Red	0.45	0.30
ESO 264-52	10:57:13.91	-47:40:11.3	Galaxy	0.016	Red	0.63	0.14
LEDA 648093	10:57:36.52	-35:30:15.8	Galaxy	–	Blue	1.00	0.00
2MASX J10584423-1909304	10:58:44.25	-19:09:31.1	Galaxy	0.012	Blue	1.00	0.00
EC 10566-3120	10:58:59.03	-31:36:34.1	CataclyV*	–	Blue	0.52	0.08
2MASX J10590982-2759589	10:59:09.86	-27:59:59.3	Galaxy	0.005	Blue	0.91	0.04
Gaia DR2 5386613537284200960	11:01:51.26	-46:53:04.5	Candidate RRLyr	–	Blue	1.00	0.00
Gaia DR2 353711743043448320	11:01:57.97	-23:47:27.3	PM*	–	Blue	0.53	0.10
V* TU Crt	11:03:36.57	-21:37:45.9	CataclyV*	–	Blue	0.58	0.09
NGC 3513	11:03:46.16	-23:14:42.1	GinPair	0.004	Blue	0.76	0.04
FAUST 2807	11:03:59.06	-18:46:36.1	UV	–	Blue	1.00	0.00

Table B1: –continued

Id Object	RA	Dec	Type	Redshift	Group	P(Blue)	P(Red)
						HAC	HDBSCAN
ESO 570-5	11:07:13.10	-19:49:07.2	IG	0.012	Blue	0.89	0.05
NGC 3529	11:07:19.13	-19:33:20.0	EmG	0.013	Blue	0.96	0.03
NGC 3529	11:07:19.14	-19:33:19.5	EmG	0.013	Blue	0.96	0.02
NGC 3565	11:07:47.84	-20:01:20.2	IG	0.013	Blue	0.89	0.04
ESO 570-10	11:10:50.57	-21:58:28.3	Galaxy	0.012	Blue	0.86	0.08
LEDA 821419	11:10:57.23	-21:56:53.3	Galaxy	–	Blue	0.89	0.03
6dFGS gJ111351.0-212655	11:13:50.97	-21:26:54.8	Galaxy	0.012	Blue	0.88	0.07
NGC 3597	11:14:42.00	-23:43:39.9	EmG	0.012	Blue	0.67	0.08
[VV96] J111644.8-171127	11:16:43.58	-17:11:41.5	QSO	0.375	Blue	0.41	0.07
LEDA 861413	11:17:15.01	-18:58:24.4	Galaxy	–	–	–	–
LEDA 809402	11:17:35.06	-22:45:06.2	Galaxy	–	Red	0.29	0.49
CRTS J112256.0-242841	11:22:56.09	-24:28:40.0	EB*	–	Blue	1.00	0.00
LEDA 786212	11:29:34.18	-24:46:39.1	Galaxy	–	Blue	0.50	0.08
[VV2010c] J113128.4-195903	11:31:28.46	-19:59:02.8	AGN	0.363	Blue	0.58	0.07
CRTS SSS110509 J113219-213943	11:32:19.01	-21:39:42.9	Candidate CV*	–	–	–	–
2dFGRS TGN444Z198	11:34:24.52	01:09:15.7	Galaxy	0.017	Blue	0.88	0.04
MGC 22410	11:36:12.70	00:04:54.9	Star	–	Blue	1.00	0.00
UGC 6578	11:36:36.73	00:49:02.1	EmG	0.004	Blue	0.58	0.13
GAMA 6821	11:36:36.79	00:48:55.8	Galaxy	0.004	Blue	0.08	0.04
V* RZ Leo	11:37:22.18	01:48:58.9	CataclyV*	-0.000	Blue	0.17	0.05
Gaia DR2 3541998025080414336	11:37:49.97	-20:07:37.1	Candidate WD*	–	Blue	0.37	0.10
2dFGRS TGN238Z266	11:38:54.33	-01:38:34.1	Galaxy	0.006	Blue	0.49	0.08
CRTS J113855.5-211148	11:38:55.60	-21:11:47.7	RRLyr	–	Blue	0.97	0.03
SDSS J113901.39+012017.8	11:39:01.39	01:20:17.7	Galaxy	0.005	Blue	0.37	0.11
LBQS 1136-0109	11:39:04.35	-01:26:25.0	QSO	1.375	Blue	0.81	0.03
6dFGS gJ114135.0-181141	11:41:35.04	-18:11:40.5	Galaxy	0.012	Blue	0.95	0.02
2dFGRS TGN238Z191	11:41:45.67	-01:54:04.8	HII G	0.006	Blue	0.86	0.06
ESO 571-16	11:42:09.14	-18:10:08.7	Galaxy	0.012	Red	0.05	0.40
SDSS J114212.38+002002.5	11:42:12.33	00:20:03.4	PartofG	0.019	Blue	0.98	0.02
2QZ J114214.5-023154	11:42:14.64	-02:31:53.3	Galaxy	0.319	Blue	0.90	0.02
CRTS J114238.0-202722	11:42:37.96	-20:27:21.8	RRLyr	–	Blue	0.99	0.01
2QZ J114250.9+013057	11:42:50.95	01:30:58.2	Seyfert 1	0.361	Blue	0.80	0.08
SDSS J114329.34-020319.7	11:43:29.34	-02:03:19.5	QSO	3.304	–	–	–
SDSS J114329.34-020319.7	11:43:29.35	-02:03:19.9	QSO	3.304	–	–	–
SDSSCGB 59619.2	11:43:46.11	-01:16:34.0	Galaxy	–	–	–	–
GAMA 396970	11:43:47.41	01:30:53.9	Galaxy	0.102	Blue	0.59	0.06
LINEAR 2118419	11:44:08.82	01:24:20.7	RRLyr	0.001	Blue	0.98	0.02
2QZ J114450.8+014324	11:44:50.95	01:43:24.8	EmG	0.333	Blue	0.58	0.07
Gaia DR2 3544179185567992320	11:44:55.76	-17:56:39.4	Candidate WD*	–	Blue	0.46	0.11
2dFGRS TGN310Z256	11:45:08.04	-00:59:18.2	Galaxy	0.004	Blue	0.48	0.09
SDSS J114511.70-005402.6	11:45:11.72	-00:54:02.5	Galaxy	0.204	Red	0.15	0.75
2MASX J11451524-2044471	11:45:15.26	-20:44:47.5	Galaxy	0.012	Blue	0.70	0.08
Z 12-78	11:45:26.30	00:00:14.8	Galaxy	0.013	Blue	0.95	0.05
SDSS J114600.44+001037.4	11:46:00.45	00:10:37.0	Galaxy	0.311	Red	0.29	0.55
2dFGRS TGN310Z211	11:46:07.72	-00:27:28.7	Galaxy	0.013	Blue	0.97	0.03
SDSS J114643.10+011118.6	11:46:43.12	01:11:18.8	QSO	3.220	Blue	0.80	0.05
2QZ J114711.4-002706	11:47:11.47	-00:27:05.8	EmG	0.312	Blue	0.98	0.02
2MASX J11481815-0138230	11:48:18.21	-01:38:23.8	Seyfert 1	0.013	Blue	0.81	0.06
SDSS J114818.33-013830.8	11:48:18.35	-01:38:30.5	Galaxy	0.013	Blue	0.52	0.08
[VV2006] J114939.6+014624	11:49:39.60	01:46:25.5	QSO	1.362	Blue	0.56	0.06
2dFGRS TGN378Z115	11:50:23.78	-00:31:41.9	HII G	0.013	Blue	0.54	0.11
[P78] ACO 1392 C	11:50:36.30	-00:34:06.6	GinCl	0.006	Blue	0.58	0.13
SDSS J115036.42-003402.0	11:50:36.39	-00:34:02.6	Galaxy	0.006	Blue	0.57	0.13
[VV2006] J115049.2-005149	11:50:49.29	-00:51:49.1	QSO	1.354	Blue	0.34	0.08
LEDA 807513	11:51:13.02	-22:53:25.2	Galaxy	–	Red	0.34	0.44
SDSS J115129.42-000333.8	11:51:29.45	-00:03:33.6	Galaxy	0.326	Red	0.20	0.34
2dFGRS TGN242Z154	11:51:32.96	-02:22:21.9	Galaxy	0.004	Blue	0.26	0.09
LEDA 37102	11:51:33.35	-02:22:21.7	Seyfert 1	0.003	Blue	0.06	0.03

Table B1: –continued

Id Object	RA	Dec	Type	Redshift	Group	P(Blue)	P(Red)
						HAC	HDBSCAN
SDSS J115216.86+012327.2	11:52:16.88	01:23:27.5	Galaxy	0.304	Red	0.11	0.59
2QZ J115217.3-025303	11:52:17.34	-02:53:02.7	EmG	0.320	Blue	0.97	0.02
ESO 572-7	11:52:27.62	-20:06:14.1	GinGroup	0.005	Blue	0.80	0.03
Mrk 1307	11:52:37.30	-02:28:09.4		0.004	Blue	0.24	0.08
SDSS J115237.67-022806.3	11:52:37.67	-02:28:06.8	HII G	0.004	Blue	0.27	0.09
2dFGRS TGN311Z206	11:52:47.52	-00:40:07.7	Seyfert 1	0.005	Blue	0.25	0.09
2dFGRS TGN311Z206	11:52:47.53	-00:40:07.8	Seyfert 1	0.005	Blue	0.26	0.09
2dFGRS TGN176Z274	11:53:14.07	-03:24:32.6	Galaxy	0.004	Blue	0.66	0.07
2dFGRS TGN243Z103	11:53:28.66	-03:13:48.9	Galaxy	0.005	Blue	1.00	0.00
[VV2006] J115345.5-024320	11:53:45.44	-02:43:20.4	QSO	1.347	Blue	0.84	0.04
UM 465B	11:54:12.31	00:08:12.4	GinPair	–	Blue	0.88	0.07
SDSS J115456.54+001106.0	11:54:56.59	00:11:05.5	Galaxy	0.004	–	–	–
SDSS J115511.13+002905.1	11:55:11.19	00:29:05.5	Galaxy	0.011	Blue	0.30	0.09
SDSS J115511.67+002925.0	11:55:11.70	00:29:25.0	Galaxy	0.011	Blue	0.39	0.09
2dFGRS TGN243Z202	11:57:11.86	-02:41:12.9	Galaxy	0.005	Blue	0.57	0.13
SDSS J115712.38-024111.2	11:57:12.29	-02:41:11.3	Galaxy	0.005	Blue	0.58	0.14
ESO 572-25	11:57:28.04	-19:37:26.5	Galaxy	0.006	Blue	0.52	0.08
2QZ J115737.0-020138	11:57:37.08	-02:01:37.3	Galaxy	0.328	Blue	0.80	0.07
2QZ J115737.0-020138	11:57:37.09	-02:01:37.2	Galaxy	0.328	Blue	0.84	0.04
[VV2006] J115748.0+014320	11:57:48.02	01:43:20.9	QSO	1.364	Blue	0.56	0.05
[VV2006] J115754.2-013815	11:57:54.26	-01:38:16.0	QSO	4.380	–	–	–
LEDA 839904	11:57:56.69	-20:33:56.4	Galaxy	–	Blue	0.39	0.11
2MASX J11580803-1753363	11:58:08.00	-17:53:36.2	Galaxy	0.008	Blue	0.83	0.04
6dFGS gJ115823.8-193103	11:58:23.80	-19:31:03.2	Galaxy	0.005	Blue	0.54	0.07
ESO 572-34	11:58:58.18	-19:01:47.7	EmG	0.004	Blue	0.55	0.13
GAMA 137854	11:59:23.49	-01:43:22.3	Galaxy	0.304	Blue	0.59	0.16
SN 1996W	11:59:28.93	-19:15:22.8	SN	–	Blue	0.85	0.04
LEDA 836770	12:00:19.81	-20:48:07.5	Galaxy	–	Blue	0.78	0.05
2MASX J12002013-0106229	12:00:20.20	-01:06:23.8	Galaxy	0.005	Blue	0.89	0.04
SDSS J120021.76-024331.0	12:00:21.77	-02:43:30.9	QSO	3.248	Blue	0.81	0.03
[BKD2008] WR 14	12:00:26.30	-01:06:07.0	PartofG	0.005	Blue	0.51	0.08
[VV2006] J120038.3+011246	12:00:38.29	01:12:46.5	QSO	1.358	Blue	0.68	0.08
QSO B1158-1842	12:00:44.95	-18:59:44.5	QSO	2.453	Blue	0.53	0.07
2dFGRS TGN244Z048	12:00:47.47	-03:25:12.1	Galaxy	0.005	Blue	0.99	0.01
[RDS2004] MGS sure 22	12:00:47.72	-00:01:24.3	HI	0.006	Blue	0.97	0.03
UGC 7000	12:01:10.85	-01:17:50.2	GinPair	0.005	Blue	1.00	0.00
QSO B1158+007	12:01:23.26	00:28:28.5	QSO	1.369	Blue	0.78	0.08
LEDA 802182	12:01:30.48	-23:19:06.8	Galaxy	–	Blue	0.71	0.02
[CEB2007] Cluster 2	12:01:50.41	-18:52:12.4	Cl*	–	Blue	0.54	0.08
CXOU J120150.4-185221	12:01:50.41	-18:52:19.8	HMXB	–	Blue	0.56	0.07
[ZBF2015] Arp244 82	12:01:50.49	-18:52:02.5	HII	–	Blue	0.94	0.06
[NU2000] 9 3	12:01:51.13	-18:52:28.8	Radio	–	Blue	0.85	0.03
[NU2000] 13 5	12:01:51.24	-18:51:45.3	Radio	–	Blue	0.60	0.04
[MLT2008] S2-2	12:01:51.90	-18:52:28.2	Cl*	–	Blue	0.78	0.03
[ZBF2015] Arp244 123	12:01:52.28	-18:52:19.4	HII	–	Blue	0.99	0.01
[ZBF2015] Arp244 80	12:01:52.96	-18:52:03.5	HII	–	Red	0.31	0.60
[ZBF2015] Arp244 5	12:01:52.98	-18:52:08.7	HII	–	Blue	0.98	0.02
[ZBF2015] Arp244 14	12:01:53.52	-18:51:44.2	HII	–	Blue	0.92	0.03
[WZ2002] 1	12:01:53.57	-18:53:09.0	Radio	–	Red	0.29	0.29
[BEK2006] Complex 6	12:01:54.54	-18:52:07.5	Cl*	–	Blue	0.56	0.03
[WS95] 89	12:01:54.54	-18:53:03.8	PartofG	–	Blue	0.57	0.07
[WBC2014] 180.48062-18.88025	12:01:55.35	-18:52:48.7	MolCld	0.005	Blue	0.34	0.06
[ZBF2015] Arp244 6	12:01:55.54	-18:52:22.9	HII	–	Blue	0.85	0.02
[ZFB2014] GMC 98	12:01:55.68	-18:52:14.0	MolCld	–	Blue	0.67	0.02
[WZ2002] 9	12:01:55.70	-18:52:42.8	Radio	–	Blue	0.35	0.06
[ZBF2015] Arp244 10	12:01:56.29	-18:52:38.8	HII	–	Blue	1.00	0.00
CRTS J120206.7-230305	12:02:06.75	-23:03:06.0	EB*	–	Blue	0.95	0.02
SDSS J120250.38+001931.6	12:02:50.39	00:19:31.5	Galaxy	0.333	Red	0.05	0.39

Table B1: –continued

Id Object	RA	Dec	Type	Redshift	Group	P(Blue)	P(Red)
						HAC	HDBSCAN
SDSS J120515.80-024222.6	12:05:15.80	-02:42:22.6	WD*	0.000	Blue	0.38	0.08
LEDA 913203	12:06:37.73	-15:17:17.2	Galaxy	–	Blue	0.97	0.03
6dFGS gJ120650.7-141256	12:06:50.66	-14:12:55.9	Galaxy	0.013	Blue	0.79	0.04
[VV2006] J120700.4+011155	12:07:00.41	01:11:56.4	QSO	1.520	Blue	0.75	0.07
SDSS J120920.53-002855.3	12:09:20.55	-00:28:55.3	QSO	3.237	Blue	0.83	0.05
[VV2006] J121010.8-003909	12:10:10.82	-00:39:09.7	QSO	1.008	Blue	0.07	0.06
SDSS J121026.38-000513.2	12:10:26.41	-00:05:13.2	Galaxy	0.310	Blue	0.70	0.04
SDSS J121043.55-003907.2	12:10:43.59	-00:39:08.5	Seyfert 1	0.331	Red	0.03	0.06
2QZ J121101.0+012024	12:11:01.05	01:20:25.0	EmG	0.333	Blue	0.96	0.04
Mrk 1313	12:12:14.73	00:04:20.6	Seyfert 1	0.008	Blue	0.77	0.08
2dFGRS TGN246Z007	12:12:15.90	-00:33:53.2	Galaxy	0.008	Blue	0.54	0.07
2MASS J12125978+0149231	12:12:59.78	01:49:23.2	EB*	–	Red	0.63	0.21
SDSS J121304.91-003901.2	12:13:04.93	-00:39:01.2	Galaxy	0.189	Red	0.06	0.64
2dFGRS TGN247Z167	12:13:38.79	-01:17:36.3	Galaxy	0.008	Blue	0.86	0.03
6dFGS gJ121348.2-143140	12:13:48.16	-14:31:39.8	Galaxy	0.330	Blue	0.62	0.06
SDSS J121435.24-015924.4	12:14:35.26	-01:59:24.4	QSO	3.233	Blue	0.86	0.09
[VV2006] J121515.2-013542	12:15:15.23	-01:35:40.8	QSO	1.350	Blue	0.57	0.04
2QZ J121539.4-022149	12:15:39.47	-02:21:47.2	Galaxy	0.319	Blue	0.78	0.05
2QZ J121607.5-022559	12:16:07.54	-02:25:57.6	Galaxy	0.324	Blue	1.00	0.00
SDSS J121759.99+002558.1	12:18:00.05	00:25:57.7	Galaxy	0.003	–	–	–
2dFGRS TGN181Z079	12:18:07.07	-03:06:28.8	Galaxy	0.001	Red	0.12	0.71
LEDA 927634	12:18:19.06	-14:12:19.9	Galaxy	–	Blue	0.97	0.03
LEDA 927634	12:18:19.06	-14:12:20.0	Galaxy	–	Blue	0.96	0.04
QSO B1216+0216	12:18:55.80	02:00:02.1	QSO	0.327	Blue	0.31	0.09
[VV2006] J121942.5-001821	12:19:42.47	-00:18:21.4	QSO	1.337	Blue	0.79	0.07
2dFGRS TGN385Z034	12:19:53.13	01:46:24.0	HII G	0.007	Blue	0.88	0.05
SDSS J122003.72+010632.0	12:20:03.73	01:06:32.4	Galaxy	0.315	Red	0.07	0.21
2dFGRS TGN385Z025	12:20:11.53	01:57:31.1	LSB G	0.007	Blue	0.54	0.13
2dFGRS TGN181Z173	12:20:28.80	-01:50:21.0	Galaxy	0.008	Blue	0.82	0.06
LEDA 1143004	12:20:30.39	-00:27:03.0	Galaxy	0.007	–	–	–
[VV2006] J122130.9+010727	12:21:30.97	01:07:28.1	QSO	1.370	Blue	0.66	0.04
Gaia DR2 3521773745637847552	12:21:34.41	-14:57:50.5	Star	–	Blue	0.09	0.04
LEDA 3294456	12:21:55.83	-01:35:36.0	Galaxy	0.006	Blue	0.54	0.08
Gaia DR2 3521681421020417408	12:22:39.34	-15:29:12.1	Star	–	Blue	0.43	0.09
SDSS J122322.39-000801.6	12:23:22.39	-00:08:01.7	Galaxy	0.318	Blue	0.69	0.03
MCG+00-32-004	12:24:12.47	00:34:01.0	Galaxy	0.007	Blue	0.96	0.04
2SLAQ J122421.12+002354.1	12:24:21.13	00:23:54.4	QSO	0.334	Blue	0.55	0.11
NGC 4385	12:25:42.74	00:34:21.9	AGN	0.007	Blue	0.60	0.04
2QZ J122547.3-012007	12:25:47.38	-01:20:05.7	Galaxy	0.317	Blue	0.72	0.03
SHOC 373a	12:26:22.64	-01:15:17.3	HII G	0.007	Blue	0.34	0.09
SHOC 373b	12:26:22.73	-01:15:12.3	HII G	0.007	Blue	0.21	0.07
[VV2006] J122625.7+011604	12:26:25.67	01:16:04.6	QSO	2.478	Blue	0.57	0.09
2SLAQ J122641.43-002005.1	12:26:41.45	-00:20:05.1	Seyfert 1	0.353	Blue	0.60	0.06
MCG+00-32-013	12:27:04.54	-00:54:21.5	GinPair	0.007	Blue	0.84	0.07
MCG+00-32-013	12:27:04.56	-00:54:22.0	GinPair	0.007	Blue	0.87	0.03
[VV2006] J122707.1+010811	12:27:07.13	01:08:11.3	QSO	2.189	Blue	0.16	0.04
[MIO2012] R1	12:27:46.07	01:36:01.5	Cl*	–	Blue	0.57	0.12
2dFGRS TGN387Z059	12:28:15.92	01:49:43.7	Galaxy	0.003	Blue	1.00	0.00
2QZ J122851.2-022630	12:28:51.34	-02:26:29.2	EmG	0.331	Blue	0.93	0.07
2dFGRS TGN250Z094	12:29:14.65	-01:21:55.2	Galaxy	0.007	Blue	0.51	0.08
2dFGRS TGN250Z087	12:29:46.33	-01:17:42.0	LSB G	0.008	Blue	0.76	0.15
2dFGRS TGN321Z099	12:29:58.88	00:01:37.9	RadioG	0.008	Red	0.08	0.68
2dFGRS TGN388Z078	12:30:54.31	00:57:50.5	Galaxy	0.008	Blue	0.66	0.08
[BKD2008] WR 29	12:31:48.01	-02:58:13.0	PartofG	0.008	Blue	0.80	0.03
2QZ J123202.6+003124	12:32:02.70	00:31:24.7	EmG	0.329	Blue	0.79	0.07
2dFGRS TGN251Z016	12:32:23.64	-01:44:24.3	HII G	0.007	Blue	0.77	0.03
GALEX 2414740977348515009	12:32:36.17	-03:18:39.4	Blue	–	Blue	0.57	0.05
MGC 34804	12:32:41.58	00:03:26.4	Star	–	Blue	0.74	0.11

Table B1: –continued

Id Object	RA	Dec	Type	Redshift	Group	P(Blue)	P(Red)
						HAC	HDBSCAN
[DCD2013] CSS J123702.3-151643	12:37:02.41	-15:16:43.5	RRLyr	–	Blue	0.90	0.01
Gaia DR2 3527007524064861312	12:39:19.45	-14:47:31.1	Star	–	–	–	–
2MASX J12442692-1252359	12:44:26.92	-12:52:35.9	Galaxy	0.018	Blue	1.00	0.00
LEDA 924051	12:50:47.04	-14:29:01.5	Galaxy	–	Blue	1.00	0.00
LEDA 932206	12:58:59.15	-13:51:42.3	Galaxy	–	Blue	0.52	0.08
CRTS SSS120721 J125901-133442	12:59:00.82	-13:34:42.0	Candidate CV*	–	Blue	0.48	0.09
6dFGS gJ125904.7-144623	12:59:04.67	-14:46:23.5		0.016	Blue	0.73	0.04
2MASX J12593269-1514196	12:59:32.75	-15:14:19.3	Galaxy	–	Blue	0.31	0.10
LEDA 914340	13:00:03.04	-15:12:17.2	Galaxy	–	Blue	0.98	0.02
NGC 4887	13:00:39.30	-14:39:59.3	GinPair	0.009	Blue	0.98	0.02
LEDA 936912	13:01:07.09	-13:31:02.4	Galaxy	0.004	Blue	0.33	0.09
[VV96] J130243.5-135553	13:02:43.59	-13:55:52.8	QSO	1.391	Blue	0.54	0.07
LEDA 45114	13:03:33.44	-14:19:23.1	EmObj	0.008	Blue	0.76	0.08
2MASX J13044961-1311288	13:04:49.65	-13:11:28.2	Galaxy	0.010	Blue	0.72	0.06
LCRS B130214.7-120615	13:04:52.39	-12:22:18.7	Galaxy	–	Blue	1.00	0.00
LEDA 949391	13:05:58.52	-12:40:08.5	Galaxy	–	Blue	0.62	0.07
LEDA 105081	13:10:08.77	-12:12:20.4	Galaxy	0.013	Blue	0.90	0.02
UGCA 332	13:11:58.29	-12:03:51.4	EmG	0.007	Blue	0.90	0.04
LEDA 976320	13:12:28.41	-10:35:24.4	Galaxy	–	Blue	0.86	0.07
LCRS B131057.8-121222	13:13:36.14	-12:28:15.2	EmObj	0.013	Blue	0.49	0.12
LEDA 126038	13:15:07.97	-12:31:05.1	Galaxy	0.013	Blue	1.00	0.00
LEDA 981336	13:17:40.89	-10:10:59.5	Galaxy	–	Blue	1.00	0.00
SDSS J131742.35-002015.8	13:17:42.37	-00:20:15.7	Galaxy	0.356	–	–	–
6dFGS gJ131743.9-010002	13:17:43.96	-01:00:01.1	AGN	0.004	Blue	0.08	0.04
2MASX J13192221-1509232	13:19:22.29	-15:09:23.6	Galaxy	0.009	Blue	0.96	0.04
MCG-02-34-029	13:19:42.72	-11:28:28.5	GinGroup	0.009	Blue	0.98	0.02
2SLAQ J131957.59-003446.7	13:19:57.60	-00:34:46.6	Star	–	Blue	0.97	0.03
QSO B1317-122	13:19:59.20	-12:29:16.8	QSO	0.329	Blue	0.46	0.09
NGC 5088	13:20:20.33	-12:34:18.1	Galaxy	0.005	Blue	0.89	0.03
SDSS J132023.46-004730.9	13:20:23.47	-00:47:30.8	QSO	3.255	–	–	–
6dFGS gJ132134.7-151056	13:21:34.68	-15:10:55.5	Galaxy	0.009	Blue	1.00	0.00
6dFGS gJ132137.8-145120	13:21:37.83	-14:51:19.7	Galaxy	0.009	Blue	0.97	0.01
2dFGRS TGN263Z056	13:22:17.11	-00:32:54.4	EmG	0.018	–	–	–
[SHM2017] J200.93368-12.05326	13:23:44.09	-12:03:11.8	RRLyr	–	Blue	0.96	0.03
LEDA 46982	13:25:48.67	-11:36:37.8	BlueCompG	0.004	Blue	0.06	0.03
LEDA 46982	13:25:48.68	-11:36:38.0		0.004	Blue	0.06	0.03
LEDA 991902	13:26:05.10	-09:22:12.6	Galaxy	–	Blue	0.54	0.09
BPS CS 22889-0007	13:31:59.47	-09:53:02.6	RRLyr	0.001	Blue	0.99	0.01
NVSS J133618-072251	13:36:18.64	-07:22:51.8	Radio	–	Blue	0.73	0.08
LCRS B133356.3-061328	13:36:33.05	-06:28:45.2	Galaxy	–	Red	0.07	0.85
GALEX 2697385722761974216	13:39:09.19	-08:19:40.8	Blue	–	Blue	0.65	0.03
LEDA 1025584	13:41:04.99	-07:01:05.8	Galaxy	–	Blue	0.65	0.02
[DCD2013] CSS J134330.9-151858	13:43:31.01	-15:18:58.9	RRLyr	–	Blue	1.00	0.00
V* HS Vir	13:43:38.44	-08:14:03.7	CataclyV*	–	Blue	0.86	0.06
SN 2018evt	13:46:39.20	-09:38:36.0	SN	0.029	Blue	0.83	0.04
GALEX 2697315366902694354	13:47:49.82	-04:10:10.6	Blue	–	Blue	0.61	0.05
2dFGRS TGN202Z201	13:49:42.20	-02:11:59.1	Galaxy	0.011	Blue	0.74	0.03
GALEX 2699039396840082228	13:50:33.33	-12:16:42.9	Blue	–	Blue	0.55	0.07
6dFGS gJ135123.7-060412	13:51:23.70	-06:04:11.7	Galaxy	0.010	Blue	0.98	0.02
2dFGRS TGN202Z136	13:51:35.65	-02:33:15.0	Galaxy	0.015	Blue	0.99	0.01
SDSSCGB 287.4	13:52:03.90	-02:07:22.3	Galaxy	–	Blue	0.79	0.09
SDSSCGB 287.2	13:52:04.24	-02:07:48.9	Galaxy	0.015	Blue	0.65	0.07
LEDA 126156	13:54:11.29	-03:26:27.2	Galaxy	0.014	Blue	0.80	0.08
LEDA 126156	13:54:11.40	-03:26:27.0	Galaxy	0.014	Blue	0.90	0.04
QSO B1352-104	13:54:46.53	-10:41:02.6	QSO	0.330	Blue	0.41	0.06
VV 99b	13:55:33.98	-05:58:17.0	GinPair	–	Blue	0.87	0.07
2dFGRS TGN141Z158	13:55:37.68	-04:11:43.8	Galaxy	0.012	Blue	0.33	0.10
VV 100a	13:55:45.46	-06:00:15.9	Galaxy	–	Blue	0.74	0.07

Table B1: –continued

Id Object	RA	Dec	Type	Redshift	Group	P(Blue)	P(Red)
						HAC	HDBSCAN
VV 100d	13:55:46.68	-06:00:40.8	Galaxy	–	Blue	0.56	0.14
[VV2006] J135602.8-022624	13:56:02.79	-02:26:23.3	QSO	1.373	–	–	–
2dFGRS TGN203Z232	13:56:53.48	-02:38:52.2	Galaxy	0.013	Blue	0.62	0.05
2dFGRS TGN142Z266	13:58:08.62	-04:08:43.6	Galaxy	0.015	Blue	0.75	0.02
SDSSCGB 16922.1	13:58:41.49	-01:31:15.7	Galaxy	–	Red	0.28	0.36
LEDA 1020082	14:02:45.08	-07:22:25.8	Galaxy	–	Blue	0.52	0.08
2MASS J14265388+0525172	14:26:53.89	05:25:17.4	QSO	0.323	Blue	0.45	0.10
UGC 9252	14:27:10.82	05:07:59.3	Galaxy	0.005	Blue	1.00	0.00
[LAM2019] J1428+0500 B	14:28:55.39	05:00:21.9	Possible lens	–	Blue	0.62	0.10
GALEX 2429518413625830432	14:28:55.46	05:00:19.9	Blue	–	Blue	0.81	0.07
DES J142943.42+052122.7	14:29:43.44	05:21:22.9	GinCl	–	Red	0.37	0.42
SDSS J142958.66+044611.0	14:29:58.65	04:46:11.3	BCIG	0.456	Red	0.08	0.18
LEDA 1290447	14:41:28.04	05:51:52.3	Galaxy	0.027	Blue	1.00	0.00
SDSS J145344.51+045645.8	14:53:44.52	04:56:46.0	QSO	3.328	Blue	0.71	0.03
SDSSCGB 43444.3	14:55:33.70	04:46:43.2	AGN	0.334	Red	0.38	0.38
SDSS J200143.74+004918.4	20:01:43.73	00:49:18.4	QSO	–	Blue	0.36	0.07
SDSS J200432.38+001041.3	20:04:32.39	00:10:41.4	low-mass*	–	–	–	–
[SHM2017] J302.70083-00.21773	20:10:48.20	-00:13:03.9	RRLyr	–	Blue	1.00	0.00
[SHM2017] J302.70083-00.21773	20:10:48.20	-00:13:03.9	RRLyr	–	Blue	1.00	0.00
[SSV2012] 4869177	20:22:35.51	-00:40:09.9	RRLyr	–	Blue	0.92	0.02
[SSV2012] 4472518	20:22:37.80	-00:02:50.5	RRLyr	–	Blue	0.99	0.01
UGC 11566	20:28:12.02	00:17:18.2	Galaxy	0.006	Blue	0.88	0.05
SDSS J202906.80+005453.5	20:29:06.81	00:54:53.6	QSO	–	Blue	0.97	0.03
2SLAQ J204340.03+002853.4	20:43:40.04	00:28:53.6	Seyfert 1	0.317	Blue	0.53	0.08
SDSS J204626.10+002337.7	20:46:26.11	00:23:37.8	QSO	0.332	Red	0.24	0.39
2SLAQ J204720.76+000007.7	20:47:20.76	00:00:07.8	CataclyV*	0.001	Blue	1.00	0.00
2SLAQ J204720.76+000007.7	20:47:20.76	00:00:07.7	CataclyV*	0.001	Blue	0.70	0.07
2SLAQ J204910.96+001557.2	20:49:10.95	00:15:57.5	Seyfert 1	0.363	Blue	0.41	0.07
[VV2006] J204956.6-001201	20:49:56.62	-00:12:01.7	QSO	0.369	Blue	0.46	0.09
[VV2006] J204956.6-001201	20:49:56.62	-00:12:01.7	QSO	0.369	Blue	0.53	0.08
[VV2006] J205316.7+005920	20:53:16.77	00:59:21.1	QSO	4.299	–	–	–
2SLAQ J205352.03-001601.5	20:53:52.04	-00:16:01.5	QSO	0.363	Blue	0.68	0.11
2SLAQ J205614.55-004050.9	20:56:14.55	-00:40:50.6	Star	–	–	–	–
2SLAQ J205712.69+001211.3	20:57:12.69	00:12:11.4	QSO	0.335	Blue	0.50	0.11
SDSS J205740.76+005418.5	20:57:40.75	00:54:19.0	QSO	0.332	Red	0.13	0.68
Gaia DR2 6794425304909258752	20:58:06.45	-30:08:18.1	Candidate WD*	–	Blue	0.40	0.07
LEDA 687146	20:58:24.54	-32:43:22.5	Galaxy	–	Blue	1.00	0.00
2MASX J20584976-4420243	20:58:49.69	-44:20:24.7	Galaxy	0.018	Blue	0.98	0.02
6dFGS gJ205957.5-213935	20:59:57.53	-21:39:34.9	Galaxy	-0.001	Blue	0.72	0.06
SDSS J210014.12+004446.0	21:00:14.11	00:44:45.9	CataclyV*	0.000	Blue	0.57	0.10
SDSSCGB 52599.6	21:01:55.95	-00:31:24.9	Galaxy	–	Red	0.15	0.64
LEDA 598660	21:01:56.43	-39:23:40.3	Galaxy	–	Blue	0.70	0.03
QSO B2059-330	21:02:41.71	-32:52:44.1	QSO	3.280	Blue	0.76	0.07
QSO B2059-330	21:02:41.72	-32:52:44.4	QSO	3.280	Blue	0.98	0.02
LEDA 528866	21:03:02.23	-45:14:41.1	Galaxy	–	Blue	0.88	0.04
Gaia DR2 6808104805812408064	21:03:56.66	-21:47:27.1	Star	–	Blue	0.89	0.03
ESO 286-33	21:04:08.52	-43:32:03.2	IG	0.017	Blue	0.68	0.05
ESO 286-35	21:04:11.17	-43:35:33.8	GinGroup	0.017	Blue	0.58	0.15
LEDA 720203	21:04:21.46	-30:11:50.0	Galaxy	–	Red	0.06	0.19
[GPM2009] J2104-0035 1	21:04:55.31	-00:35:21.8	EmG	0.005	Blue	0.75	0.15
LEDA 520361	21:05:20.69	-45:59:19.3	Galaxy	–	Blue	0.63	0.06
ESO 286-44	21:05:38.68	-42:46:52.4	Galaxy	0.008	Blue	0.71	0.13
PN G006.0-41.9	21:05:53.57	-37:08:40.4	PN	–	Blue	0.04	0.02
EC 21035-4032	21:06:48.02	-40:20:03.7	Star	–	Blue	0.38	0.11
2MASX J21071198-4733258	21:07:11.98	-47:33:25.2	GinPair	–	Blue	0.94	0.01
2MASX J21071385-4733258	21:07:13.86	-47:33:25.3	GinPair	0.015	Blue	1.00	0.00
[GPM2009] J2112-0016 2	21:12:00.92	-00:16:49.2	EmG	0.012	Blue	0.97	0.03
6dFGS gJ211224.6-412854	21:12:24.59	-41:28:53.3	AGN	0.349	Blue	0.66	0.05

Table B1: –continued

Id Object	RA	Dec	Type	Redshift	Group	P(Blue)	P(Red)
						HAC	HDBSCAN
CRTS J211328.1+000332	21:13:28.17	00:03:32.6	EB*	–	Blue	1.00	0.00
ESO 402-20	21:15:19.13	-33:13:34.6	Galaxy	0.018	Blue	0.93	0.07
CTCV J2118-3412	21:18:04.28	-34:13:43.5	CataclyV*	–	Blue	0.53	0.06
AT20G J212302-291504	21:23:02.82	-29:15:04.0	Radio(cm)	–	Blue	0.52	0.08
CRTS CSS120613 J212655-012054	21:26:54.54	-01:20:54.1	Candidate CV*	–	Blue	0.32	0.06
LEDA 710984	21:27:08.26	-30:57:08.4	Galaxy	–	Blue	1.00	0.00
2SLAQ J212954.20-010323.3	21:29:54.22	-01:03:23.3	EmG	0.335	Blue	0.70	0.03
LBQS 2128-4555	21:31:29.53	-45:41:50.5	QSO	0.623	Blue	0.63	0.07
2SLAQ J213242.28-010309.0	21:32:42.29	-01:03:09.2	Galaxy	–	Blue	0.87	0.05
2SLAQ J213245.24+000146.4	21:32:45.26	00:01:46.8	Seyfert 1	0.234	Blue	0.28	0.07
2MASS J21333817+0126291	21:33:38.14	01:26:29.0	QSO	1.004	Blue	0.97	0.03
SDSS J213455.08+001056.9	21:34:55.09	00:10:56.8	QSO	3.289	Blue	0.76	0.03
WISEA J213649.75-012852.2	21:36:49.75	-01:28:52.2	QSO	3.280	Blue	1.00	0.00
QSO B2134-453	21:38:07.49	-45:08:18.0	QSO	4.360	–	–	–
2MASS J21381896+0112224	21:38:18.96	01:12:22.5	Seyfert 1	0.344	Blue	0.44	0.10
CRTS J213937.6-023913	21:39:37.58	-02:39:13.0	Candidate CV*	–	Blue	0.36	0.08
2SLAQ J214106.46+004733.3	21:41:06.44	00:47:33.5	QSO	2.452	Blue	0.45	0.08
SDSSCGB 15831.2	21:41:42.73	00:45:34.9	Galaxy	–	Blue	0.91	0.02
SDSS J214155.04-011734.3	21:41:55.04	-01:17:34.2	QSO	3.286	Blue	1.00	0.00
SDSS J214155.04-011734.3	21:41:55.04	-01:17:34.3	QSO	3.286	Blue	0.47	0.06
SN 2017hxv	21:44:22.94	-29:54:59.0	SN	0.019	Red	0.12	0.19
2SLAQ J214455.94+002305.8	21:44:55.92	00:23:06.1	EmG	0.330	Blue	0.86	0.05
6dFGS gJ214540.0-291937	21:45:40.01	-29:19:36.9	Galaxy	0.341	Red	0.17	0.22
2SLAQ J214830.60-004752.6	21:48:30.61	-00:47:52.6	EmG	0.332	Blue	0.90	0.03
2SLAQ J214830.60-004752.6	21:48:30.61	-00:47:52.5	EmG	0.332	–	–	–
SDSS J215002.69+011343.8	21:50:02.70	01:13:43.8	QSO	3.267	Blue	0.98	0.02
2SLAQ J215010.52-001000.6	21:50:10.53	-00:10:00.6	QSO	0.335	Blue	0.48	0.10
2dFGRS TGS406Z223	21:53:05.55	-31:28:17.9	Galaxy	0.019	Blue	0.54	0.09
2dFGRS TGS406Z223	21:53:05.55	-31:28:17.9	Galaxy	0.019	Blue	0.54	0.09
2dFGRS TGS406Z223	21:53:05.55	-31:28:17.9	Galaxy	0.019	Blue	0.54	0.09
2dFGRS TGS406Z223	21:53:05.55	-31:28:17.9	Galaxy	0.019	Blue	0.54	0.09
2MASX J21541799+0056318	21:54:18.00	00:56:31.9	Galaxy	0.010	Blue	1.00	0.00
LEDA 214792	21:56:13.83	-01:09:42.8	Galaxy	–	Blue	0.85	0.03
LEDA 214792	21:56:13.85	-01:09:43.2	Galaxy	–	Blue	0.97	0.03
SDSSCGB 16345.1	21:56:19.79	-01:10:03.6	Galaxy	0.016	Blue	0.78	0.12
SDSSCGB 16345.1	21:56:19.81	-01:10:03.7	Galaxy	0.016	Blue	0.79	0.12
2dFGRS TGS059Z257	21:57:20.89	-25:08:02.4	Galaxy	0.009	Blue	0.96	0.04
SDSS J215824.23-004413.7	21:58:24.28	-00:44:13.7	HII G	0.016	Blue	0.94	0.03
SDSS J215902.90-003318.4	21:59:02.89	-00:33:18.0	Galaxy	–	Blue	0.73	0.08
LEDA 214793	21:59:03.11	-01:57:18.3	Galaxy	–	Blue	0.66	0.05
LEDA 1136721	22:01:50.08	-00:42:26.7	Galaxy	0.018	Blue	0.96	0.04
2dFGRS TGS114Z230	22:02:07.08	-26:26:38.0	Galaxy	0.309	Blue	0.59	0.11
PB 5049	22:03:15.14	01:17:21.0	Star	–	Blue	0.06	0.03
2dFGRS TGS115Z105	22:04:53.68	-25:03:05.2	Galaxy	0.009	Blue	0.97	0.03
2SLAQ J220529.34-003110.6	22:05:29.34	-00:31:10.7	QSO	2.454	Blue	0.66	0.05
NGC 7204	22:06:55.31	-31:03:10.6	IG	0.009	Red	0.25	0.29
2dFGRS TGS251Z159	22:07:34.55	-28:39:29.3	Galaxy	0.018	Blue	0.58	0.14
NGC 7208	22:08:24.43	-29:03:03.6	GinGroup	0.009	Blue	0.96	0.04
2dFGRS TGS333Z140	22:08:51.96	-30:38:58.8	Galaxy	0.008	–	–	–
[VV2006] J220852.0-010603	22:08:51.97	-01:06:03.7	QSO	0.351	Blue	0.46	0.09
[VV2006] J220852.0-010603	22:08:51.97	-01:06:03.7	QSO	0.351	Blue	0.48	0.08
MCG-05-52-033a	22:08:55.90	-27:13:22.0	GinPair	0.009	Blue	0.78	0.06
2dFGRS TGS061Z180	22:09:19.05	-24:07:12.4	QSO	0.320	Red	0.16	0.17
2dFGRS TGS116Z088	22:09:22.91	-25:25:04.6	Galaxy	0.008	Blue	0.58	0.08
2QZ J220948.6-301357	22:09:48.63	-30:13:55.8	WD*	–	Blue	0.21	0.08
SDSSCGB 41857.2	22:09:51.35	01:09:00.0	Galaxy	0.149	Red	0.38	0.38
SDSS J220954.57-012717.6	22:09:54.57	-01:27:17.6	QSO	3.296	Blue	0.57	0.03
2QZ J221000.7-311400	22:10:00.75	-31:14:00.0	EmG	0.328	Blue	0.63	0.05

Table B1: –continued

Id Object	RA	Dec	Type	Redshift	Group	P(Blue)	P(Red)
						HAC	HDBSCAN
2dFGRS TGS116Z082	22:10:03.74	-25:20:07.3	Galaxy	0.009	Blue	0.99	0.01
2QZ J221005.7-275439	22:10:05.76	-27:54:38.7	Galaxy	0.330	Blue	0.95	0.03
6dFGS gJ221058.1-250431	22:10:58.01	-25:04:31.1	Galaxy	0.017	Blue	0.78	0.03
2QZ J221058.3-273930	22:10:58.33	-27:39:29.4	Galaxy	0.313	Blue	0.81	0.07
LSQ 12dw1	22:12:41.57	00:30:43.1	SN	0.014	Blue	0.51	0.10
[VV2006] J221335.7-282542	22:13:35.65	-28:25:41.7	QSO	2.469	Blue	0.41	0.08
2dFGRS TGS175Z009	22:14:02.86	-27:32:21.4	Galaxy	0.014	Blue	1.00	0.00
2dFGRS TGS175Z009	22:14:02.88	-27:32:21.5	Galaxy	0.014	Blue	0.96	0.04
NGC 7229	22:14:03.23	-29:22:57.8	EmG	0.014	Blue	0.77	0.05
2dFGRS TGS254Z244	22:14:05.10	-29:22:52.9	Galaxy	0.015	Blue	0.97	0.03
ESO 467-25	22:14:24.23	-29:58:51.5	EmG	0.015	Blue	0.74	0.03
2dFGRS TGS254Z138	22:14:41.93	-28:26:39.6	Galaxy	0.012	Blue	1.00	0.00
2dFGRS TGS334Z074	22:14:47.16	-29:41:12.4	Galaxy	0.006	Blue	0.76	0.02
2QZ J221517.1-285358	22:15:17.10	-28:53:57.5	EmG	0.312	Blue	0.74	0.07
[VV2006] J221532.6-281805	22:15:32.58	-28:18:03.9	QSO	1.330	Blue	0.67	0.04
2QZ J221630.0-290054	22:16:30.07	-29:00:53.3	EmG	0.330	Red	0.18	0.09
6dFGS gJ221706.5-303447	22:17:06.52	-30:34:46.1	Galaxy	0.337	Red	0.34	0.24
[VV2006] J221722.5+010436	22:17:22.44	01:04:36.3	QSO	1.403	Blue	0.10	0.05
2dFGRS TGS176Z011	22:17:41.15	-27:21:54.6	Galaxy	0.009	Blue	0.76	0.03
SDSS J221813.90+001625.1	22:18:13.91	00:16:25.3	Galaxy	0.333	–	–	–
2MASX J22181503+0115169	22:18:15.03	01:15:16.9	Galaxy	0.049	Blue	0.80	0.04
SDSS J221817.26+003623.6	22:18:17.26	00:36:23.7	AGN	0.331	Red	0.08	0.20
2QZ J221819.4-271544	22:18:19.39	-27:15:44.2	Seyfert 1	0.355	Blue	0.44	0.09
2SLAQ J221846.76-011119.0	22:18:46.74	-01:11:18.8	Galaxy	–	Blue	0.77	0.03
2SLAQ J221846.76-011119.0	22:18:46.74	-01:11:18.8	Galaxy	–	Blue	0.84	0.03
SDSS J221852.63-010310.1	22:18:52.65	-01:03:10.5	Galaxy	0.016	Blue	0.69	0.11
2QZ J221925.9-305108	22:19:25.92	-30:51:07.7	EmG	0.307	Blue	0.66	0.04
SDSSCGB 28259.2	22:19:44.75	-00:14:40.0	Galaxy	–	Red	0.21	0.38
2QZ J221945.1-293414	22:19:45.08	-29:34:13.4	EmG	0.343	Blue	0.97	0.03
[DD2013] W4+2-1 115196	22:19:53.86	00:29:04.8	Galaxy	0.087	Blue	0.61	0.11
2SLAQ J222021.37+004040.2	22:20:21.36	00:40:40.5	Star	–	Blue	0.57	0.06
2QZ J222113.6-280421	22:21:13.62	-28:04:20.9	Seyfert 1	0.332	Red	0.27	0.18
2dFGRS TGS337Z130	22:22:54.92	-30:42:28.4	Galaxy	0.014	Blue	0.94	0.02
6dFGS gJ222313.7-285844	22:23:13.70	-28:58:44.6	Galaxy	0.006	Blue	0.45	0.11
2SLAQ J222332.83-010614.8	22:23:32.84	-01:06:14.8	QSO	2.460	Blue	0.52	0.06
2QZ J222336.0-283140	22:23:36.03	-28:31:39.6	EmG	0.333	Blue	0.82	0.07
2SLAQ J222403.36-005724.2	22:24:03.35	-00:57:24.2	QSO	0.313	Blue	0.56	0.11
2SLAQ J222403.36-005724.2	22:24:03.36	-00:57:24.1	QSO	0.313	Blue	0.48	0.11
2QZ J222416.2-292421	22:24:16.26	-29:24:21.7	Candidate CV*	–	Blue	0.59	0.11
2dFGRS TGS338Z083	22:27:38.90	-31:08:10.3	Galaxy	0.015	Blue	0.80	0.06
2SLAQ J222825.11-002217.4	22:28:25.12	-00:22:17.2	Galaxy	–	Red	0.51	0.18
LEDA 711478	22:28:47.80	-30:54:43.2	Galaxy	–	Blue	0.41	0.12
LEDA 711478	22:28:47.82	-30:54:43.2	Galaxy	–	Blue	0.43	0.11
2dFGRS TGS337Z266	22:28:53.67	-30:58:51.4	Galaxy	0.013	Blue	0.85	0.05
2dFGRS TGS337Z266	22:28:53.67	-30:58:51.4	Galaxy	0.013	Blue	0.80	0.03
SDSS J222923.00-020042.7	22:29:23.00	-02:00:42.4	QSO	3.294	–	–	–
2SLAQ J222956.53+003126.5	22:29:56.54	00:31:26.5	QSO	1.340	Blue	0.45	0.07
2dFGRS TGS338Z165	22:30:01.84	-29:35:52.7	Galaxy	0.010	Blue	0.83	0.02
2dFGRS TGS338Z165	22:30:01.85	-29:35:52.6	Galaxy	0.010	Blue	0.80	0.05
NAME Kinman Dwarf	22:30:36.83	-00:06:35.8	BlueCompG	0.006	Blue	0.58	0.14
LEDA 1149494	22:31:06.00	-00:11:43.9	Galaxy	–	Blue	1.00	0.00
2QZ J223114.0-312005	22:31:13.95	-31:20:04.4	Star	–	Blue	0.77	0.08
[VV2006] J223251.7-303250	22:32:51.74	-30:32:49.6	QSO	0.350	Blue	0.31	0.07
2QZ J223342.5-301936	22:33:42.56	-30:19:35.4	Galaxy	0.324	Blue	0.80	0.06
2MASS J22340663+0001199	22:34:06.67	00:01:20.8	Star	–	Red	0.06	0.20
FASTT 1560	22:34:39.93	00:41:27.5	CataclyV*	0.001	Blue	0.54	0.07
2dFGRS TGS414Z208	22:34:56.56	-31:08:44.1	Galaxy	0.009	Blue	1.00	0.00
2dFGRS TGS414Z208	22:34:56.57	-31:08:44.1	Galaxy	0.009	Blue	1.00	0.00

Table B1: –continued

Id Object	RA	Dec	Type	Redshift	Group	P(Blue)	P(Red)
						HAC	HDBSCAN
SDSS J223508.41-005359.3	22:35:08.42	-00:53:59.4	Seyfert 2	0.328	Red	0.26	0.32
SDSS J223508.41-005359.3	22:35:08.43	-00:53:59.4	Seyfert 2	0.328	Red	0.33	0.61
2QZ J223532.2-294634	22:35:32.24	-29:46:33.0	EmG	0.325	Blue	0.82	0.03
2SLAQ J223543.05-005436.5	22:35:43.04	-00:54:36.6	Galaxy	–	Blue	0.81	0.11
2SLAQ J223543.05-005436.5	22:35:43.05	-00:54:36.6	Galaxy	–	Blue	0.67	0.02
2SLAQ J223543.05-005436.5	22:35:43.06	-00:54:36.4	Galaxy	–	Blue	0.50	0.07
SDSS J223543.94-003931.4	22:35:43.93	-00:39:32.1	low-mass*	0.000	Red	0.15	0.18
[EKS96] NGC 7314 28	22:35:44.87	-26:02:27.4				0.84	0.05
[EKS96] NGC 7314 43	22:35:45.40	-26:02:10.8	HII	–	Blue	0.68	0.02
[EKS96] NGC 7314 71	22:35:46.29	-26:04:29.1	HII	–	Blue	0.80	0.09
[EKS96] NGC 7314 130	22:35:48.23	-26:01:24.0	HII	–	Blue	0.91	0.07
[VV2006] J223633.5+002652	22:36:33.54	00:26:52.8	QSO	1.354	Blue	0.69	0.07
SDSS J223649.60+005413.5	22:36:49.60	00:54:13.8	QSO	3.313	–	–	–
2SLAQ J223723.84-010120.3	22:37:23.88	-01:01:19.2	Galaxy	–	Blue	0.97	0.03
SDSS J223729.86-010549.1	22:37:29.86	-01:05:49.3	HB*	-0.001	–	–	–
PHL 354	22:38:23.25	-00:57:08.2	QSO	0.361	Blue	0.34	0.06
PHL 354	22:38:23.26	-00:57:08.1	QSO	0.361	Blue	0.43	0.08
2SLAQ J223844.30-005655.3	22:38:44.29	-00:56:55.3	QSO	1.357	Blue	0.53	0.08
LEDA 131686	22:41:19.49	-39:58:23.3	Galaxy	–	Blue	0.72	0.05
2QZ J224149.5-301945	22:41:49.50	-30:19:44.5	Galaxy	0.322	Blue	0.66	0.08
[GDB2008] 503	22:43:16.38	-39:51:39.9	Galaxy	0.007	Blue	0.80	0.05
[GDB2008] 504	22:43:19.40	-39:52:44.4	Galaxy	0.007	Blue	0.49	0.13
[GDB2008] 509	22:43:25.11	-39:55:20.0	Galaxy	0.327	Red	0.11	0.88
SDSS J224352.11-002259.7	22:43:52.21	-00:22:59.9	Galaxy	0.010	Blue	0.97	0.03
2SLAQ J224531.20-004509.4	22:45:31.20	-00:45:09.4	QSO	1.368	Blue	0.58	0.05
2SLAQ J224531.20-004509.4	22:45:31.20	-00:45:09.3	QSO	1.368	Blue	0.31	0.06
SDSS J224539.94-002419.7	22:45:39.94	-00:24:19.6	QSO	3.280	Blue	0.98	0.02
2MASS J22495608+0002182	22:49:56.08	00:02:18.4	QSO	3.307	Blue	0.88	0.07
2SLAQ J225012.91-003959.0	22:50:12.92	-00:39:58.9	Galaxy	–	Blue	0.78	0.08
SDSS J225149.74-002811.7	22:51:49.75	-00:28:11.4	QSO	3.228	Blue	0.97	0.03
2QZ J225157.1-292451	22:51:57.10	-29:24:50.8	EmG	0.318	Blue	0.39	0.06
2SLAQ J225257.45+002731.5	22:52:57.44	00:27:31.6	Star	–	Blue	0.59	0.12
2QZ J225352.9-300944	22:53:52.96	-30:09:43.7	Seyfert 1	0.326	Blue	0.26	0.09
[VV2006] J225411.2-312712	22:54:11.15	-31:27:11.3	QSO	1.360	Blue	0.71	0.04
SDSS J225411.96-004949.5	22:54:11.96	-00:49:49.4	QSO	3.297	Blue	0.50	0.06
SDSS J225411.96-004949.5	22:54:11.96	-00:49:49.3	QSO	3.297	Blue	0.99	0.01
2QZ J225503.9-301914	22:55:03.89	-30:19:13.3	EmG	0.326	Blue	0.99	0.01
2QZ J225908.1-312717	22:59:08.12	-31:27:16.7	Star	–	Blue	0.30	0.07
2SLAQ J230030.09-003005.9	23:00:30.09	-00:30:05.8	Galaxy	–	Blue	0.61	0.07
2SLAQ J230201.20+003047.2	23:02:01.20	00:30:47.3	QSO	1.344	Blue	0.63	0.05
[VV2006] J230235.5-285630	23:02:35.44	-28:56:29.7	QSO	0.368	Blue	0.60	0.07
2SLAQ J230316.40-001211.5	23:03:16.41	-00:12:11.4	QSO	1.516	Blue	0.60	0.08
V* HY Psc	23:03:51.63	01:06:51.4	CataclyV*	-0.000	Blue	0.67	0.07
SDSS J230428.31+005701.2	23:04:28.34	00:57:01.2				0.56	0.11
2SLAQ J230444.16-010251.7	23:04:44.16	-01:02:51.5	QSO	1.377	Blue	0.44	0.08
LEDA 1122038	23:08:10.78	-01:17:58.5	Galaxy	–	Blue	0.74	0.06
SDSS J230855.49+003705.6	23:08:55.49	00:37:05.7	QSO	1.784	Blue	1.00	0.00
ESO 469-15	23:08:55.60	-30:51:28.2	GinGroup	0.005	Blue	0.73	0.14
[VV2006] J230914.4-305913	23:09:14.31	-30:59:12.5				0.61	0.05
2MASS J23094616+0000496	23:09:46.15	00:00:49.1	Seyfert 1	0.352	Blue	0.61	0.10
2MASS J23094616+0000496	23:09:46.16	00:00:49.0	Seyfert 1	0.352	Blue	0.65	0.11
[GPM2009] J2310-0109 2	23:10:41.99	-01:09:48.0	EmG	0.012	Blue	0.78	0.07
[VV2006] J231135.1-312644	23:11:35.12	-31:26:44.1	QSO	1.350	Blue	0.58	0.04
2dFGRS TGS422Z155	23:12:08.96	-31:04:13.3	Galaxy	0.165	Red	0.43	0.21
2SLAQ J231231.36-011137.5	23:12:31.36	-01:11:37.3	QSO	1.360	Blue	0.71	0.05
SDSS J231259.07+010805.6	23:12:59.06	01:08:05.9	QSO	3.295	Blue	0.84	0.04
[VV2006] J231311.9-004538	23:13:11.91	-00:45:38.0	QSO	1.364	Blue	0.54	0.04
SDSS J231351.87-011031.9	23:13:51.86	-01:10:30.8	HII G	0.012	Blue	0.84	0.08

Table B1: –continued

Id Object	RA	Dec	Type	Redshift	Group	P(Blue)	P(Red)
						HAC	HDBSCAN
2MASX J23145046+0123280	23:14:50.52	01:23:26.7	LSB G	0.016	Blue	1.00	0.00
[VV2006] J231519.4-303857	23:15:19.39	-30:38:57.2	QSO	1.356	Blue	0.81	0.05
V* CC Scl	23:15:31.78	-30:48:48.7	CataclyV*	–	Blue	0.70	0.10
[VV2006] J231652.0+005125	23:16:52.04	00:51:25.9	QSO	3.229	Blue	0.80	0.03
3XMM J231742.5+000535	23:17:42.61	00:05:35.3	Seyfert 1	0.321	Blue	0.56	0.06
[VV2006] J231942.8-302629	23:19:42.76	-30:26:29.5	QSO	2.473	Blue	0.83	0.08
LEDA 71137	23:20:35.21	-00:52:50.9	Galaxy	0.015	Blue	0.64	0.08
LEDA 71137	23:20:35.22	-00:52:50.8	Galaxy	0.015	Blue	0.56	0.08
2QZ J232126.5-310730	23:21:26.51	-31:07:29.5	Galaxy	0.309	Blue	1.00	0.00
[SIG2010] 389821	23:23:31.32	01:08:06.0	RRLyr	–	Blue	0.86	0.02
GALEX 2417063145906373262	23:24:20.34	-00:06:25.0	HII	–	Blue	0.10	0.04
[GPM2009] J2324-0006	23:24:21.37	-00:06:29.4	HII G	0.009	Blue	0.24	0.08
2SLAQ J232457.75+002153.2	23:24:57.75	00:21:53.4	QSO	0.345	Blue	0.20	0.07
2SLAQ J232524.40+004612.0	23:25:24.43	00:46:12.2	Galaxy	0.016	Blue	0.87	0.06
2MASS J23255145-0140232	23:25:51.48	-01:40:23.8	CataclyV*	–	Blue	0.33	0.10
[VV2006c] J232555.5-003710	23:25:55.51	-00:37:10.7	Seyfert 1	0.332	–	–	–
SDSS J232743.68-020055.8	23:27:43.70	-02:00:55.7	BlueCompG	0.018	Blue	0.13	0.05
6dFGS gJ232744.4-020047	23:27:44.38	-02:00:46.8	Galaxy	0.018	Blue	0.10	0.04
LEDA 1127711	23:28:12.30	-01:03:44.8	HII G	0.009	Blue	0.79	0.06
GD 1662	23:29:00.44	-29:46:46.0	CataclyV*	0.000	Blue	0.55	0.08
SDSS J233104.38-004237.2	23:31:04.40	-00:42:37.1	QSO	1.353	Red	0.53	0.09
2MASS J23315973-0048192	23:31:59.77	-00:48:18.5	Galaxy	0.017	Blue	0.99	0.01
2QZ J233254.8-305844	23:32:54.78	-30:58:43.8	EmG	0.329	Blue	0.58	0.07
SDSS J233256.68+011122.9	23:32:56.68	01:11:23.1	BCIG	0.382	–	–	–
SDSS J233300.21-002030.5	23:33:00.22	-00:20:30.5	QSO	3.328	Blue	0.95	0.05
[VV2006] J233438.5+002341	23:34:38.55	00:23:41.9	QSO	1.385	Blue	0.46	0.07
2MASX J23352102+0110271	23:35:20.98	01:10:27.4	Galaxy	0.085	Red	0.45	0.31
2SLAQ J233522.69-000635.2	23:35:22.69	-00:06:35.2	QSO	1.373	Blue	0.53	0.07
LEDA 135900	23:36:46.97	00:37:23.8	LSB G	0.009	Blue	0.99	0.01
[VV2006] J233722.0+002239	23:37:22.02	00:22:39.2	QSO	1.377	Blue	0.46	0.06
2XMM J233731.7+002559	23:37:31.79	00:25:59.9	AGN	0.314	Blue	0.72	0.13
DES J233747.57+001742.6	23:37:47.57	00:17:42.8	GinCl	–	–	–	–
RESOLVE rf772	23:40:38.43	-00:53:30.6	Galaxy	0.019	Blue	0.66	0.07
[VV2006] J234329.1-300200	23:43:29.16	-30:02:00.1	QSO	1.358	Blue	0.53	0.07
2SLAQ J234440.53-001205.8	23:44:40.53	-00:12:06.1	CataclyV*	–	Blue	0.40	0.06
LEDA 1109937	23:48:23.99	-01:47:31.1	Galaxy	–	Blue	1.00	0.00
2dFGRS TGS356Z227	23:50:01.55	-30:11:07.1	Galaxy	0.010	Blue	0.63	0.07
2SLAQ J235115.66-000000.0	23:51:15.66	-00:00:00.0	Galaxy	–	Blue	0.23	0.05
2SLAQ J235115.66-000000.0	23:51:15.68	-00:00:00.2	Galaxy	–	Blue	0.55	0.08
[VV2006] J235546.2-002342	23:55:46.14	-00:23:42.8	QSO	3.245	Blue	0.99	0.01
[VV2006] J235718.4+004350	23:57:18.37	00:43:50.5	QSO	4.366	Red	0.04	0.10
SDSS J235805.25-012153.9	23:58:05.25	-01:21:53.9	QSO	1.368	Blue	0.63	0.04

Table B2: Espectra from SDSS DR16

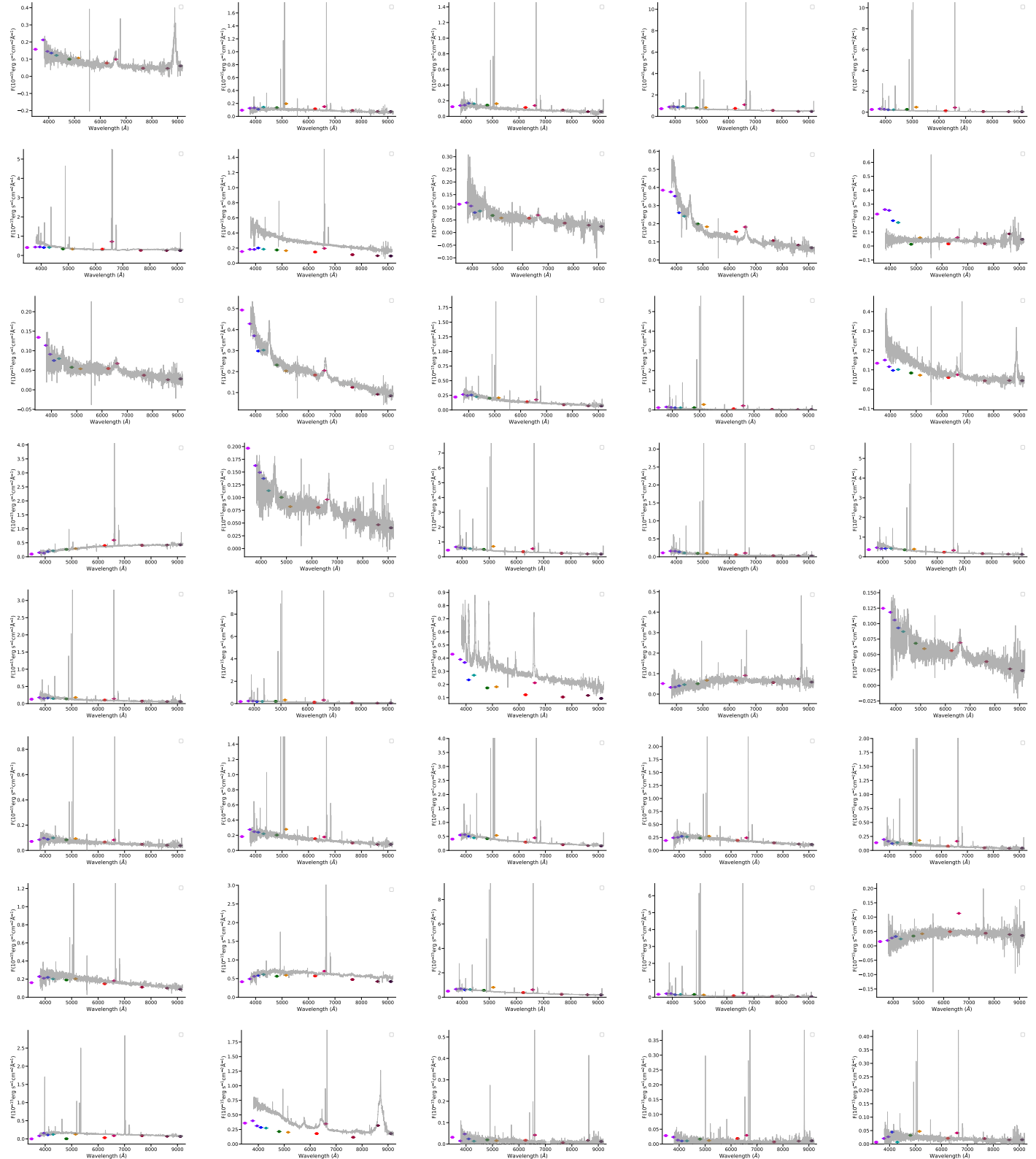


Table B2: –continued

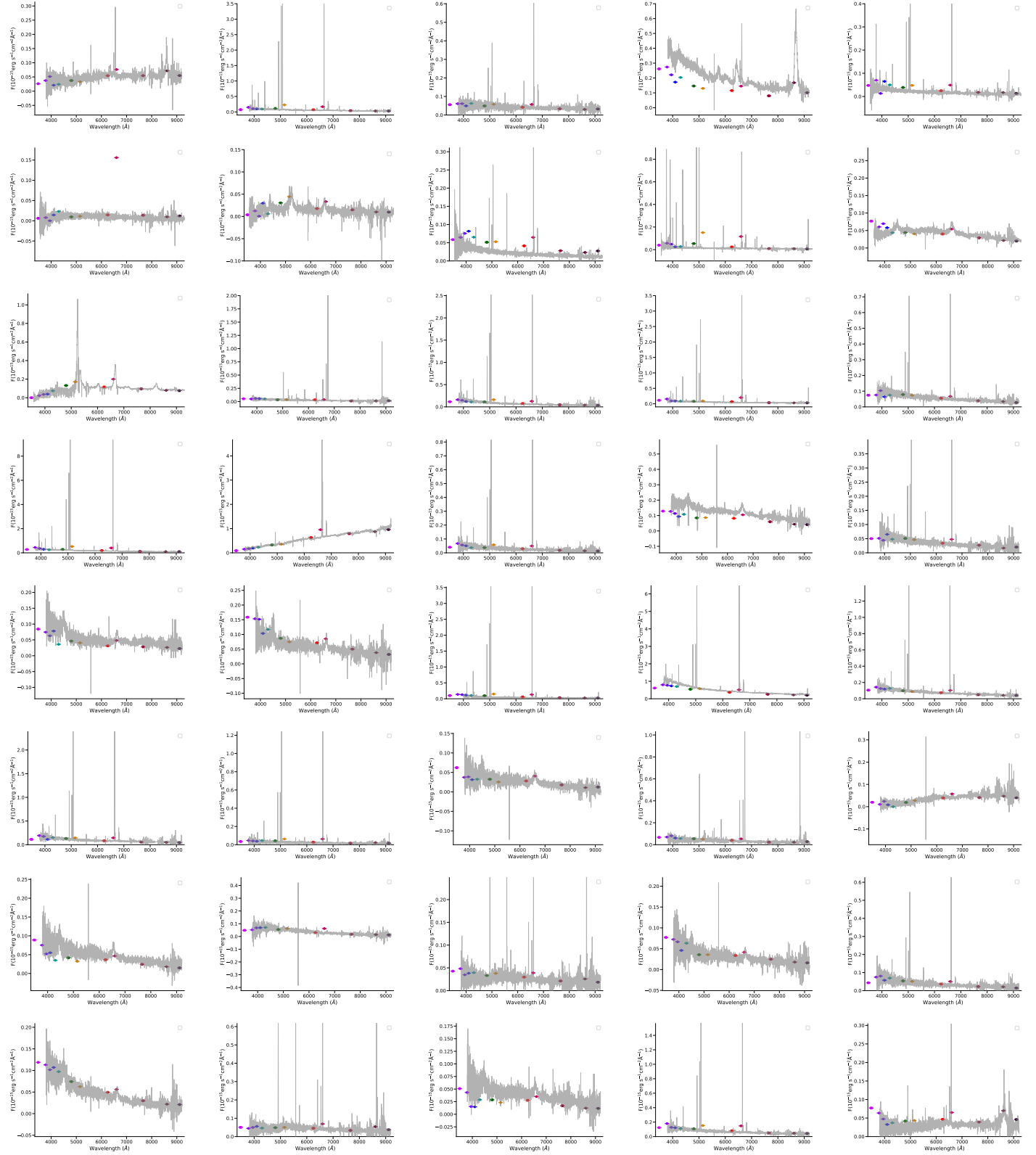


Table B2: –continued

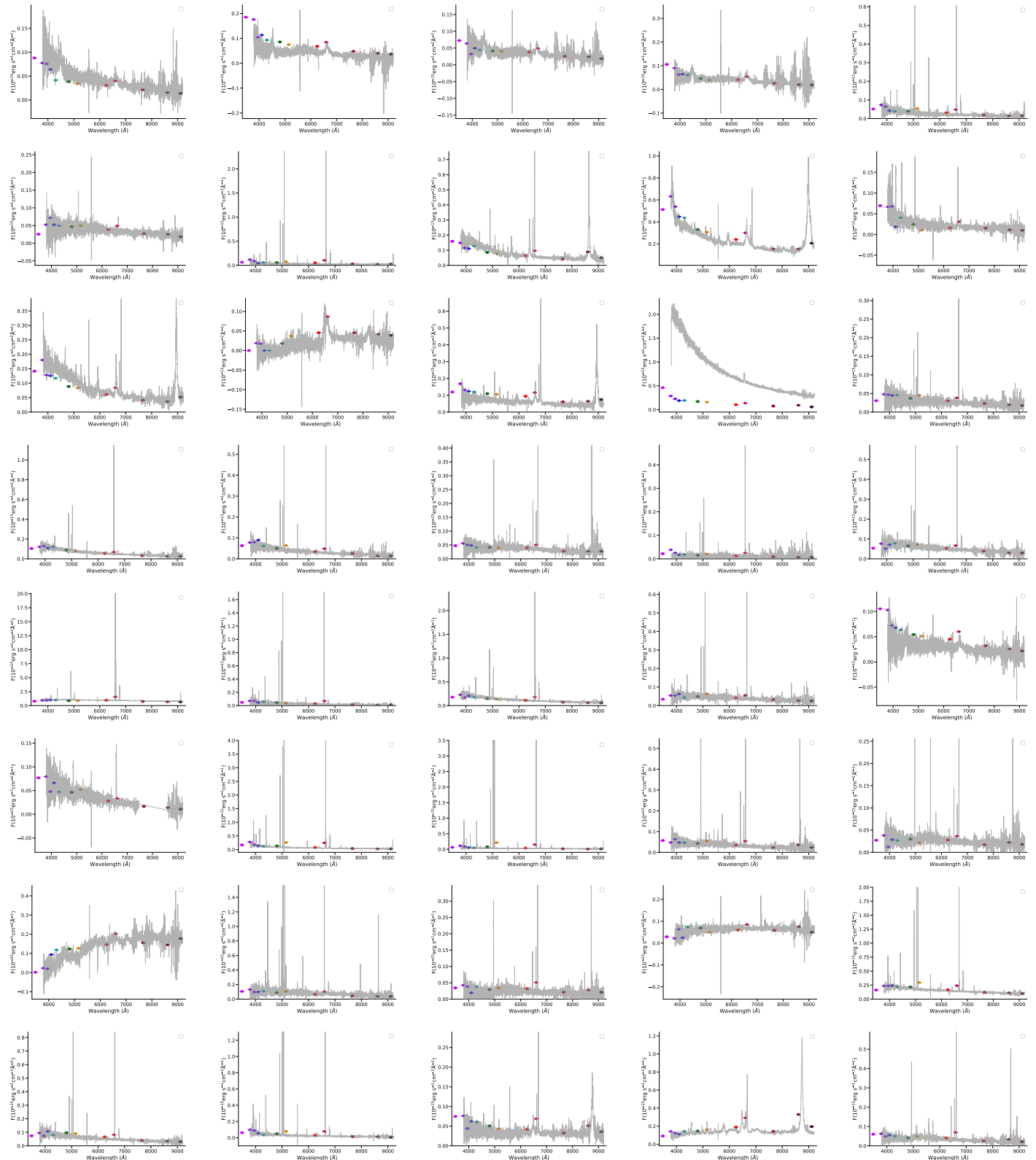


Table B2: –continued

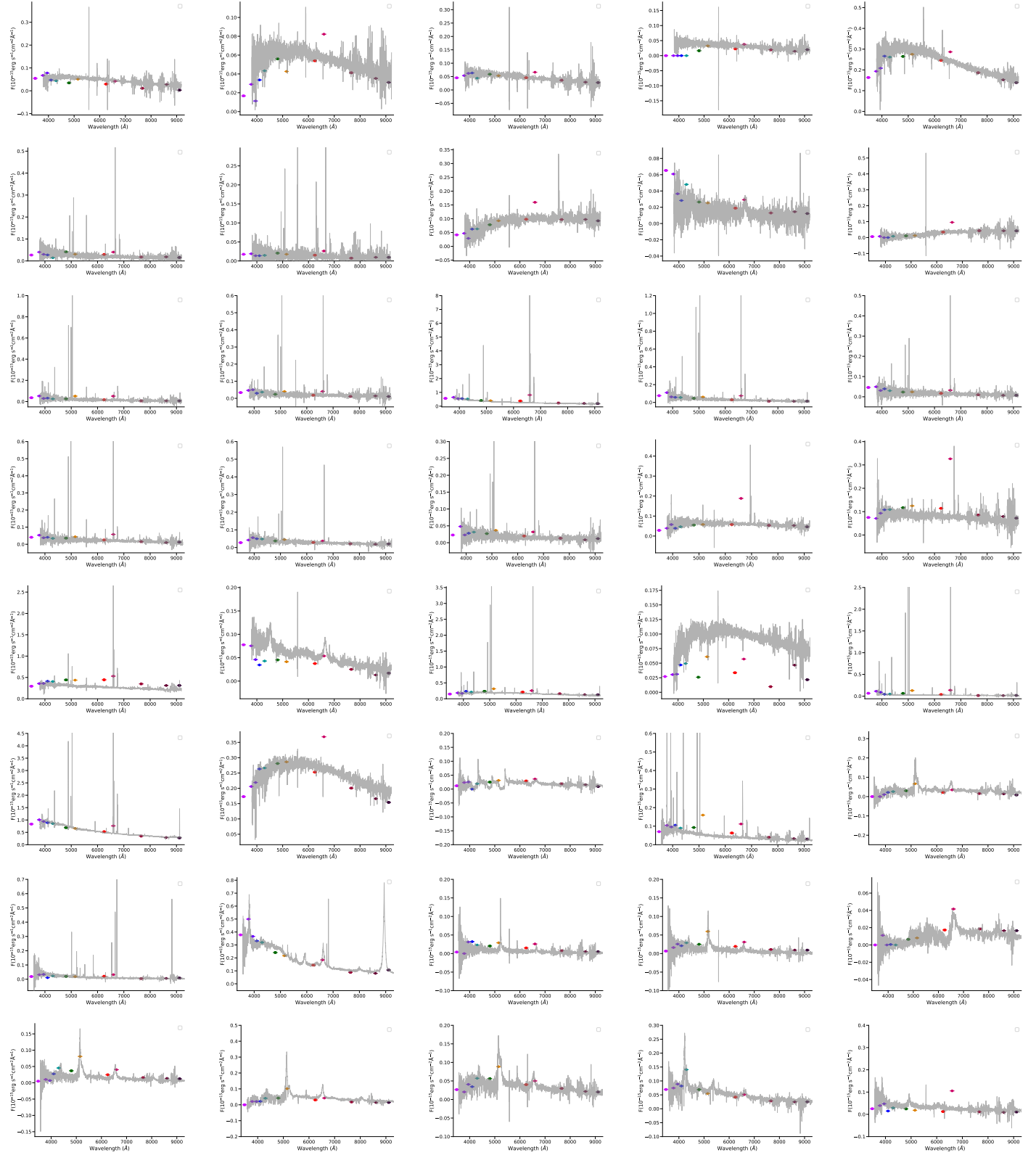


Table B2: –continued

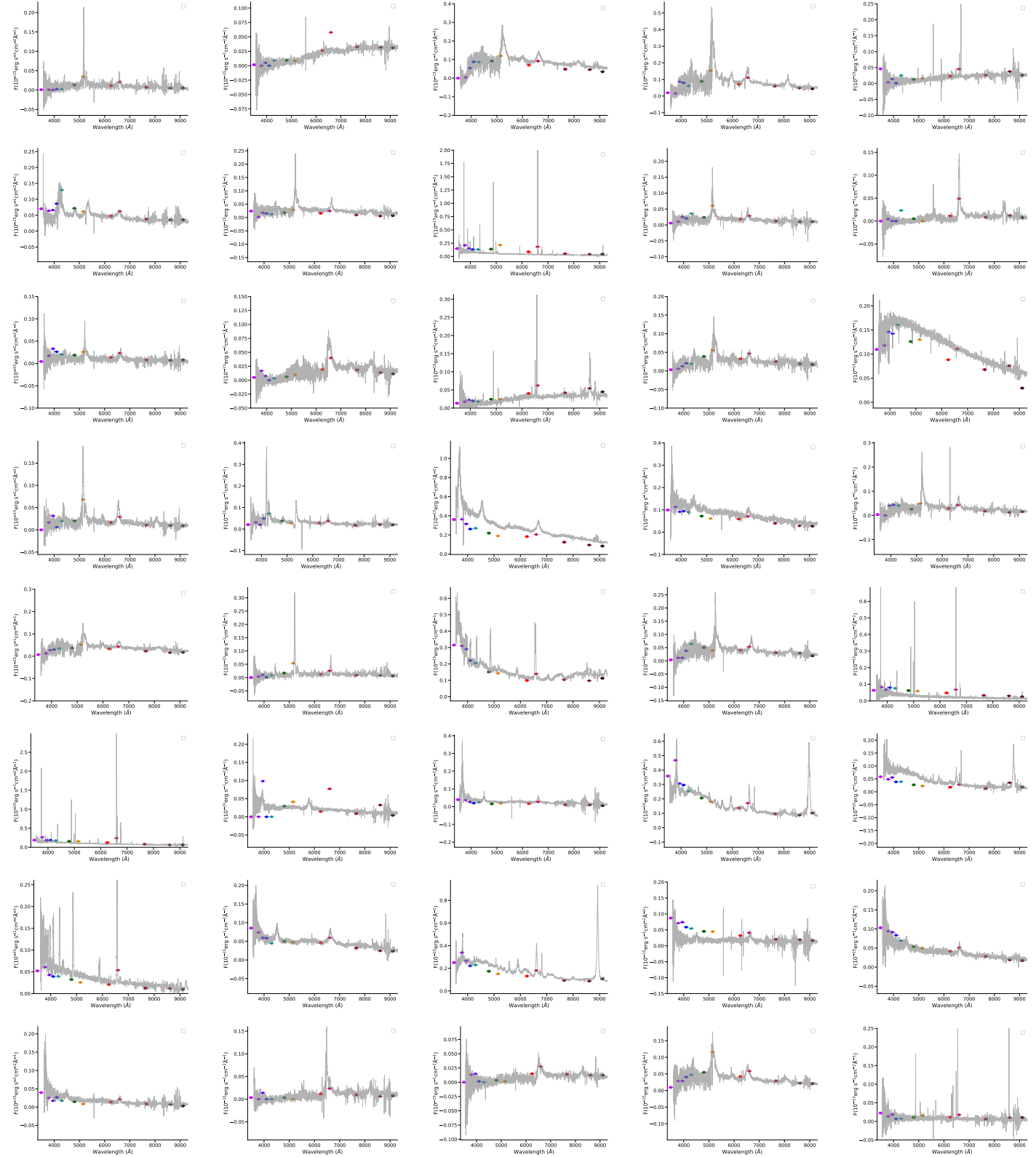


Table B2: –continued

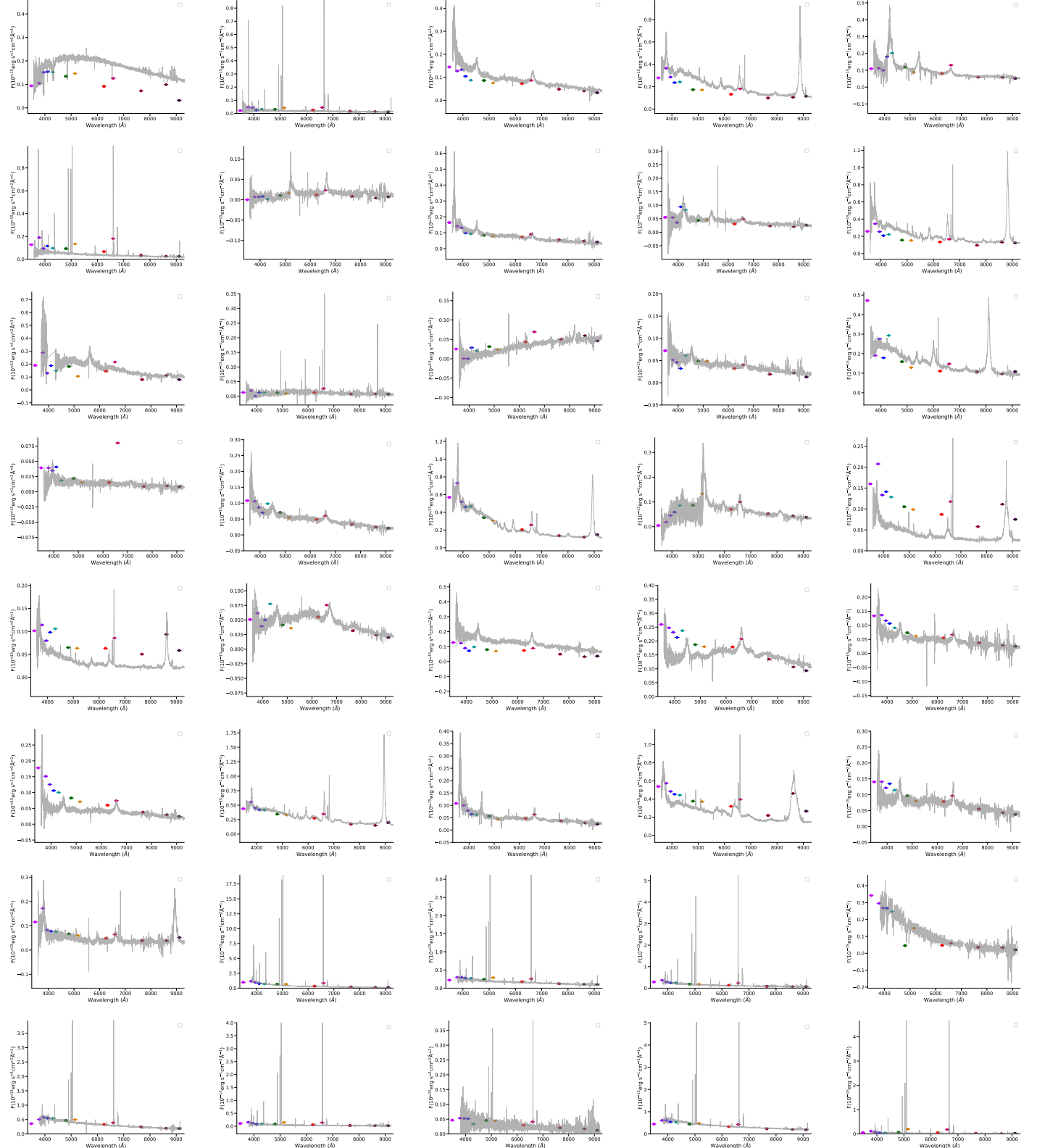


Table B2: –continued

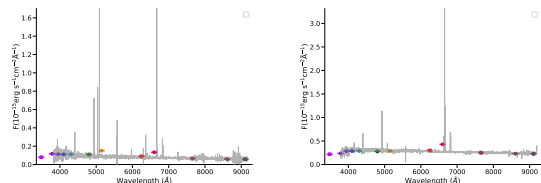


Table B3: Espectra from LAMOST DR6

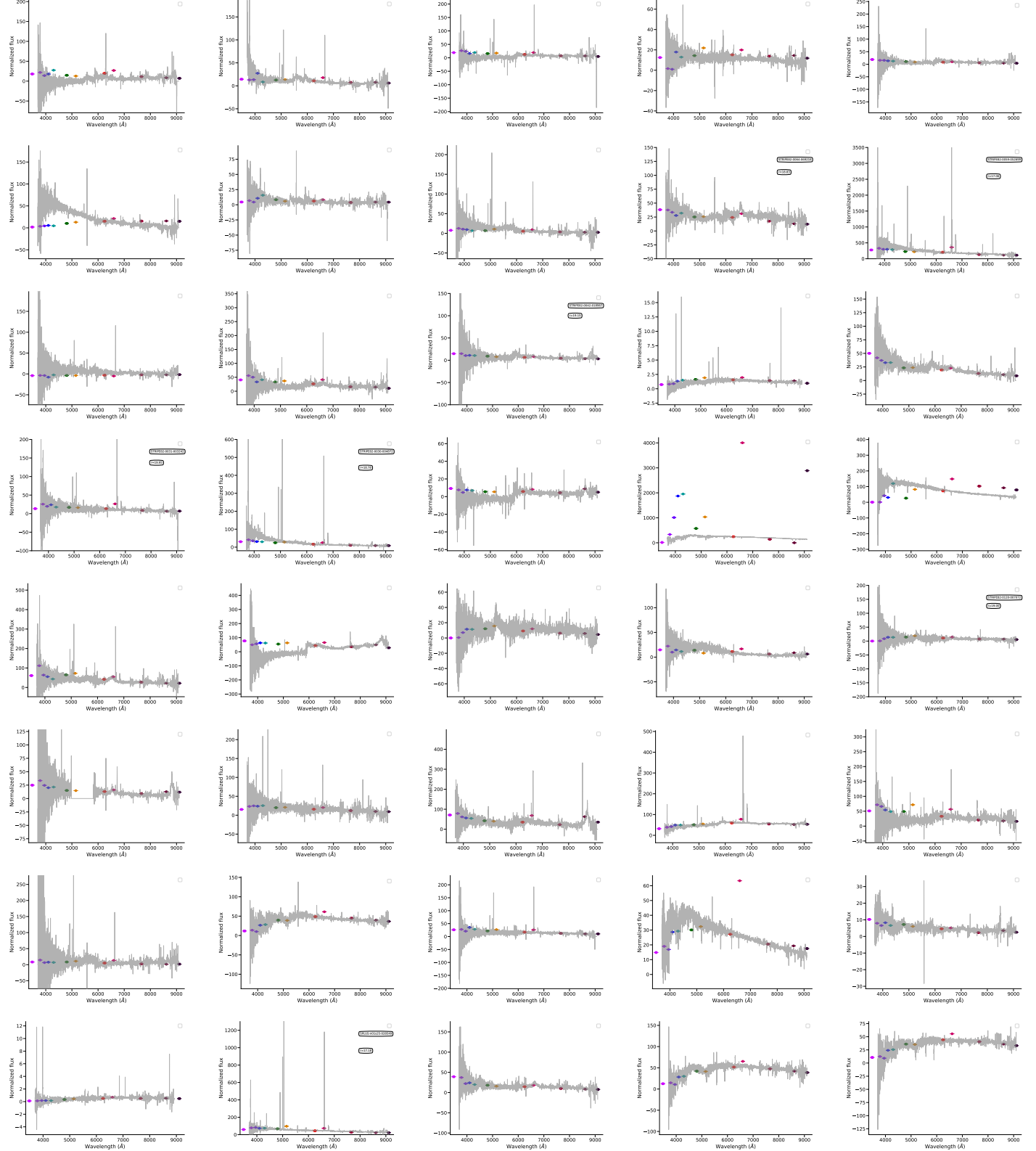


Table B3: –continued

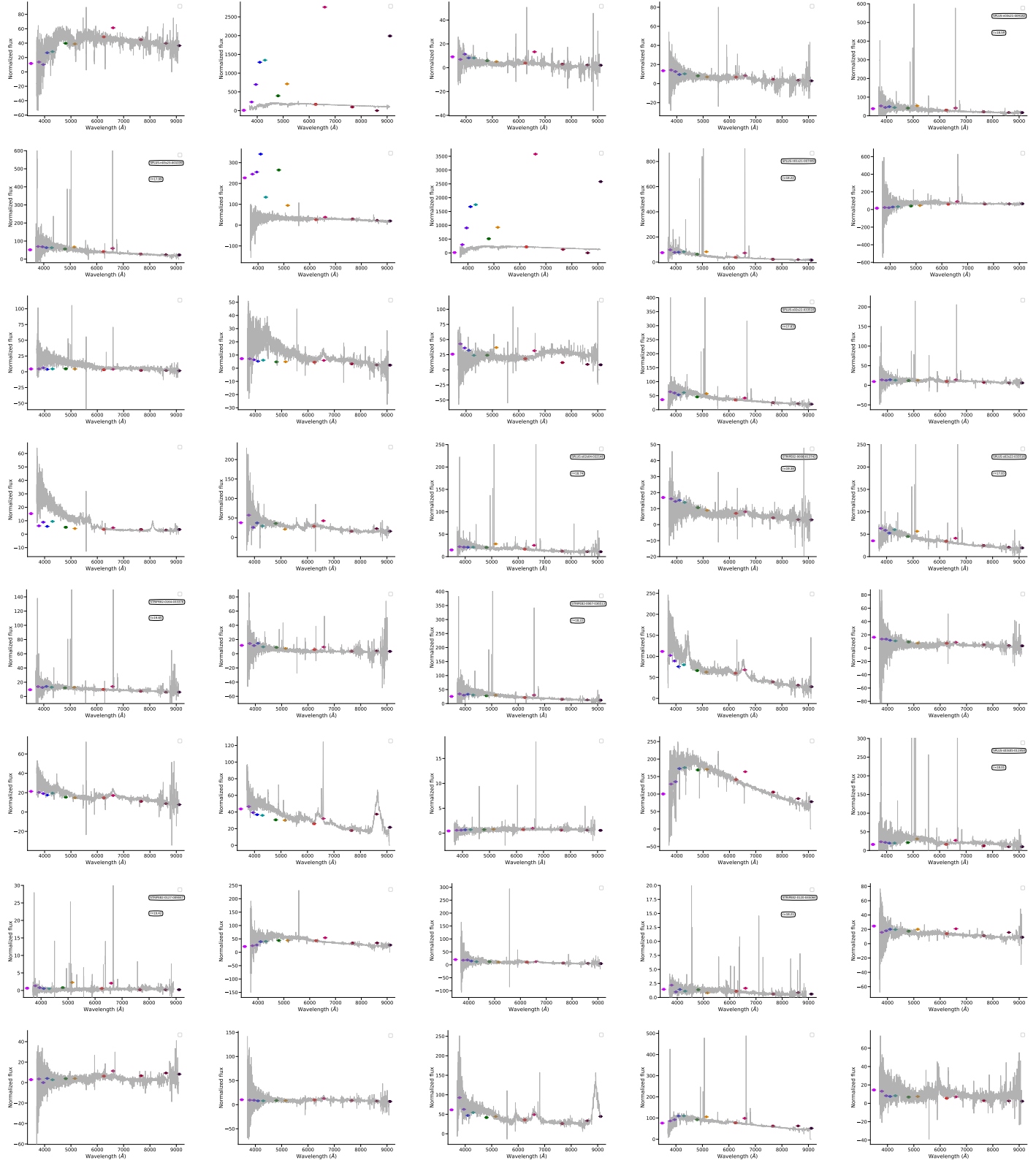
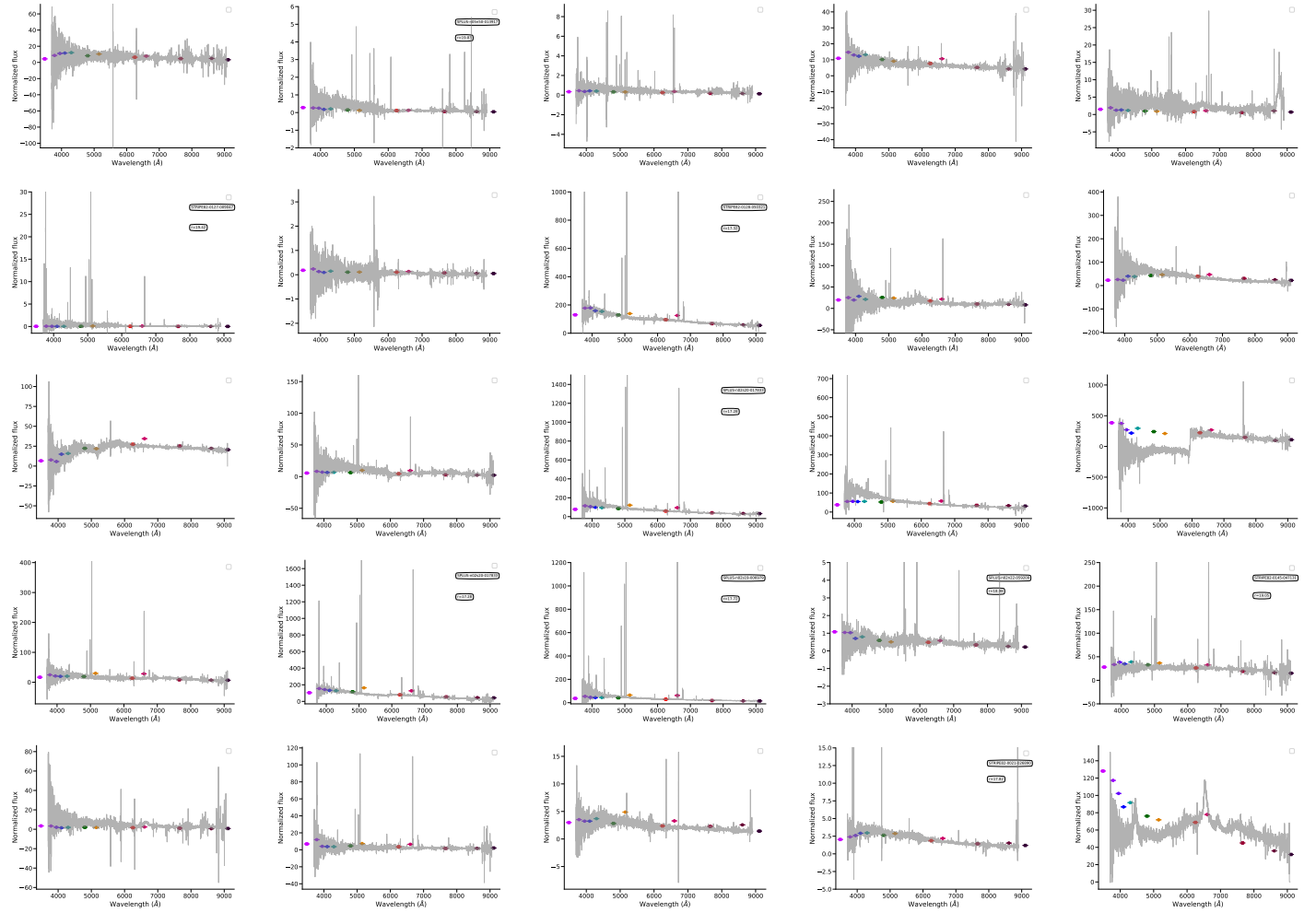


Table B3: –continued



This paper has been typeset from a \TeX / \LaTeX file prepared by the author.